DISSERTATION

MEMBRANE ORGANIZATION OF LUTEINIZING HORMONE

RECEPTORS DURING SIGNAL TRANSDUCTION

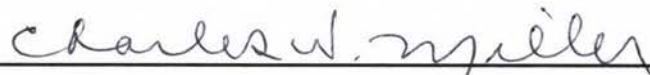Submitted by

Amber L. Wolf-Ringwall

Department of Biomedical Sciences

COLORADO STATE UNIVERSITY

May 28, 2010

WE HEREBY RECOMMEND THAT THE DISSERTATION PREPARED UNDER OUR SUPERVISION BY AMBER L. WOLF-RINGWALL ENTITLED MEMBRANE ORGANIZATION OF LUTEINIZING HORMONE RECEPTORS DURING SIGNAL TRANSDUCTION BE ACCEPTED AS FULFILLING IN PART REQUIREMENTS FOR THE DEGREE OF DOCTOR OF PHILOSOPHY.
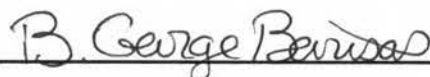
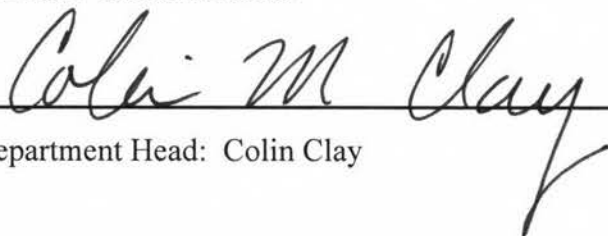Committee on Graduate Work

Charles Miller

James Graham

B. George Barisas

Advisor: Deborah Roess

Department Head: Colin Clay

ii

ABSTRACT OF DISSERTATION

MEMBRANE ORGANIZATION OF LUTEINIZING HORMONE RECEPTORS DURING SIGNAL TRANSDUCTION

Mechanisms involved in signal transduction by luteinizing hormone (LH) receptors are important for regulating key events in mammalian reproduction, such as ovulation, sex hormone production and maintenance of pregnancy. Studying the organization of LH receptors in the plasma membrane during hormone-mediated signaling provides insights into the protein interactions needed for important physiological responses.

We used biochemical and biophysical methods to examine the role of the plasma membrane in contributing to LH receptor desensitization. Using single particle tracking and sucrose gradient ultracentrifugation, we determined that individual human LH receptors are confined in small membrane compartments and localize in membrane rafts for several hours following desensitization. These receptors do not demonstrate signaling via cyclic adenosine monophosphate (cAMP) while they are confined, suggesting that the microenvironment within these compartments may be different for desensitized versus actively signaling receptors.

We also investigated self-association of human LH receptors using homotransfer fluorescence resonance energy transfer (homo-FRET) and fluorescence correlation spectroscopy. We determined that human LH receptors self-associate following desensitization and in response to increasing concentrations of human chorionic gonadotropin (hCG). LH receptors demonstrated the highest degree of aggregation in response to saturating concentrations of 100 nM hCG.

Using single particle tracking, we examined whether native LH receptors expressed on KGN human granulosa-like tumor cells, or M17 human neuroblastoma cells, become confined in small membrane compartments in response to hormone binding. We found that confinement of native LH receptors in small plasma membrane compartments depended on hCG concentration. With increasing concentrations of hCG, more LH receptors became confined in small membrane compartments with an average diameter of less than 100 nm. These receptors also exhibited slower rates of lateral diffusion. We reported the movement of non-functional hormone-receptors, labeled with deglycosylated hCG, into small membrane compartments in response to hCG treatment that saturated other available LH receptors on the membrane. This finding suggests that interactions between functional and non-functional LH receptors may occur in membrane microdomains during signal transduction.

Amber L. Wolf-Ringwall
Department of Biomedical Sciences
Colorado State University
Fort Collins, CO 80523
Summer 2010

ACKNOWLEDGEMENTS

First I would like to recognize the members of my graduate committee. Thank you to Dr. Miller and to Dr. Graham for your excellent instruction in a number of physiology and endocrinology courses that have enriched my undergraduate and graduation education at Colorado State University. Thank you to Dr. Sanborn for always offering moral support and guidance along the way in my graduate education. Over the years, I have realized how fortunate I am to be given the opportunity to work in the laboratory of Dr. Barisas and Dr. Roess, and I thank both of them very much for allowing me to work under their supervision. Thank you to Dr. Barisas for sharing your vast knowledge of analytical and biophysical chemistry and also for your willingness and patience in teaching me. Finally, a very special thank you to my advisor, Dr. Deborah Roess, whose support and guidance has meant the world to me in many aspects of my personal and professional life. Thank you for helping me believe in myself and in my career goals.

I have had the great pleasure of working with a number of extraordinary people in this lab that have helped me in countless ways. A very special thank you to Dr. Steven Smith, who single-handedly sparked my interest in teaching and research, and fostered my confidence in pursuing a career in science. In addition, thank you to Dr. Ying Lei, Dr. Guy Hagen, Dr. Jingjing Liu and Shirley Crenshaw for the many hours spent teaching me laboratory techniques and data analysis. Thank you to Dr. Jinming Song, Dr. Jun

Zhou and Peter Winter for their help in many areas of microscopy and laboratory techniques. And a very special thank you to members of the group past and present that have offered their friendship, advice, support and encouragement, especially Dr. Steven Smith, Dr. Mary Cahill, Chelsea Roan, Dr. Ann Baker and Abeer Al-Qatati. Each of you have made a significant impact on my life and I will always value the friendships that we have formed. Finally, a special thanks to my husband, Kris, and to all of my family and friends for listening to me, supporting me, and encouraging me throughout this journey.

For Keely

TABLE OF CONTENTS

LIST OF TABLES

LIST OF FIGURES

CHAPTER I

BACKGROUND HISTORY

INTRODUCTION

The luteinizing hormone-choriogonadotropin (LH) receptor is critical for the successful reproduction of mammals. If the LH receptor is not functioning properly, ovulation does not occur in females, Leydig cells do not develop properly in males, and early pregnancy will be compromised due to inadequate maintenance of elevated progesterone (1). Therefore it is of great importance to fully understand the biology of the LH receptor and, in particular, to understand the underlying mechanisms of receptor activation, signal transduction and regulation of receptor-mediated signaling. In addition, increasing evidence for the presence of extragonadal LH receptors implicates possible roles for gonadotropins and their receptors in both normal and disease processes outside of reproduction. For example, the presence of elevated LH in postmenopausal women and the identification of LH receptors in the brain have led to exciting new avenues in neuroendocrinology and Alzheimer's Disease research.

HYPOTHALAMIC-PITUITARY-GONADAL AXIS

The pituitary gonadotropins, LH and follicle-stimulating hormone (FSH), work together to regulate functions of the ovary and testis including gametogenesis and steroidogenesis. LH and FSH are secreted from the anterior lobe of the pituitary gland in response to the pulsatile secretion of the decapeptide hormone gonadotropin releasing hormone (GnRH). GnRH is released from the hypothalamus into the hypophyseal portal capillaries. GnRH is not diluted in the systemic circulation before it reaches its target cells in the pituitary, making it a rapid and economical signal from the brain (2). GnRH binds its G protein-coupled receptor on the gonadotrope cells in the pituitary, causing release of the gonadotropins into the peripheral circulation (3). The gonadotropins then affect the target organs (the gonads) where LH and FSH receptors are expressed. In the gonads, LH and FSH bind their high-affinity receptors and stimulate production and release of the sex steroid hormones testosterone, estrogen and progesterone (1). The gonadal sex hormones can exert negative feedback on GnRH secretion at the hypothalamus and at the level of the pituitary affecting gonadotropin secretion.

The gonadotropins play a central role in a highly regulated system known as the hypothalamic-pituitary-gonadal (HPG) axis as depicted in Figure 1. Maintaining homeostasis of these hormones is crucial in mammalian reproduction and is carried out by feedback mechanisms at all levels in the axis. The HPG axis is regulated by a number of G protein-coupled receptors, including the GnRH, LH and FSH receptors. Both LH and placentally-derived human chorionic gonadotropin (hCG) can bind the LH receptor with high affinity.
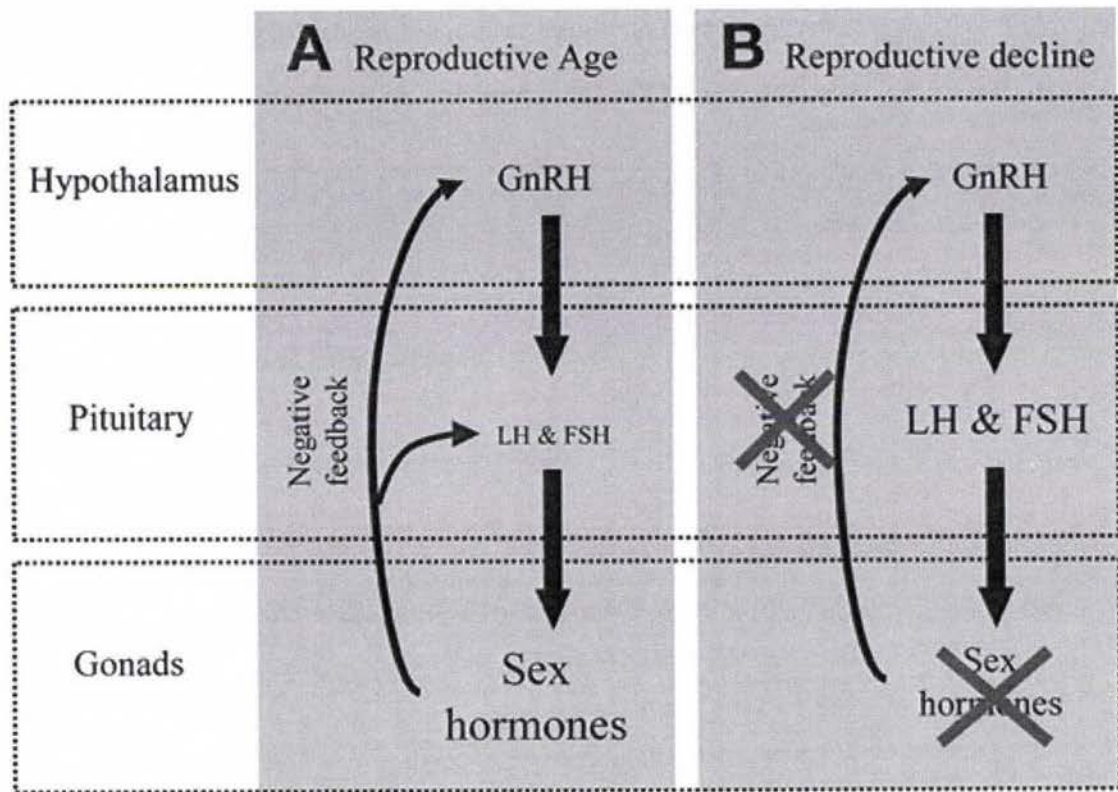
Figure 1: HPG axis interactions at reproductive age (A) and during reproductive decline (B). During reproductive decline, the gonads fail to produce the sex hormones estrogen and testosterone, shutting down negative feedback on the hypothalamus and pituitary. As a consequence, secretion of the gonadotropins rises, leading to marked increases in LH and FSH (4). (Adapted from Barron AM et al., 2006 *Endocrine* 29(2):257-269)

ROLE OF THE LH RECEPTOR IN REPRODUCTION

Fertility and normal reproductive function in mammals is dependent on functional LH receptors. The main physiological role of the LH receptor is found in its actions in the follicles and corpus luteum of the ovary, and in Leydig cells of the testis (1). In the ovary, LH receptor is expressed in theca cells, interstitial cells, differentiated granulosa cells, and luteal cells. On luteal cells, the LH receptor functions to promote ovulation, corpus luteum formation and progesterone secretion. On granulosa and thecal cells, the LH receptor promotes maturation of the follicle and steroidogenesis. In the testis, the LH receptor regulates the development and function of Leydig cells, which leads to the secretion of testosterone required for sexual development (1).

To understand the nature of LH secretion, it is necessary to understand how GnRH is released. In the hypothalamus, GnRH neurons coordinate to release GnRH episodically in pulses. Secretion of GnRH is intermittent, consisting of pulses of secretion which occur regularly at intervals of 20 minutes or more (2). The pulsatile release pattern of GnRH is essential for sustaining normal secretion and synthesis of the gonadotropins, as continuous administration of GnRH does not sustain gonadotropin release. The neurons and their processes that function to release GnRH rhythmically are collectively referred to as the GnRH pulse generator (2). Similarly, LH is secreted in a pulsatile manner. The nature of LH release is important in understanding LH receptor-mediated signaling because continuous or excessive release of a hormone can result in downregulation – a decrease in the number of active receptors on the surface of target cells (2).

In females, gonadotropins are released cyclically and are characterized by a marked increase or surge prior to ovulation. Rising levels of estrogen in the blood stimulate the preovulatory LH surge and these events result in ovulation. The LH surge also initiates luteinization – the transformation of the mature ovarian follicle into a corpus luteum after ovulation (2). This process involves the conversion of granulosa cells into luteal cells, formation of the corpus luteum from the mature follicle and, overall, a decline in proliferation of granulosa cells and an increase in the enzymes needed for progesterone synthesis. LH receptors appear on granulosa cell membranes when the antrum forms in large preovulatory follicles. LH causes increased synthesis of progesterone mainly by stimulating cholesterol transport and activating the cholesterol side chain cleavage enzyme P450. The corpus luteum (CL) was named by early anatomists from the Latin *corpus* (body) and *luteum* (yellow) to describe the yellow-colored tissue that fills the cavity of the ruptured ovulatory follicle (2). The CL is a critical steroidogenic organ that is required for the maintenance of pregnancy by providing high levels of progesterone. If pregnancy does not occur, the CL stops producing progesterone. Conversely, if pregnancy does occur, a stimulating factor such as chorionic gonadotropin in primates and equids acts to prolong the life of the CL.

hCG is synthesized in women by the syncytiotrophoblastic cells of the placenta and is secreted as early as one day after embryo implantation (5). In the same way, equine choriogondotropin (eCG) is secreted by chorion-derived uterine endometrial cells in equids (2). hCG levels peak in the first 2 to 3 months of gestation, where it functions to stimulate the CL to maintain the secretions of both estrogen and progesterone needed for maintenance of pregnancy (6). However as the placenta grows,

it gains the ability to produce enough progesterone to maintain pregnancy, and hCG production consequently diminishes (2).

Studying the mechanisms of signal transduction in LH receptors is particularly interesting because naturally-occurring mutations in the receptor can result in human disease. A large number of point mutations in the human LH receptor have been identified and can lead to constitutive activation or inactivation of LH receptor signaling (7). Constitutively activating mutations are dominant and cause familial male-limited precocious puberty (8), while inactivating mutations are recessive and can lead to Leydig cell hypoplasia (7). Loss-of-function mutations of the LH receptor gene cause pseudohermaphroditism in men and lead to amenorrhea in women (9). Women who are homozygous for loss-of-function mutations of the LH receptor are infertile.

EXTRAGONADAL LH RECEPTORS

There is increasing evidence that LH receptors are expressed in extragonadal tissues based upon the detection of LH receptor mRNA (1). In particular, the LH receptor has been identified in the uterus of many different species although the location within the uterus varies. For example LH receptors were identified in the endometrial endothelium of humans but in the uterine stroma and subepithelial cells of mice (10). Rao and colleagues have reported the presence of LH receptors in a variety of tissues including mucosa of the human fallopian tube, human sperm, human seminal vesicles, rat and human prostate, human prostate carcinomas, human skin, human breast cell lines from breast cancer biopsies and benign breast lesions, lactating rat mammary gland, human adrenals, neural retina, neuroendocrine cells, rat brain, and human thyroid

(11-13). Because there have been no clinically-observed abnormalities in individuals with either loss-of-function or gain-of function LH receptor mutations in these tissues, it is predicted that signaling through extragonadal LH receptors plays a subtle role in the physiology of these systems (1).

One example demonstrating a role for functional extragonadal LH receptors is found in the studies performed by Lacroix et al. on a postmenopausal woman with "luteinizing hormone-dependent Cushing's syndrome" (14). This patient also developed Cushing's syndrome during each of her four full-term pregnancies, suggesting that elevated LH after menopause and elevated hCG during pregnancy led to hypercortisolism and adrenal hyperplasia. A series of experiments administering GnRH, hCG, recombinant hLH, and/or the long-lasting GnRH analog leuprolide acetate were performed. It was determined that her cortisol production was controlled by LH/CG, which suggested inappropriate expression of functional LH receptor in the adrenal cortex. Additional studies of this kind are needed to fully understand the functional significance of the expression of the LH receptor in other nongonadal tissues.

AGING AND REPRODUCTIVE HORMONE CHANGES

Depletion of ovarian follicles is the primary event that causes reproduction to cease in aging female primates and marks the onset of menopause. Without endocrine cells, the ovaries do not release estrogen or progesterone in response to gonadotropins. Negative feedback exerted by the sex hormones is inhibited, and results in high-frequency, high-amplitude pulses of circulating gonadotropins that begin to rise after age 35 until postmenopause (4). As a result, menstrual cycles become irregular and

eventually cease. In contrast, aging males experience a similar phenomenon referred to as andropause, however it is characterized by a more slow and subtle decline in testicular function that corresponds with decreasing testosterone levels that begins at around age 30 (4). In both sexes, a decrease in sex hormones results in a loss of negative feedback on the hypothalamus that translates to marked increases in LH. In postmenopausal women, serum LH levels are up to 18-fold higher and FSH levels are 3-fold higher than in women at reproductive age (15). In addition, increases in both gonadotropins have been found specifically in cerebrospinal fluid, indicating that modest increases in circulating LH and FSH may be affecting the central nervous system (4). A similar but less profound increase is observed in postandropausal men, where a 2- to 3-fold higher increase is observed in serum LH and FSH compared to men at reproductive age (16).

Of particular importance is the fact that pulse amplitude and frequency also appear to increase with age, from the time of reproductive maturity to reproductive senescence. This phenomenon has been observed in female rhesus monkeys, where the average GnRH levels and pulse amplitudes both increased with age, as did corresponding LH secretion (17). In addition, a comparison between younger and older premenopausal women also demonstrated that LH pulse amplitude increases with age (18). This trend continues past menopause as seen in postmenopausal women, who exhibit higher pulse amplitudes and more frequent pulses when compared to premenopausal women (19, 20). The hormonal changes associated with dysregulation of the HPG axis following menopause have been implicated in the pathogenesis of Alzheimer's Disease.

Alzheimer's disease (AD) is a neurodegenerative disorder primarily affecting the elderly. It is a progressive disease that is initially characterized by memory loss and eventually results in a complete loss of cognitive functions. Early-onset or familial AD accounts for about 5% of AD cases and has been linked to mutations in the amyloid-β protein precursor (AβPP) and presenilin genes, leading to the overproduction and deposition of amyloid-β (Aβ) in neuritic placques. In contrast, late-onset or spontaneous AD accounts for the majority (about 95%) of AD. For late-onset AD, aging appears to be the strongest risk factor among others such as diet, exercise and gender. However, epidemiological studies have also revealed an increased prevalence for AD in females, suggesting that the major changes in serum concentrations of HPG axis hormones displayed in postmenopausal women may play a role in the development of AD.

In an attempt to explain this finding, research has primarily focused on the role of the sex hormone estrogen, since lower levels of estrogen have been reported in female AD subjects compared to age-matched controls (21). The use of hormone-replacement therapy (HRT) in delaying the onset of AD was observed in animal models (22), however a large Women's Health Initiative study found that combined HRT given to postmenopausal women did not protect against dementia or cognitive decline, and in fact substantially increased their risk of dementia and cognitive decline (23).

Since LH levels were found to be 2-fold higher in AD patients than in age-matched controls (4), Bowen and colleagues established the "gonadotropin hypothesis" of AD, proposing that the gonadotropins, particularly LH, play a role in the pathogenesis of AD. Hallmarks associated with AD are neuronal and synaptic loss,

deposition of amyloid-β in extracellular neuritic plaques, neurofibrillary tangles in neuronal cytoplasm containing abnormally hyperphosphorylated bundles of tau protein, oxidative stress, and metal ion dysregulation (24). However the causative factors of AD, including the role that high unopposed levels of LH could play, are not known.

The classical role of LH is in modulating sex hormone production. However, recently it has been suggested that an increase in overall LH levels may lead the activation of LH receptors in the postmenopausal brain, making this an interesting area to study when looking for possible molecular mechanisms of AD. In the rodent brain, LH receptors have been identified in a number of regions including the amygdala, cerebellum, preoptic area, cerebral cortex and in particular the hypothalamus (25, 26). Furthermore, a small percentage of LH and hCG, but not FSH, has been shown to cross the blood-brain barrier in rodents (27), and radiolabeled hCG was found to localize to the hippocampus (28). The hippocampus is a region of the brain involved in memory that is also severely affected in AD. Mechanisms for how gonadotropins cross the blood-brain barrier are not clear, however receptor-mediated transcytosis has been suggested (29), which has been observed in the testes for the transport of radiolabeled hCG to cross the blood-testes barrier (30).

Of further interest is the effect of the pregnancy hormone, hCG, on the behavior and brain function of the mother. During pregnancy, hCG levels have been shown to correlate with nausea, fatigue, insomnia, food preference and with impaired cognitive function and memory loss. The term "maternal amnesia" has been coined to describe this phenomenon that could be explained by the action of a hormone such as hCG on the hippocampus (31).

Bowen et al. investigated if LH was involved in the formation of Aβ (32). *In vitro* studies showed that gonadotropins can alter the processing of amyloid-β precursor protein (AβPP) in M17 neuroblastoma cells, resulting in elevated secretion of Aβ. In addition, *in vivo* studies demonstrated that a GnRHR antagonist, leuprolide acetate that lowers gonadotropin levels, decreased Aβ levels in mice. This work suggests that GnRH agonists and antagonists may represent a novel treatment strategy for AD. However it is difficult to determine cause and effect relationships with the HPG axis hormones because the regulation of gonadotropins and sex hormones depend on each other (4). Alternatively, Barron and colleagues propose that elevated LH could act through LH receptors to modify cholesterol synthesis and stimulate Aβ production in neuronal cells. Increased levels of LH could also activate LH receptor signaling on glial cells, stimulating inflammation and oxidative stress. These events combined with the effects of low sex hormone levels, could contribute to the neurodegenerative effects that eventually result in AD (4).

STRUCTURE OF LH AND hCG

LH and hCG are members of the glycoprotein hormone family that includes FSH and thyroid-stimulating hormone (TSH). The glycoprotein hormones are heterodimers that contain a conserved α-subunit and a unique but homologous β-subunit that determines receptor binding specificity. Resolution of the three-dimensional crystal structure of hCG by Lapthorn and colleagues in 1994 revealed important information about hormone-receptor interactions, and about specific locations of receptor-binding domains on hCG (33). The α- and β-subunits of hCG are linked by noncovalent

interactions that are stabilized by a segment of the β-subunit that wraps around the α-subunit forming a unique "seat-belt" arrangement. This distinctive structural feature appears to be essential for holding the α- and β-subunits together, and for receptor binding of the glycoprotein hormones. There are five disulphide bonds in the α-subunit and six disulphide bonds in the β-subunit. Both subunits are members of the structural superfamily of cysteine-knot growth factors that include nerve growth factor (NGF), transforming growth factor-β (TGF-β), and platelet-derived growth factor-β (PDGF-β). A number of residues are involved in receptor binding and were identified by a variety of different methods including chemical modification, site-directed mutagenesis, and the use of synthetic peptides in competitive inhibition studies (33).

hCG is the most heavily glycosylated glycoprotein hormone. It contains four additional *O*-linked carbohydrates on the β-subunit. In its native form, about 34% of the weight of hCG is attributed to complex carbohydrates. The presence of carbohydrate on glycoprotein hormones is essential for full biological activity and modifies the rate of clearance from the body. Due to its stability and abundance, hCG is often used as the radioligand in LH receptor-binding studies (34). Much of the carbohydrate contained on the hCG molecule can be removed by the process of chemical deglycosylation, which involves treating hCG with anhydrous hydrofluoric acid (35). Deglycosylated hCG (DG-hCG) binds to the LH receptor with a similar high affinity, but results in little to no stimulation of adenylate cyclase (36), making it a useful tool in biochemical and biophysical studies of the LH receptor because it is a non-functional hormone.

The LH receptor binds LH as well as hCG. In a study comparing the functionality of LH and hCG, single-cell fluorescence energy transfer (FET) was

measured between LH or hCG molecules labeled with FITC- and TrITC, where energy transfer was evaluated based on the reduced rate of irreversible photobleaching of FITC fluorophores when TrITC fluorophores were present (37). The observed energy transfer efficiency (%E) was higher between LH receptors binding the fluorescent hCG molecules than between the receptors binding the LH molecules. In addition, a study by Roess and coworkers examining the rotational diffusion of LH receptors with time-resolved phosphoresence anisotropy techniques determined that LH-occupied receptors were rotationally mobile on MA-10 cells, while hCG-occupied receptors were rotationally immobile (38). It is thought that there could be additional interactions between hCG and nearby membrane proteins, perhaps as a result of the additional glycosylation of the hCG molecule (39). For example, Calvo and Ryan have suggested that there may be lectin-like binding sites in cell membranes that interact with carbohydrates on hCG (40). Interactions of hCG with such lectin-like sites on the membrane may result in the formation of large molecular weight complexes that result in slow rates of receptor rotational diffusion. Furthermore, binding of chemically deglycosylated hCG to LH receptors does not appear to slow receptor rotational diffusion (41). Additional studies examining differences in the molecular motions of the LH receptor following binding of LH or hCG may reveal important differences in the biological activity of these hormones.

STRUCTURE OF THE LH RECEPTOR

The human LH receptor is a single polypeptide comprised of 699 amino acids encoded by a single gene located on the short arm of chromosome 2 (2p21) (42, 43).

The rat and human LH receptor genes are approximately 80 kb in size and each contains 10 introns and 11 exons (44, 45). In 1989, two papers simultaneously reported the cloning, sequencing and expression of complementary DNA (cDNA) for the rat and porcine LH receptors (46, 47). It was established that the LH receptor is a polypeptide chain that binds glycoprotein hormones (46, 48) and is a member of subfamily A, the rhodopsin/β_2-adrenergic receptor-like subfamily of G protein-coupled receptors (GPCRs). The cloning of cDNAs for the human LH receptor followed shortly afterwards (43, 49).

GPCRs are the largest class of membrane receptors with over 1000 members (50, 51). Currently half of the drugs used in clinical practice can directly or indirectly alter GPCR activity (52, 53). GPCRs share a similar structure, characterized by a hydrophobic serpentine domain consisting of seven membrane-spanning α-helical segments, each composed of 25-35 amino acids, and connected by three extracellular and three intracellular loops (46). Given their characteristic structure, GPCRs are also known as seven transmembrane (TM) receptors, and this nomenclature is perhaps more accurate since GPCRs can also interact with other signaling molecules that are not G proteins (54).

When cDNAs for the rat and human LH receptor are transfected into mammalian cells, three distinct LH receptor species are displayed in SDS gels. The mature glycoprotein LH receptor present at the cell surface is represented with an 85- to 95-kDa band, the immature precursor to the cell-surface receptor, thought to be localized in the endoplasmic reticulum, is found at 65- to 75-kDa, and an oligomer/aggregate of the

immature receptor is found at 165- to 200-kDa (1). About 15 kDa of the mature receptor is made up of carbohydrate chains.

The mature cell-surface LH receptor, like other GPCRs, can be divided into three well-defined domains (Figure 2). The first domain is a long, heavily glycosylated extracellular N-terminal domain containing about 340 amino acid residues which functions in ligand binding (55). The second domain is a highly conserved serpentine region containing seven α-helical transmembrane (TM) segments connected by three extracellular loops and three intracellular loops. The third domain is a shorter, intracellular C-terminal cytoplasmic domain, consisting of about 70 amino acid residues that plays roles in signal transduction, desensitization (56) and internalization of the receptor (57). The amino acid sequence homology between the hLHR and the rLHR is approximately 88% in the extracellular domain, 92% in the seven TM region, and 69% in the C-terminal cytoplasmic tail (1).

The extracellular domain of the LH receptor is known as the ligand-binding domain because it is primarily responsible for the recognition and high affinity binding of its ligands. It can be divided into three distinct regions – an N-terminal cysteine-rich region, a leucine-rich motif region, and a C-terminal cysteine-rich region also known as the hinge region (1). The glycoprotein hormone receptor family (LH/CG receptor, FSH receptor and TSH receptor) make up their own subfamily of GPCRs that is characterized by the presence of a large N-terminal extracellular domain containing several leucine-rich repeats (1). For this reason the glycoprotein hormone receptors have been renamed the leucine-rich repeat-containing GPCR (LGR) family (58). A leucine-rich repeat (LRR) is a structural motif containing 8 to 9 residues of hydrophobic amino acids

15
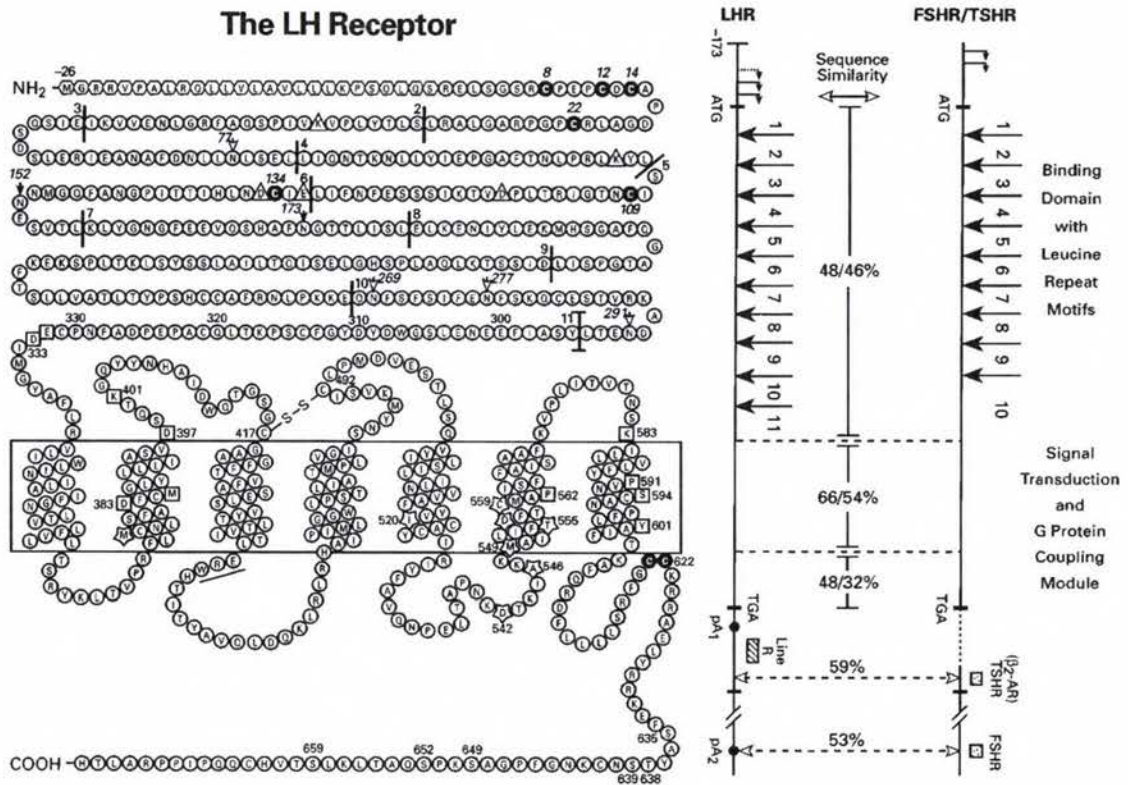
Figure 2: The amino acid sequence of the LH receptor and the nucleotide similarities between the regions of the glycoprotein hormone receptor sequences (34).

(Adapted from Dufau ML, 1998 *Annu Rev Physiol* 60:461-496)

involved in protein-protein interactions. Tandem arrays of LRRs have been found in many hormone receptors and hormone-binding proteins (59, 60).

The extracellular domains of the rat and human LH receptor also contain six conserved consensus sites (AsnXxxSer/Thr) for N-linked glycosylation, however these carbohydrate chains do not seem to be needed for binding hormone or for signal transduction (1). Interestingly, a single N-linked carbohydrate on the α-subunit of hCG is necessary for hCG to stimulate G_s coupling by the LH receptor (61, 62). It is thought that N-linked carbohydrates of the LH receptor may play a facilitative role with the chaperone protein, calnexin, in aiding the folding and trafficking of glycoproteins out of the endoplasmic reticulum (1).

The C-terminal tail of the LH receptor is the most divergent domain between the rat and human LH receptors. It is the site of two posttranslational modifications – palmitoylation and phosphorylation. Palmitoylated sites are only found on the mature cell-surface LH receptor, suggesting that palmitoylation occurs during the maturation and transport of the immature receptor to the plasma membrane, or once the LH receptor has reached the plasma membrane (1). Palmitoylation of an intracellular cysteine residue located in the juxtamembrane region of the C-terminal tail is highly conserved in all members of the rhodopsin/β₂-adrenergic subfamily of GPCRs. The LH receptor also contains at least two additional palmitoylated sites at two adjacent cysteine residues (Cys[621,622]) (63, 64). Mutations in either of these sites resulted in an increase in hormone-induced receptor downregulation (63). In addition, a C-terminal truncation deleting these sites impaired receptor processing, which led to intracellular

accumulation of LH receptors (64).   However unlike the β_2-adrenergic receptor (β_2-AR), palmitoylated cysteine is not a requirement for G_s coupling of the LH receptor (65).

Both rat and human LH receptors can become phosphorylated when expressed in transfected cells, which occurs at the cell-surface upon stimulation with hCG or phorbol esters (66, 67).   Phosphorylation of the LH receptor occurs only on serine residues and is presumed to be carried out by members of the GPCR kinase family (68).   Little is known about the importance of phosphorylation of the LH receptor, but mutating at least five of these serine residues resulted in a strong reduction in basal and LH/CG-stimulated phosphorylation of the human LH receptor (67).   Similar mutagenesis studies of the rat LH receptor led to the impairment and delay of β-arrestin-dependent internalization of receptors (69, 70).

A number of naturally occurring mutations in the human LH receptor gene leading to reproductive disorders have been reported.   Loss-of-function mutations are found throughout the human LH receptor and have been found to prevent hCG binding and/or signal transduction.   The vast majority of these mutations seem to be involved in impairing maturation and/or transport of the human LH receptor precursor, resulting in reduced expression of the receptor at the cell surface (1).   All gain-of-function mutations identified in the human LH receptor have been localized to exon 11 in the transmembrane region of the receptor located in helix VI and adjacent structures.   These mutations display some degree of constitutive activation and have provided valuable information about mechanisms of signal transfer and G protein coupling.

18

SIGNAL TRANSDUCTION BY LH RECEPTORS

The LH receptor was one of the first GPCRs known to demonstrate dual coupling – the ability to independently activate two G protein-dependent signaling pathways (71). The LH receptor interacts with the heterotrimeric ($\alpha\beta\gamma$) G proteins leading to activation of the enzyme adenylate cyclase (AC) as well as phospholipase C (PLC), as shown in Figure 3. Although the LH receptor interacts primarily with the G-protein G_s, it has also been shown to interact with $G_{q/11}$, G_{13} and G_i (34).

The LH receptor binds LH and hCG on its extracellular domain with high affinity. Activation of the LH receptor, like other GPCRs, is initiated by agonist binding, which evokes a change in conformation in the ligand binding domain, leading to a rotation in the sixth transmembrane domain. It is thought that the intracellular loops, particularly the 3i loop, forms contact sites for interaction with G proteins such as G_s (34). A model of the hCG-LHR-G_s signaling complex is illustrated in Figure 4.

Recently, a new mechanism for receptor activation of the glycoprotein hormone receptors, termed *trans*-activation, has been proposed in contrast to the traditional mechanism known as *cis*-activation (72). *Cis*-activation of receptors occurs when ligand binds to the receptor's large exodomain followed by interactions between the receptor's transmembrane domains and extracellular loops. In contrast, *trans*-activation occurs when a ligand-occupied exodomain on one receptor interacts with the signaling domain of an adjoining receptor.

19
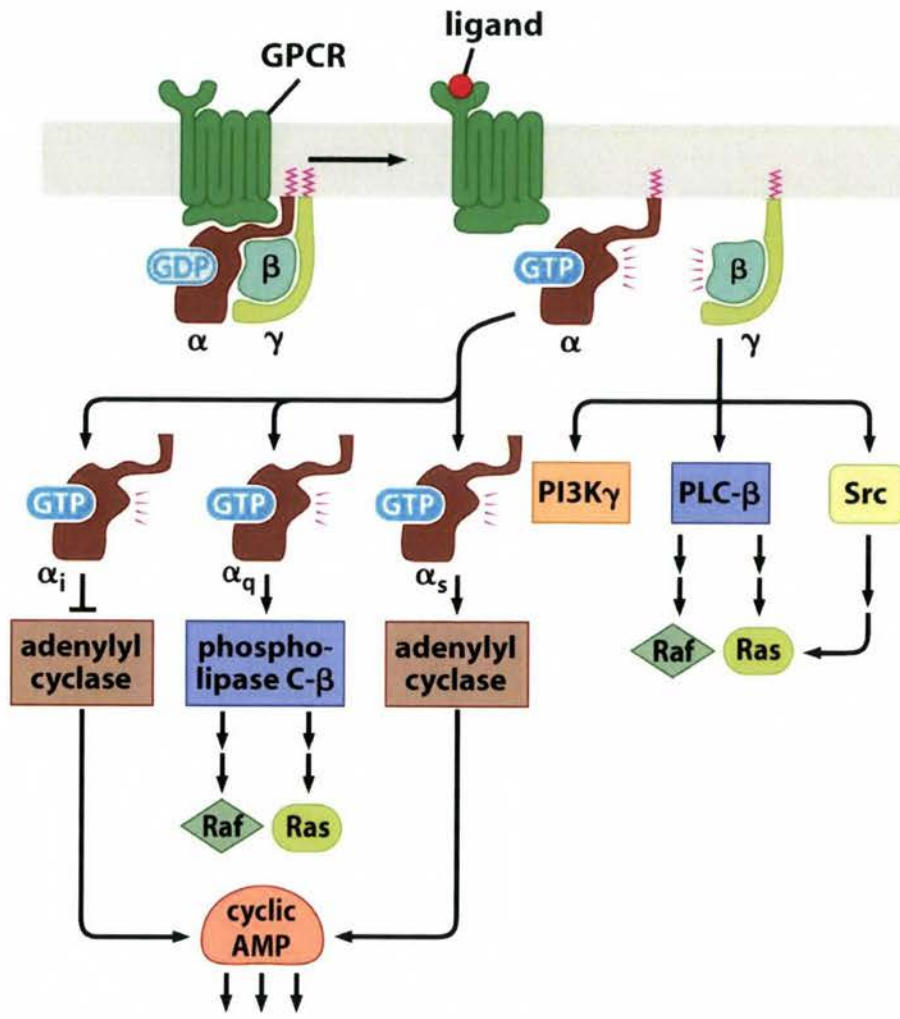
Figure 6-28 The Biology of Cancer (© Garland Science 2007)

Figure 3: G protein-coupled receptors like the LH receptor are able to activate a variety of heterotrimeric G proteins that differ in the identity of their G_α subunits. Activation of enzymes such as AC and PLC can have mitogenic or anti-mitogenic influences on target cells (73). (Adapted from Weinberg RA, 2007 The Biology of Cancer)
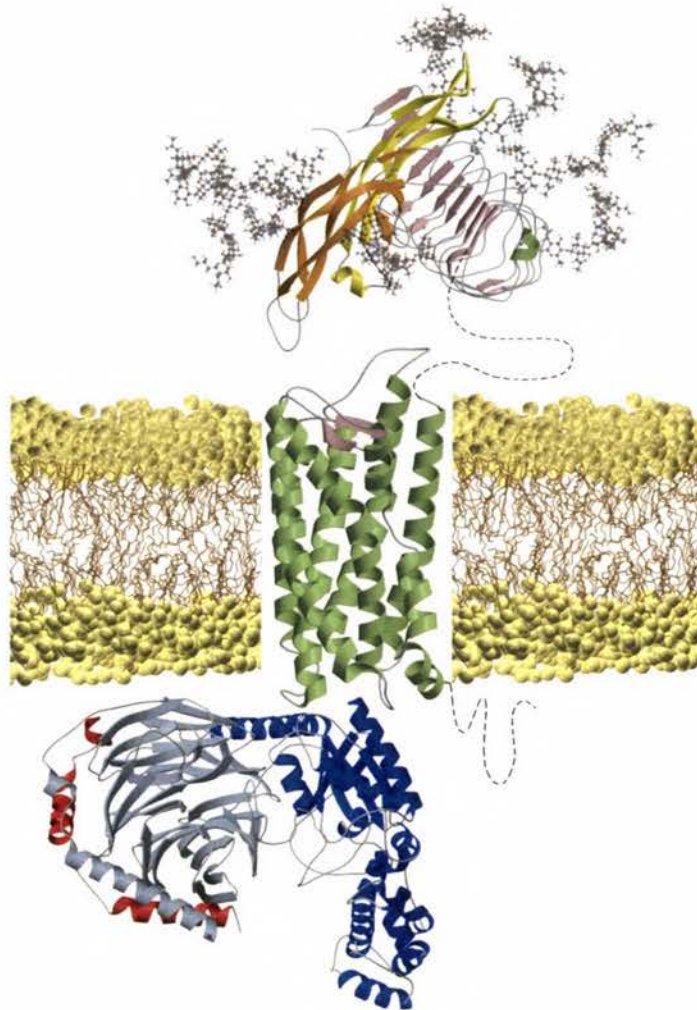
Figure 4: Schematic representation of the hCG–LHR–G_s complex for illustrative purposes only. Some of the regions are based on structural data and molecular modeling. This illustration shows a complex containing the heterodimeric hormone, hCG, bound to the LHR-ECD and the transmembrane portion of LHR bound to the heterotrimeric G protein (74).

(Adapted from Puett D et al., 2007 *Mol and Cell Endocrinology* 260-262:126-136)

The AC-cAMP-PKA Pathway

The LH receptor primarily signals through the cyclic adenosine monophosphate (cAMP)/protein kinase A (PKA) pathway (34). Receptor activation catalyzes the rate-limiting release of guanosine diphosphate (GDP) from the G_α subunit of the heterotrimeric stimulatory G protein G_s. Activated G_α binds guanosine triphosphate (GTP) and dissociates from both the receptor and membrane-anchored $G_{\beta\gamma}$ subunits. G_α is then free to activate the transmembrane adenylate cyclase (AC) enzyme, which converts adenosine triphosphate (ATP) to the second messenger molecule cAMP. Hydrolysis of GTP to GDP turns off the activation of G_α, and is followed by its reassociation with $G_{\beta\gamma}$. As long as hormone is available and signal transduction machinery can be activated, this series of molecular events persists. A downstream effect of cAMP production is activation of protein kinase A (PKA), which functions in phosphorylating serine hydroxyl groups on a variety of target proteins. The enzyme cyclic nucleotide phosphodiesterase rapidly degrades cAMP.

The PLC-IP3-Ca^{2+} Pathway

Gudermann and colleagues first demonstrated that the mouse LH receptor expressed in L cells, or the endogenous LH receptor present in bovine luteal membranes, activated G_s *and* G_{i2} (71). This led to the idea that activation of phospholipase C (PLC) is mediated by $G_{\beta\gamma}$ subunits released from LH receptor-induced activation of G_s and G_i (75). Although activation of AC is detectable in all cells types, activation of PLC is not (1). It is thought that LH receptor activation via PLC requires both high receptor expression and high agonist concentration (76). Because high concentrations of LH/CG

22

are required, it is thought that the PLC signaling pathway is activated only in females during the preovulatory LH surge and during pregnancy when hCG levels are high (71, 77). In these circumstances it is thought that maximal levels of $\beta\gamma$ are produced by increased stimulation of hormone (34). Additional factors such as variations in receptor density, G protein subunits and specific inhibitors in individual tissues at specific stages of differentiation must also be taken into consideration (34).

Events in the PLC-IP3-Ca^{2+} pathway are similar to the AC-cAMP-PKA pathway, except that $GTP_{\alpha q}$ binds the enzyme PLC instead of AC. PLC hydrolyzes the membrane lipid, phosphatidylinositol 4,5-biphosphate (PIP2), yielding two active products, inositol 1,4,5-triphosphate (IP3) and 1,2-diacylglycerol (DAG). IP3 leads to the release of stored intracellular Ca^{2+} ions from the endoplasmic reticulum, while DAG in the presence of Ca^{2+} ions increases the catalytic activity of protein kinase C (PKC) isoforms (2).

REGULATION OF LH RECEPTOR SIGNAL TRANSDUCTION

After binding ligand, LH receptors appear to remain in the plasma membrane and undergo time-dependent changes in their functional status. A number of events occur that reduces the receptor's responsiveness to continuous stimulation of additional hormone (78). This phenomenon, characteristic of GPCRs, is termed receptor desensitization (79) and occurs when receptors are unable to activate G proteins (80). Desensitization of LH receptors is initially characterized by uncoupling of the receptor from its signaling machinery, rather than by a decrease in receptor number (81).

Despite the continual presence of hormone, desensitization of the LH receptor is followed by a decrease in intracellular cAMP levels.

Desensitization is followed by endocytosis in a number of GPCRs, including the β_2-AR, which utilizes a clatherin-coated vesicle pathway. In addition, GPCRs may become sequestered, particularly after phosphorylation of the receptor, which may play a role in its reactivation along with dephosphorylation and recycling to the cell surface (82). Receptor sequestration is the movement of agonist-occupied receptor from a site where the receptor is accessible to ligand, to a location where the receptor is no longer accessible (82). Hormone-bound receptor complexes can also be internalized into the cell via an endosome, where fusion with a lysosome causes degradation of both the hormone and the receptor. In addition, some of the receptors can be recycled from the plasma membrane in a process known as ligand-mediated receptor downregulation (2). This mechanism, combined with receptor desensitization, may be critical regulatory steps in preventing target cells from becoming overstimulated by agonists.

RECEPTOR DESENSITIZATION

Desensitization of GPCRs

Receptor desensitization, also known as agonist-induced uncoupling, is a phenomenon in which a receptor is unable to bind ligand after subsequent hormone challenge. This is a common form of regulation in cell surface receptors, in which a change in receptor function occurs, while maintaining a constant number of receptors on the plasma membrane (79). Desensitization can be induced *in vitro* by binding hormone and then removing it with a low pH buffer. This protocol will effectively mimic *in vivo*

desensitization by uncoupling the receptor. It is important to note that receptors are functionally undamaged by this treatment and will still bind hormone; however their ability to activate the effector system and produce cAMP has been affected (78).

The β_2-AR has served as a model for GPCR desensitization. However it is becoming increasingly clear that the diversity of GPCR structure and function results in different patterns of intracellular signaling (79). Signal transduction of the β_2-AR is well-studied. It is known that the β_2-AR is desensitized within seconds to minutes and, after removal of ligand, the receptor recovers from the desensitized state in about 20 minutes (83). Like many GPCRs, desensitization of the β_2-AR depends on phosphorylation of the C-terminal domain and/or 3rd intracellular loop by two different classes of serine/threonine kinases, the second messenger dependent kinases such as PKA, and the G protein-coupled receptor kinases (GRK) (84). Phosphorylation of these residues promotes interaction of the receptor with regulatory molecules like β-arrestin (79).

Desensitization of the LH receptor

The LH receptor exhibits desensitization in response to treatment with saturating hormone concentrations. This has been observed *in vitro* in granulosa, luteal and Leydig cells (1). Desensitization of the LH receptor is very important in the physiology of the female. LH receptor desensitization occurs in ovarian follicles in response to the mid-cycle LH surge that promotes ovulation. It also occurs in corpora lutea in response to elevated levels of hCG during pregnancy (85). One hour following the removal of hormone, rebinding of LH or hCG causes no cAMP response (56). This is functionally

significant because decreased cAMP is a requirement for the initiation of oocyte meiosis. It appears that either inhibition or stimulation of mammalian oocyte maturation occurs depending on the pattern of exposure of the oocyte-cumulus cell complex to cAMP (86). Early work by Lindner and coworkers in 1977 demonstrated that cAMP participates in the transduction of a positive meiosis-inducing signal within the preovulatory ovarian follicle in response to gonadotropin stimulation (87). Dekel and colleagues later hypothesized that a constant exposure of the oocyte to elevated levels of cAMP maintains meiotic arrest, however a transient increase in cAMP may lead to the promotion of meiosis by triggering germinal vesicle breakdown (88).

Unlike the β_2-AR, desensitization of the LH receptor requires about one hour and takes several hours for the receptor to again become responsive to hormone (56). Little is known about the molecular mechanisms by which LH receptor desensitization occurs, but studies have focused on phosphorylation events in the C-terminal domain. Removal of the last 43 amino acid residues of the C-terminal domain has shown to slow desensitization (56). Removal or mutation of specific serine and/or threonine residues in the C-terminus abolished phosphorylation and demonstrated that phosphorylation was necessary, but not alone sufficient for hCG-induced uncoupling (69). This finding was determined because a delay in the time course of desensitization occurred, but no effect was observed on the magnitude of desensitization detected upon prolonged incubation with agonist (69). In contrast, work by Hunzicker-Dunn and colleagues on a cell-free model using porcine follicular membranes has shown that phosphorylation of the LH receptor is not necessary for LH receptor desensitization (89). In addition, these membranes were treated with antibodies against β-arrestin-1 as well as synthetic 3i

26

peptides which prevent desensitization, implicating roles for β-arrestin-1 and the 3rd intracellular loop in the LH receptor uncoupling mechanism (90, 91).

Role of Arrestins in Desensitization

One of the few molecules identified in LH receptor desensitization is β-arrestin-1, also known as arrestin 2. Arrestins are a family of proteins named for their ability to "arrest" signal transduction. They act by sterically hindering the ability of the receptor to interact with G proteins, thereby uncoupling the receptor from molecules involved in signaling (83). β-arrestin-1 is a member of the family of arrestins that includes visual arrestin which are expressed ubiquitously in all cells and function in desensitization of most of the GPCRs (92). It is well-known that the binding of β-arrestin-1 to phosphorylated G protein-coupled receptors interferes with the receptors' ability to interact with G proteins and therefore terminates signaling (83). GPCRs are the most important target of clinically-used drugs and, with the recent discovery of β-arrestin-mediated signalling, a class of novel therapeutic agents termed "super-receptor blockers" has been suggested (51).

It has been reported that preovulatory porcine follicular membranes contain membrane-associated β-arrestin-1, which selectively binds to the third intracellular loop (3i) of the LH receptor following receptor activation (91). As in other GPCRs, it is the binding of β-arrestins to cytoplasmic domains of the receptor that leads to LH receptor uncoupling. Mukherjee and colleagues found that LH receptor desensitization is blocked when monoclonal arrestin antibodies that recognize common epitopes on all arrestins are added to membrane preparations (91). The addition of a synthetic peptide

27

corresponding to the antibody-binding site on β-arrestin-1 effectively reverses this desensitization. It was also determined that LH receptor desensitization depends on the presence of GTP, and that GTP attributes to the binding of β-arrestin-1 to the 3i loop of the LH receptor by an unknown mechanism (91).

Role of ARF6 and ARNO in LH Receptor Desensitization

With β-arrestin-1 identified as the primary molecule responsible for desensitization of the LH receptor, discovering mechanisms that regulate the availability of β-arrestin-1 has become a priority for better understanding desensitization of all GPCRs. Using the porcine follicular membrane model, Mukherjee and colleagues identified a highly expressed, ubiquitous membrane-localized small G protein called ADP ribosylation factor 6 (ARF6) as a protein whose activation state is regulated by the LH receptor (93). ARF6 is a monomeric G protein that functions in regulating the availability of β-arrestin-1. ARF6 cycles between a GDP-bound inactive state and a GTP-bound active state. A class of ARF nucleotide exchange factors called ARNO catalyzes the release of GDP by ARF6. It is believed that β-arrestin-1 is bound to ARF6 when ARF6 is in the GDP-bound inactive state. As illustrated in Figure 5, when ARF6 becomes activated, β-arrestin-1 is released and is free to bind the LH receptor thereby promoting desensitization (93). It is particularly interesting to ask whether ARF6 is unique to LH receptor desensitization, or whether it plays a more universal role in desensitization and perhaps in the internalization of GPCRs.
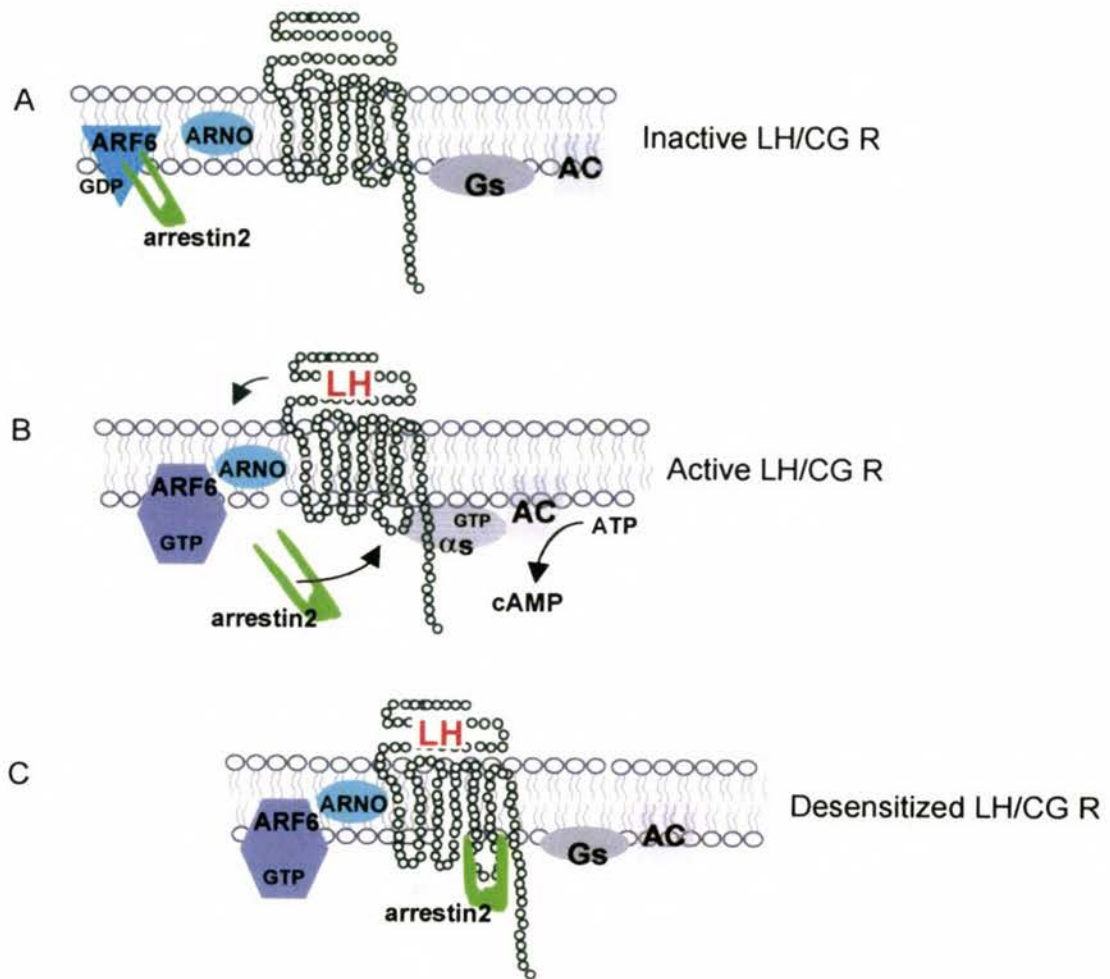
Figure 5: Model of LH receptor desensitization. Panel (A) shows the docking of arrestin 2 (β-arrestin-1) in association with inactive ARF6$_{GDP}$ at a membrane location away from the inactive receptor. Activation of the LH receptor upon agonist binding promotes activation of ARF6 and therefore liberates arrestin 2 (Panel B). ARNO promotes GDP release from ARF6 in response to LH receptor activation. In Panel (C), arrestin 2 binds to the 3i loop of the active receptor and mediates desensitization by interfering with the receptor's ability to activate G$_s$ (93).

(Adapted from Hunzicker-Dunn M et al., 2002 *FEBS* 521:3-8)

Biophysical Studies of LH Receptor Desensitization

Aggregation of LH receptors following binding of hormone has been widely reported. Early studies by Luborsky and colleagues using electron microscopy demonstrated the presence of small groups or microaggregates of LH receptors on the surface of rat luteal cells following exposure to high concentrations of ovine LH (94). In addition, immunofluorescence studies of the LH receptor on rat granulosa cells by Amsterdam et al. demonstrated the formation of large, punctate structures on the cell membrane following hCG treatment (95). Interestingly, larger clusters of LH receptors were observed on the cell surface following prolonged exposure to hCG (up to 4 hours) that coincided with a diminished cAMP response after the addition of fresh hormone.

Hunzicker-Dunn and colleagues performed unique studies utilizing a cell-free model to compare the membrane organization of actively signaling LH receptors that cannot undergo desensitization, with that of desensitized receptors (90). Studying plasma membrane preparations offers the advantage of studying desensitization as an event that is distinctly different from that of receptor sequestration and internalization. To investigate the organization of LH receptors in the membrane during desensitization, they performed time-resolved phosphorescence anisotropy (TPA) on endogenous LH receptors in porcine follicular membranes. Desensitized LH receptors exhibited rotational correlation times approximately 3-fold slower than actively signaling LH receptors. This data suggests that desensitized LH receptors become organized into larger protein complexes following the molecular events that trigger desensitization. Desensitized LH receptors on follicular membranes were found to organize into large, microscopically-visible complexes exhibiting slow rotational diffusion. To determine if

30

desensitization was required for aggregation of LH receptors into these larger protein complexes, membranes were incubated with anti-arrestin antibodies or synthetic 3i peptides to prevent desensitization. Neutralizing anti-arrestin antibodies bind arrestin molecules, reducing the availability of arrestins to bind to LH receptors. Synthetic 3i peptide binds to the corresponding 3rd intracellular loop of the LH receptor, preventing arrestins from binding the receptor. Pretreatment of membranes with either anti-arrestin antibodies or the synthetic 3i peptide followed by treatment with hCG and GTP resulted in faster rotational diffusion of the LH receptor. The rotational diffusion times of these receptors were equivalent to those of actively signaling LH receptors. These results indicate that inclusion of the LH receptor into larger, slower rotating complexes is dependent on desensitization (90).

To assess self-association of LH receptors during desensitization, Horvat et al. performed fluorescence resonance energy transfer (FRET) experiments between FITC- and TrITC-derived hCG bound to active or to desensitized LH receptors (96). FRET experiments allow further investigation into whether receptors are present as monomers or organized into dimers or oligomers in the large complexes that form during desensitization. Although there was measurable energy transfer between active receptors, desensitized LH receptors exhibited a 2.4-fold increase in FRET, indicating that there were more self-associated receptors in the large receptor complexes formed during LH receptor desensitization. This study suggests that actively signaling LH receptors are self-associated, and convert to a state of further self-association into receptor oligomers that are contained in large, higher-ordered structures containing β-arrestin-1 molecules.

Perhaps binding of β-arrestin-1 to the 3i loop of the receptor leads to oligomerization of LH receptors and clustering into large, slowly diffusing structures.

GPCR OLIGOMERIZATION

The ability of membrane proteins such as tyrosine-kinase receptors to form dimers or higher-ordered oligomers is widely accepted. Receptor tyrosine-kinases are activated by ligand-induced dimerization. The functional significance of clustered receptors was first hypothesized by Agnati and colleagues in 1982. They hypothesized that islands or clusters of receptors are capable of interacting and may be involved in synaptic plasticity contributing to memory (97). Early techniques such as radiation inactivation, photo-affinity labeling, crosslinking, and gel filtration experiments have supported the idea that GPCRs also form higher-ordered structures (98). More recently, domain-swapping experiments utilizing a number of GPCR types have provided clues about how GPCRs form dimers and oligomers. In addition to homodimers of a given GPCR, specific heterodimerization between distinct GPCRs has also been documented.

In a classical study by Maggio et al., two chimeric GPCRs – one containing the first five TM domains of the α2-adrenergic receptor and the last two TM domains of the M3 muscarinic acetylcholine receptor, and the other vice versa – resulted in partial restoration of binding for both receptors (99). This and similar studies of mutant GPCRs led to the "domain-swapping" model of dimerization, where "two independent folding units of the receptor separate and recombine between the two protomers of the dimer" (54). The folding units are believed to be made up from the first five and the last

two TM domains, connected by the third intracellular loop which serves as a "hinge" (100). However, additional studies investigating GPCR dimerization such as co-expression of V2 vasopressin receptors, and D_2 dopamine mutant receptors did not exhibit functional rescue (101, 102). Instead their behavior supports the notion of contact dimerization, where GPCRs need to come into direct contact with each other perhaps through using interaction sites on the exterior of the TM domains such as a disulfide bond (54). Thus early work examining GPCR oligomerization seemed to depend on the type of GPCR in question.

Today, co-immunoprecipitation is a commonly used biochemical technique used in identifying GPCR oligomerization, indicating both the homo- and hetero-oligomerization of different GPCRs. Co-immunoprecipitation was first applied to studying receptor dimerization of β_2-adrenergic receptors, which were tagged with influenza hemagglutinin and myc-tags and co-expressed in Sf9 cells (103). Co-immunoprecipitation is performed with cells expressing two receptors, where the cells are solubilized and the lysate is incubated with an antibody directed against one of the receptors or against the receptor's epitope tag (54). The complex is then bound to a medium, electrophoresed, blotted and visualized using an antibody against the other receptor of interest or its epitope tag (54). There are a number of drawbacks for using co-immunoprecipitation to detect the oligomeric state of receptors. For example, glycosylation of GPCRs does not allow the proper estimation of the molecular weight of the receptor, as interacting GPCRs are detected as higher molecular weight complexes that may have formed *in vivo*. In addition, lysis and solubilization steps indicate that receptor interactions cannot be studied in living cells. The hydrophobic nature of GPCR

7 TM domains can lead to the GPCRs forming aggregates during solubilization, which depends on the detergent concentration and lysis conditions. Another drawback of co-immunoprecipiation is the possibility of overexpressing receptors. This can possibly be avoided by using cell lines that stably express receptors at a low level (54). In conclusion, additional methods should be used to verify any interactions detected in co-immunoprecipitation experiments.

In recent years, the question of whether members of the large, functionally-diverse family of GPCRs can oligomerize has produced conflicting data. A central question is whether oligomerization is fundamentally important for all GPCRs, and whether GPCRs exist as homo- or heterodimeric or oligomeric complexes in their resting states. In addition, it is unclear when and if they form higher-ordered complexes during receptor activation by ligand, when being trafficked to the cell surface, when internalized, and when inhibited such as in a desensitized state (54). This is particularly interesting in the case of the LH receptor, which is desensitized for uniquely long times where the receptor remains clustered into higher-ordered structures for extended periods of time.

GPCR oligomerization represents a new shift in paradigm for GPCR signal transduction mechanisms, and suggests the need for a reevaluation of how ligands, hormones, neurotransmitters and other pharmacological ligands act on GPCRs (54). The advent of biophysical techniques such as resonance energy transfer (RET) has revolutionized the study of receptor oligomerization and should continue to reveal clues about the functional importance of GPCR oligomerization (54). RET methods including fluorescence imaging and bioluminescence resonance energy transfer (BRET) are able

to sensitively detect protein-protein interactions in *live* cells, allowing us to monitor dynamic properties of GPCR complexes (104).

STRUCTURE AND ORGANIZATION OF THE PLASMA MEMBRANE

The Two-Dimensional Fluid Mosaic Model

The motion of a membrane protein such as the LH receptor depends on a number of factors, including its interactions with other molecules and with its environment, namely the plasma membrane. In 1972 Singer and Nicolson proposed the "fluid mosaic model" of the structure of cell membranes – a mosaic structure of globular proteins with a phospholipid bilayer (105). The mosaic appears to be fluid or dynamic, and was thought of as a two-dimensional oriented viscous solution. The fluid mosaic model of membrane structure applies to all functional/biological membranes such as cell organelles like the mitochondria and chloroplast. Two kinds of noncovalent interactions are important in understanding the structure of the phospholipid bilayer, hydrophobic and hydrophilic. Hydrogen bonding and electrostatic interactions play a secondary role. A phospholipid bilayer consists of two layers of phospholipids, oriented in such a way that the ionic and polar head groups of the phospholipids make contact with the aqueous extracellular region. The organization of the bilayer is based on the fact that hydrophobic and hydrophilic interactions are maximized, achieving the lowest free energy state. Therefore nonpolar amino acid residues of the proteins and the fatty acid chains of the phospholipids should be sequestered from contact with the aqueous environment, while the ionic and polar head groups of the proteins, lipids and oligosaccharides should be in contact with aqueous solution.

Based on Singer and Nicolson's model, proteins and lipids in biological membranes should be capable of both lateral and rotational motions. One of the earliest experiments exemplifying the dynamic cell surface was performed by Frye and Edidin in 1970 who showed that membrane antigens are not stationary but instead can move within the plane of the membrane (106). In this experiment, mouse and human cells were fused with two different fluorescent labels (red or green) for membrane proteins. Colors were initially separate, but over time they mixed. Additionally, Loor and colleagues observed the ability of membrane proteins to move within the plasma membrane when they witnessed the aggregation of surface proteins on lymphocytes (107). They observed an initial uniform "ring" distribution of surface proteins on the surface of cells, followed by "patching" and "capping" after treating cells with concanavalin A, which crosslinked membrane glycoproteins. Experiments of this type performed in the last forty years have provided evidence that rearrangement of membrane proteins is an essential mechanism of cell regulation.

The ability of LH receptors to move into different areas of the plasma membrane agrees with the classic fluid mosaic model proposed by Singer in 1972, in which proteins and lipids are able to freely diffuse through the membrane (105). However, recent advances in light microscopy, live-cell imaging and single molecule techniques have shown that a certain degree of heterogeneity exists in the plasma membrane, suggesting a more complex organization (108). This is evident in the formation of specialized membrane domains and in the localization of signaling events which rely on spatiotemporal coordination of specific molecules. The diverse plasma membrane is

composed of a wide variety of lipid and protein components, as well as containing multiple classes of membrane domains.

Membrane Microdomains

Diffusion measurements of molecules in model membranes have been shown to be 50 times faster than that of the same molecules in live cells (109). This suggests that membranes are heterogeneous and contain multiple classes of microdomains that function in slowing the diffusion of membrane proteins and lipids (110). Examples of membrane microdomains that have been shown to play a role in GPCR signal transduction are clathrin-coated pits, membrane/lipid rafts, teteraspanins and caveolae, a subset of membrane rafts that are enriched in the protein caveolin (111).

A stoichiometric ratio of GPCR signaling components has been determined to be approximately 1:100:3 for GPCR that act via G_s and G_i to regulate the activity of AC (112). However, it is thought that membrane microdomains such as membrane rafts can further concentrate G proteins and downstream signaling molecules like AC in order to deliver a quick, efficient response to GPCR agonists (111). In addition, the role of the cytoskeleton has also been identified in slowing protein diffusion by a number of fluorescence recovery after photobleaching (FRAP) studies which report the presence of a mixture of micrometer-size protein-rich and protein-poor domains in the plasma membrane (113, 114). Cytoskeletal elements are thought to participate in forming the boundaries for some membrane domains that may confine membrane receptors and components involved in signal transduction. In addition, signaling molecules may also exhibit slow diffusion because they are anchored to the actin cytoskeleton (110).

Currently, a number of biophysical techniques such as FRAP, single particle tracking (SPT) and fluorescence correlation spectroscopy (FCS) are being used to characterize properties of dynamic membrane microdomains, particularly membrane rafts, through measurements of protein and lipid diffusion (110).

Membrane Rafts

Membrane rafts are specialized membrane microdomains composed of dynamic clusters of sphingolipids, cholesterol and GPI-anchored proteins, as well as a variety of transmembrane proteins located in the outer leaflet of the lipid bilayer of the plasma membrane (Figure 6) (115). The special lipid composition in rafts creates regions of the membrane that have greater order or less fluidity than more disordered portions of the membrane with less densely packed phospholipids (116). Because rafts are insoluble in the detergent Triton X-100 at 4°C, they tend to float to a low density during gradient centrifugation (115). This property makes rafts and raft-associated proteins easy to isolate biochemically. Membrane rafts were first described by Brown and Rose for sorting GPI-anchored proteins and glycosphingolipids to the apical surface of polarized epithelial cells (117-119). Fractionating membranes treated with detergent resulted in the isolation of GPI in membrane fractions that were enriched in sphingolipids (119). These membrane fractions were termed detergent-resistant membrane domains, or DRMs. Simons and Ikonen first described "functional rafts" as detergent-insoluble, glycolipid-enriched complexes (DIGs) (115). More recently, a consensus definition of membrane rafts has emerged that defines rafts as "small (10-200 nm), heterogeneous, highly dynamic, sterol- and sphingolipid-enriched domains that

38
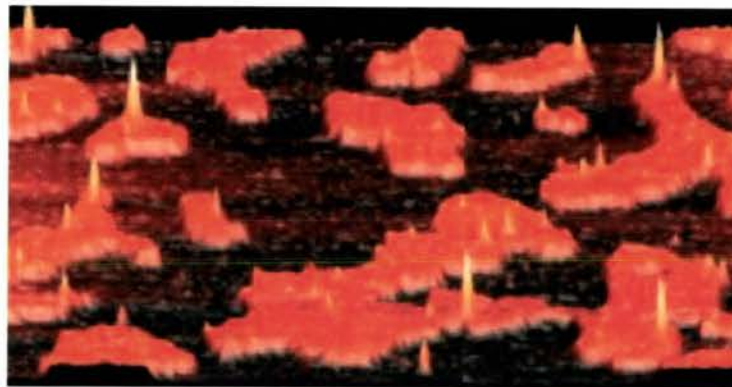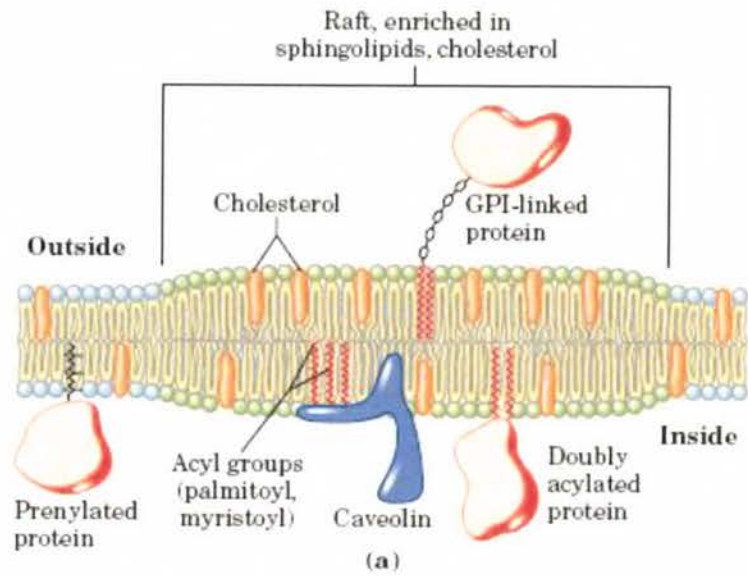
Figure 6: Panel (a) identifies components of membrane rafts in the plasma membrane. Panel (b) demonstrates raft regions visualized by atomic force microscopy. Rafts protrude from the lipid bilayer and sharp peaks within rafts represent GPI-linked proteins (120).

(Adapted from Saslowsky DE et al., 2002 *J Biol Chem* 277(30): 26966-26970)

compartmentalize cellular processes;" in addition, "small rafts can sometimes be stabilized to form larger platforms through protein-protein and protein-lipid interactions" (111).

To study the functional significance of cellular compartments such as membrane rafts or caveolae in signal transduction, biochemical approaches such as cell fractionation techniques have been used extensively. There are four general types of cell fractionation methods (121). The first and most commonly used method takes advantage of the detergent-insolubility and light buoyant density of rafts on sucrose gradients. Triton X-100 is often used as the detergent that can be used to isolate detergent-insoluble light membrane fractions from either isolated plasma membrane or from the whole cell. The second method uses 500 mM sodium carbonate at pH 11 in place of Triton X-100. The third method uses sonication to break apart isolated plasma membrane into small pieces with separation based on their buoyant density. The fourth method uses cationized silica to purify rafts from isolated plasma membranes by homogenization, density gradient centrifugation and immunoadsorption. It should be noted that cell fractionation methods do *not* result in the isolation of "pure" individual compartments and each method does not necessarily produce the same fraction of membranes. This is important in studying aspects of signal transduction.

Membrane rafts are of particular interest because they can limit the lateral movement of specific membrane proteins (122). It has been suggested that rafts serve as signaling platforms which function in concentrating signaling molecules necessary for productive ligand-mediated signal transduction (122). It is well-documented that a number of GPCRs, including the β_2-AR, M3 muscarinic, and delta opioid receptors

move into rafts upon agonist binding during signal transduction. However, some GPCRs localize in membrane rafts *prior* to agonist exposure, and yet others appear to *exit* rafts after binding agonist, perhaps as a prelude to receptor internalization/endocytosis and desensitization (111). In addition, rafts on certain cell types have been shown to contain high concentrations of proteins needed for cell signaling, such as G proteins (123) and AC (124). One example comes from Baird and colleagues, who demonstrated that native, monomeric type I Fcε receptors (FcεRI) occupied by IgE are primarily localized within membrane regions referred to as the bulk plasma membrane (125). However, after binding antigen by IgE, approximately 50% of the total population of receptors was found to localize in membrane fractions containing membrane rafts. These isolated membrane structures also contained heterotrimeric G proteins G_s and G_i as well as glycosylphosphatidylinositol-(GPI)-anchored membrane proteins (123, 126). In addition, the role of lipid modification of proteins, such as palmitoylation and myristoylation has been determined to be important in the localization of G protein signaling components to rafts (111). Finally, it has been demonstrated that the interaction of cytoskeletal components with membrane rafts/caveolae may regulate downstream signaling components. For example, Head and colleagues disrupted membrane rafts using methyl-β-cyclodextrin, a cholesterol sequestering agent, colchicine, a microtubule disruptor, or cytochalasin D, a microfilament disruptor, and found that AC relocated to non-buoyant membrane fractions while generating an increase in β-AR-agonist-stimulated cAMP (127).

It is thought that if rafts exist *in vivo* they are probably small and highly dynamic, therefore biophysical techniques may be more beneficial in understanding their dynamic

41

nature than current biochemical approaches. For example experiments investigating the large-scale movements of rafts can be performed, as well as using techniques to compare the properties of "raft" and "non-raft" markers. One of the most studied markers of membrane rafts is the cholera toxin B subunit, which can be labeled with fluorescent GM1. Unfortunately, visualizing rafts has proven difficult and has revealed that clustering of raft molecules can be induced with the use of crosslinkers such as antibodies and fixatives, as well as by cooling to room temperature (128). It is suggested that rafts may be smaller than the optical diffraction limit of approximately 300 nm in resting cells (128). Single particle tracking has suggested that rafts range in size from 50-200 nm in diameter (129). An overwhelming problem with the existence of membrane microdomains, particularly of membrane rafts, is the lack of consensus in defining them. For example, future studies are needed to determine if membrane rafts are in fact small dynamic domains, or alternatively, a complex of slowly diffusing clusters of individual rafts (110).

The Compartmentalized Fluid Model

For 30 years, there have been two major problems regarding the Singer-Nicolson, two-dimensional fluid model of biological membranes. The first problem, already mentioned, is the observation that diffusion coefficients for both proteins and lipids in the plasma membrane are on the order of 5- to 50-fold smaller than diffusion coefficients measured in artificially reconstituted membranes or liposomes (128). The second problem is the observation of dramatically reduced diffusion coefficients when molecules such as membrane receptors form oligomers or enter large molecular

complexes. It appears that these membrane receptors become "temporarily immobilized." This behavior indicates that the plasma membrane cannot be considered a two-dimensional continuum fluid (128).

With the advent of high-speed single-molecule tracking pioneered by Kusumi and colleagues, tracking single molecules in the plasma membrane on live cells has led to a paradigm shift from the plasma membrane as a two-dimensional continuum model to a more accurate model called "the compartmentalized fluid model" (128). The compartmentalized fluid model attempts to explain the two major shortcomings of the Singer-Nicolson model. In this model, the plasma membrane is partitioned into submicron-sized compartments and both membrane proteins and lipids undergo "hop diffusion" over these compartments to access adjacent compartments. Therefore hop diffusion explains the slower diffusion rates of membrane molecules in the plasma membrane compared to those found in artificial membranes (128). Sako and Kusumi were the first to observe "hop diffusion" of membrane molecules when they used single particle tracking (SPT) to track the transmembrane proteins transferrin receptor and α2-macroglobulin receptor (130). To date, plasma membrane compartmentalization appears to be universal as it has been observed in a wide range of mammalian cell types, with compartment sizes varying from 30 nm to 230 nm. In addition, nearly all of the transmembrane proteins examined so far including a number of GPCRs have been shown to undergo hop diffusion.

The Membrane-Skeleton Fence Model and Oligomerization-induced Trapping

To determine what makes up the boundaries between compartments found in the plasma membrane, SPT studies were used to elucidate a "membrane-skeleton fence" or "membrane-skeleton corralling" model (128). In this model, illustrated in Figure 7, a membrane-skeleton fence functions to confine the movement of transmembrane proteins and to form membrane compartments (131). The fences are made up of actin microfilaments and form corrals that can separate membrane regions, restricting the movement of transmembrane proteins that are anchored to the inner leaflet (110).

The compartmentalized fluid model predicted by SPT studies can be further described by the observation of temporal corralling or "transient confinement" of transmembrane proteins (132). Partial disruption of the cytoskeleton with cytochalasin D affected the diffusion of membrane receptors that were labelled with ligand-bound gold particles (130). The transmembrane proteins that are directly anchored to the actin cytoskeleton form pickets along the fences like posts. Both the actin fence and the pickets can impede the movements of molecules in both leaflets of the lipid bilayer (133).

Recently, the relationship between membrane protein dynamics and actin-defined domains has been directly visualized. Andrews and colleagues examined FcεRI using quantum dot-labeled IgE simultaneously with GFP-tagged actin (134). They showed that the FcεRI-quantum dot diffusion was confined with actin-poor regions of the plasma membrane when they overlayed the trajectory of quantum dot-IgE-FcεRI complex on images of actin distribution. They also found that the location and the size of the actin fences underwent dynamic reorganization over time, in a matter of seconds.
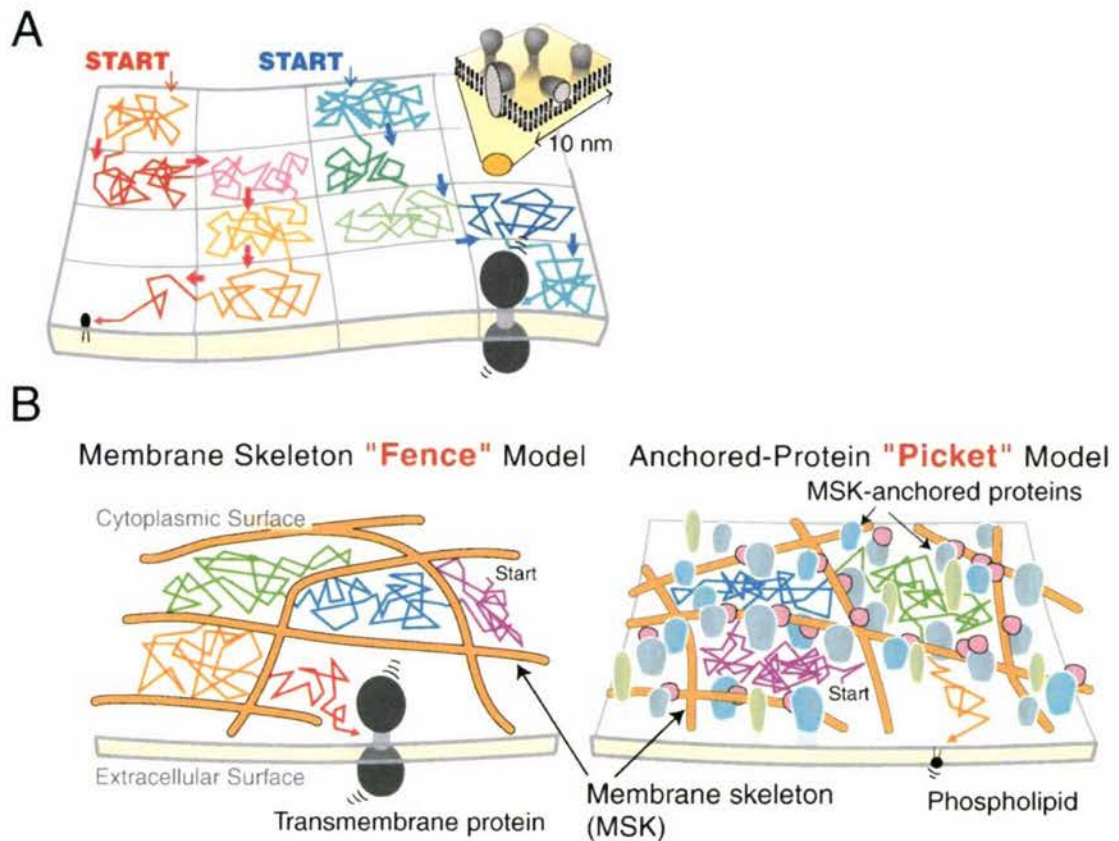
Figure 7: A paradigm shift for the concept of the plasma membrane structure: from the two-dimensional continuum fluid model (A) to the partitioned fluid model (B). Effects of the membrane-skeleton fence (MSK) and the anchored-protein "pickets" partition the plasma membrane into many small compartments with an average size between 30 nm and 230 nm (131).

(Adapted from Kusumi A et al., 2005 *Biochimica et Biophysica Acta* 1746: 234-251)

Additional studies of this kind will help to better describe the nature of the barriers of diffusion formed by the cytoskeleton.

A physiologically important consequence of membrane compartmentalization caused by membrane skeleton fences and anchored-protein pickets is oligomerization-induced trapping. This phenomenon is defined as the reduced diffusion of membrane molecules when they form oligomers or higher-ordered structures (128). Oligomerization-induced trapping might represent the temporary confinement of membrane receptors as well as signaling molecules. For example, studies using SPT to monitor diffusion properties of the Ras protein revealed that upon EGF or insulin activation, Ras was greatly immobilized and confined to small diameter compartments of 20 nm (135). This data supports the formation of signaling complexes composed of clusters of membrane receptors and signaling molecules as illustrated in Figure 8.
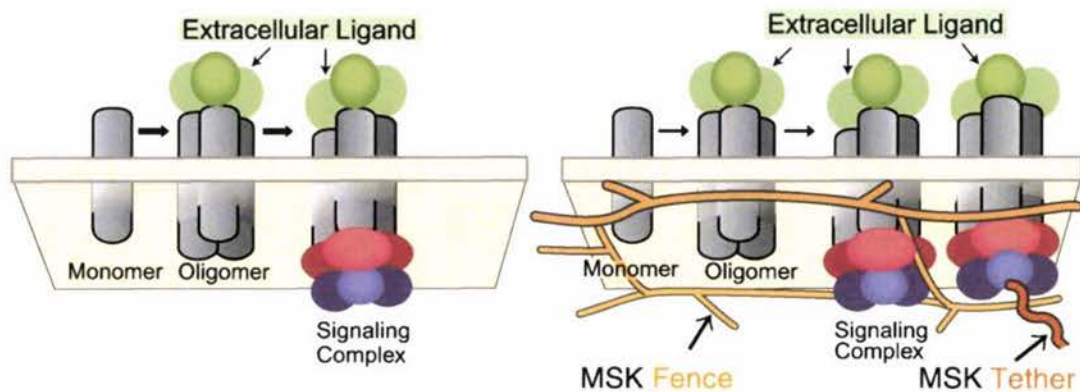
Figure 8: Oligomerization-induced trapping model for membrane molecules. Slowing or immobilization of membrane molecules may be induced upon oligomerization or the formation of greater molecular complexes. In addition, molecular complexes are more likely to be tethered to the membrane skeleton, perhaps temporarily, which also reduces . their overall diffusion rate (128).

(Adapted from Kusumi A et al., 2005 *Seminars in Immunology* 17:3-21)

Biological Significance of Compartmentalization of the Plasma Membrane

An intricate organization of the plasma membrane may be a requirement for signaling events, and specialized areas of the membrane may exist to concentrate signaling molecules to ensure efficient signal transduction. Alternatively, membrane compartments may function in sequestering membrane proteins leading to desensitization and subsequent internalization in order to prevent overstimulation of the receptor. Integral membrane proteins, such as LH receptors, exhibit lateral motions and self-association during and after cell signaling. These motions are dependent upon how proteins interact with the lipid bilayer, in addition to protein-protein interactions. Changes in lipid composition, clustering of receptors into large molecular weight complexes or associations between membrane proteins and the cytoskeleton will affect the movement of a particular protein within the plasma membrane, therefore affecting its function. Using biophysical methods and single molecule techniques in living cells will enhance our understanding of how the cell functions in signal transduction. Such methods will reveal how signaling molecules move around in the cell, how they transmit signal to the downstream effector molecules, and how molecules that associate with membrane rafts assemble/disassemble the raft structure (128).

STUDYING MEMBRANE PROTEIN DYNAMICS WITH BIOPHYSICAL TECHNIQUES

Biophysical techniques utilizing optical microscopy can be used to provide important information about the mobility, diffusion, concentration and aggregation state of proteins in the plasma membrane on live cells (136). Such methods include

fluorescence recovery after photobleaching (FRAP), fluorescence correlation spectroscopy (FCS), single particle tracking (SPT) and fluorescence resonance energy transfer (FRET).

Early work studying the lateral diffusion of membrane proteins occurred in 1976, when Axelrod and colleagues developed fluorescence photobleaching recovery (FPR), a method used to measure the lateral diffusion coefficient of membrane proteins (137). FPR, or FRAP, involves labeling a lipid or protein of interest with a fluorescent probe. A small patch of the membrane containing the fluorophores is then irreversibly bleached with a brief laser pulse at high intensity. Using low intensity laser excitation, the lateral diffusion of the unbleached fluorophores found outside the bleached site can be monitored, as can the lateral diffusion of the bleached molecules that move out of the region of interest. Plotting the change in fluorescence intensity in the region of interest versus time and fitting the curve to an appropriate equation yields the average rate of diffusion of the membrane molecule of interest. FRAP also yields the mobile fraction (M_f) of a membrane protein by determining the percentage of the recovered fluorescence in the region of interest, compared to the fluorescence lipid analogs (110).

Alternatively, a more recent ensemble method called fluorescence correlation spectroscopy (FCS) can be used to characterize the dynamics of fluorescent-labeled molecules. FCS measures the fluctuations of photons arising from fluorescent molecules contained within a small three-dimensional excitation volume over time (110). Constant illumination at the excitation wavelength of the fluorophore in a fixed beam waist size allows changes in emitted photons to be measured as a function of time (110).

The fluctuations in the fluorescence light are detected and analyzed in real-time using a signal autocorrelator (136).

Single Particle Tracking

Single particle tracking (SPT) is a method that is becoming widely available for examining the interactions of individual molecules on the cell surface. These methods include single fluorescent molecule video imaging (SFVI) using fluorescent probes, SPT using colloidal-gold probes, and optical tracking (128). In the experiments performed on LH receptors, large gold particles (30-40 nm) were used as probes for labeling the receptors on the surface of living cells and imaged using light microscopy. In particular, 40 nm gold particles can be attached to single lipid or protein molecules on the cell surface and particle Brownian motion can be recorded by light microscopy. Although the particle image is 300 nm in diameter, its center can be tracked to ± 5 nm, making SPT a very precise technique.

Colloidal gold was first introduced by Faulk and Taylor in 1971 when they used their "immunocolloid method" to study the distribution of antigens on cell surfaces by electron microscopy (138). The electron-dense colloidal gold particles had previously proven to be excellent markers for transmission electron microscopy by Feldherr and Marshall (139). Colloidal gold is a valuable tool in immunocytochemistry because it will stably and rapidly adsorb proteins without changing their biological activities (140). Colloidal gold particles carry a net negative charge, therefore positively charged proteins in solution will form complexes after mixing with colloidal gold particles by electrostatic interactions (141). Gold markers can be prepared in a size range of 5-150 nm, and the

50

interaction of gold and protein is influenced by factors such as ionic concentration, pH and protein concentration (142).

Single particle tracking is a novel biophysical technique that offers numerous advantages over other current light microscope techniques for evaluating protein diffusion (143). Single particle tracking allows us to measure the individual trajectories of a particle and to resolve the modes of motion of individual molecules (108). The trajectories resulting from SPT experiments are used to make plots of the mean square displacement (MSD) of the diffusing receptor versus time. The MSD is a measure of the average distance travelled by the particle in a given time period (136). The shape of the MSD plot can be used to classify the different modes of diffusion. For example, free diffusion leads to a linear relationship between MSD and time, while confined diffusion results in a plateau curve. The MSD can be related to the diffusion coefficient (D) through these models by taking the slope of the plot (144). For SPT data of LH receptors presented here, the diffusion coefficient within a compartment was calculated from the first two points of the MSD vs. time plot as described by Daumas et al. (145) and is indicated as D_{0-1}. In addition, the diffusion coefficient within a compartment is calculated from compartment size (L_r) and particle residence time (t) as $D = L_r^2/4t$ as described by Saxton (144).

When compared with FRAP, the spatial resolution of single particle tracking is approximately two orders of magnitude higher than FRAP, and the minimum detectable diffusion coefficient is lowered by about two orders of magnitude (144). Single particle tracking yields valuable characteristics about the compartments that are accessed by individual membrane receptors. SPT can yield a single rate of diffusion representing one

51

molecule, unlike FRAP, which uses all of the diffusion coefficients for a given population of molecules.

Fluorescence Resonance Energy Transfer

Interactions between membrane receptors such as LH receptors can be evaluated using fluorescence resonance energy transfer (FRET), a biophysical technique including hetero-FRET and homo-FRET. The result of FRET indicates whether two molecules physically interact with each other and can be an accurate measurement at Angstrom distances. FRET reports proximity between molecules on a length scale of 1 to 10 nm (146). Importantly, FRET methods remain the only way to assess physical interactions between membrane receptors on viable cells.

The fundamental phenomenon of FRET is the transfer of excitation energy from a donor singlet excited state to an acceptor singlet ground state. During the fluorescence process, a photon of energy is supplied by an external source such as a laser and absorbed by the fluorophore. Different aspects of the transfer phenomenon give rise to multiple ways of observing or measuring FRET. For instance, energy transfer causes quenching of donor fluorescence and sensitized fluorescence of the acceptor. FRET is especially valuable in determining the oligomeric state of GPCRs during all stages of signal transduction. FRET between ligands is another way to measure GPCR oligomerization, where ligands are conjugated to fluorophores. This technique is particularly useful in studying interactions between endogenous receptors.

Hetero-FRET

Hetero-FRET refers to the FRET between two different fluorescent proteins such as cyan fluorescent protein (CFP) and yellow fluorescent protein (YFP). Cyan and

yellow variants of GFP make a good FRET pair since excitation of CFP at 440 nm does not excite YFP. Excitation of the fluorescence donor (CFP) leads to energy transfer to the fluorescence acceptor (YFP) and emission by the acceptor (YFP) when the donor-acceptor pair are in close proximity at distances of less than 100 Å (146).

Acceptor photobleaching is a method that can be used to image FRET between CFP and YFP. First the donor and acceptor are imaged separately before bleaching. Then YFP is photobleached for approximately 5 minutes. Finally CFP and YFP are imaged again. The intensity of the CFP signal before and after YFP photobleaching can be used to evaluate energy transfer efficiency (%E). %E is calculated as fluorescence of the donor after bleaching YFP, minus the fluorescence of the donor before bleaching YFP, divided by the donor fluorescence after bleaching, times 100. A diagram of this energy transfer method is illustrated in Figure 9.

$$\%E = [(D_{after} - D_{before}) / D_{after}] \times 100$$

Epac

Recently, FRET has been used to monitor real-time signaling events in live cells with a number of different FRET-based indicators. This technology has allowed monitoring of intracellular Ca^{2+}, kinase activities, protein-protein interactions, cAMP dynamics, and clustering in membrane rafts (147). An example of a FRET-based indicator is Epac, an *e*xchange *p*rotein *a*ctivated by *c*AMP. In Epac, FRET occurs between enhanced cyan (ECFP) and citrine fluorescent proteins. When Epac binds cAMP, a conformational change results in the separation of ECFP and citrine, resulting in a decrease in energy transfer efficiency (%E). Conversely, in the absence of cAMP, the fluorophores are in close enough proximity to transfer energy.

53
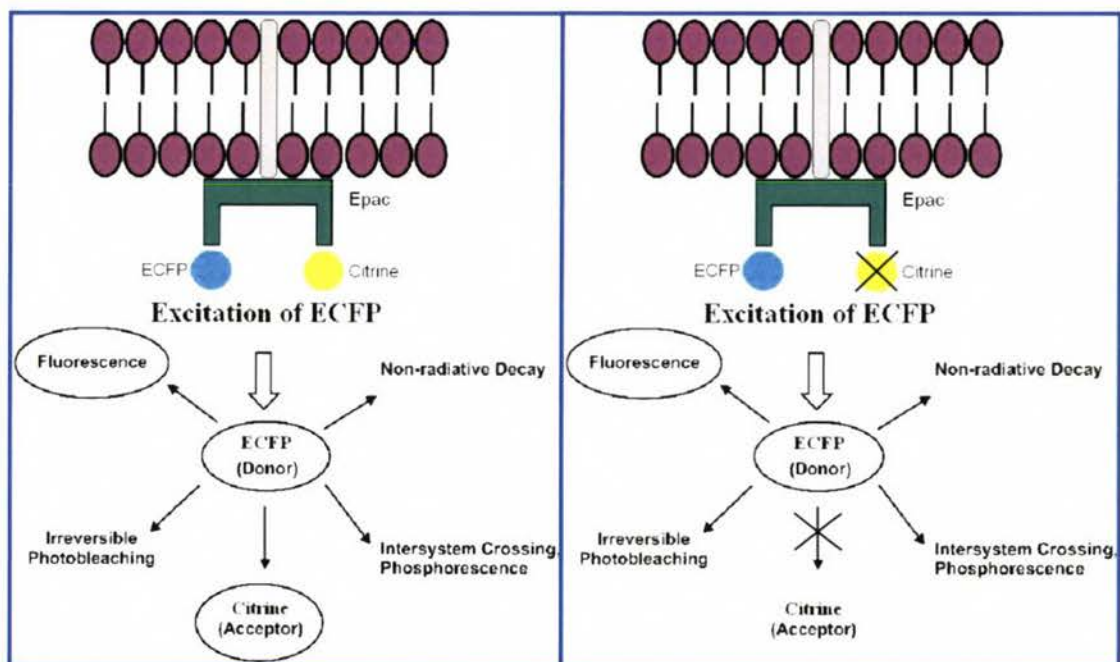
Figure 9: Fluorescence resonance energy transfer (FRET) between ECFP, the fluorescence donor, and citrine, the fluorescence acceptor, on Epac, an *exchange protein activated by cAMP*. The extent of energy transfer can be evaluated by acceptor photobleaching, comparing the ECFP fluorescence before and after irreversible photobleaching of the acceptor, citrine. Photobleaching of citrine results in an increase in fluorescence emission from ECFP, and the energy transfer phenomenon is represented by high values of energy transfer efficiency (%E).

Polarization homo-FRET

Homo-FRET is the energy transfer between *identical* donor and acceptor molecules, such as between two YFP molecules (148). This is possible because the only requirement for a FRET pair is that the acceptor and donor spectrums overlap (146). Therefore two of the same fluorophores can serve as both the donor and the acceptor. Homo-FRET is useful in tracking the movement of receptors on an individual cell when we also consider its effect on anisotropy, or the measure of the degree of polarization. Homo-FRET has a substantial effect on polarization.

As there are different ways of measuring energy transfer between molecules, homo-FRET utilizes the principle that sensitized emission is polarized along the same axis as exciting radiation. In the absence of energy transfer, the acceptor molecule emits with a polarization reflecting the orientation of the donor molecule (148). But if two molecules are in close enough proximity for energy transfer, the emitted energy is polarized like the donor fluorescence, but with much less anisotropy. The acceptor molecule is thereby orientated differently in the presence of FRET (148). If the polarization increases, the self-association decreases therefore suggesting that the receptor or protein is in a monomeric state. If polarization decreases then the receptor self-association has increased which suggests that the observed molecules exist as dimeric or oligomeric structures.

To measure anisotropy, fluorescence images are collected using polarizers to obtain parallel and perpendicular images simultaneously. Total intensity and fluorescence anisotropy (r) are calculated using the following formulae:

$$\text{Total Intensity} = I_{\parallel} + 2I_{\perp}$$

$$\text{Anisotropy (r)} = \frac{I_{\parallel} - I_{\perp}}{\boxed{I_{\parallel} + 2I_{\perp}}} \longleftarrow \text{Total Intensity/Emission}$$

where I is the intensity and $I_{\parallel}$ and $I_{\perp}$ are the parallel and perpendicular polarized emission components generated by excitation with linearly polarized light (148, 149).

Homo-FRET offers numerous advantages over other methods used for examining interactions between proteins on individual cells. Homo-FRET allows us to look at a single living cell using either confocal or wide-field microscopy. We can localize a signal to the cell surface as well as in the nucleus and in specific organelles in the cytoplasm. Compared to photobleaching and other methods of tracking molecules, it is the easiest to analyze and most importantly it has the fewest artifacts or false positives. Homo-FRET can be used to analyze the aggregation state of LH receptors during desensitization, revealing how receptor desensitization can affect the oligomeric state of GPCRs.

SUMMARY AND STATEMENT OF RESEARCH GOALS

A number of studies have reported that desensitized LH receptors remain self-associated and cluster into large, microscopically-visible structures that diffuse slowly in the membrane for several hours (90, 95, 96). Here, we used sucrose gradient ultracentrifugation and single particle tracking (SPT) to determine whether LH receptors are located in plasma membrane microdomains such as detergent-resistant membrane rafts, and in cytoskeletally-defined membrane compartments following desensitization. In addition, we used a novel polarization-based fluorescence resonance energy transfer approach known as homo-FRET to examine whether LH receptors are self-associated in the plasma membrane during desensitization. The following questions are addressed in Chapter II:

- Does LH receptor desensitization occur within specialized membrane microdomains such as membrane rafts?

- How is LH receptor lateral diffusion affected by desensitization?

- Are LH receptors aggregated during desensitization?

Our basic hypothesis is that LH receptors will aggregate, perhaps forming dimers or oligomers in response to hormone treatment and following desensitization by low pH buffer. Desensitized LH receptors will associate with membrane rafts and/or small membrane compartments detected by SPT. This may be a result of becoming confined and/or localized in rafts for signaling. Perhaps molecules such as β-arrestin, ARF6 and ARNO are localized in membrane rafts and/or small membrane

compartments, and their interactions with LH receptors ultimately lead to desensitization.

In an additional study, we used SPT to examine the effects of hormone concentration on receptor motions. We investigated the effects of increasing hormone concentrations on hCG-occupied LH receptors expressed on KGN human granulosa-like tumor cells, and receptors tagged using a form of hCG that lacks glycosylation. Additionally, we investigated whether extragonadal LH receptors endogenously expressed on a neuron-like cell line, M17 neuroblastoma cells, become confined within small membrane compartments following exposure to increasing concentrations of hormone. We also examined the effect of low amplitude hormone pulses typically seen in younger, premenopausal women on LH receptor compartmentalization. Finally, because slower lateral diffusion can result from self-association of LH receptors, we used homo-FRET to detect the oligomerization state of LH receptors in response to increasing concentrations of hormone. The following questions are addressed in Chapters III and IV:

- Does hormone concentration affect lateral diffusion characteristics of LH receptors during signal transduction?

- Are native, hormone-occupied LH receptors confined in small membrane compartments on KGN human granulosa-like tumor cells and M17 human neuroblastoma cells?

- How do non-functional hormone-receptor complexes behave when cells are exposed to hormone?

- How does hormone concentration affect the aggregation state of LH receptors?

58

CHAPTER II[1]

LUTEINIZING HORMONE RECEPTORS AGGREGATE AND LOCALIZE IN PLASMA MEMBRANE MICRODOMAINS FOLLOWING RECEPTOR DESENSITIZATION

INTRODUCTION

The desensitization of luteinizing hormone (LH) receptors is an important regulatory event in the reproductive function of mammals. After binding either glycoprotein hormone, LH or human chorionic gonadotropin (hCG), LH receptors become unresponsive to further stimulation by additional hormone. Receptor desensitization is a common feature shared by many G protein-coupled receptors (GPCRs) including the well-characterized β_2-adrenergic receptor (β_2-AR). However desensitization of the LH receptor has a unique time course. Desensitization requires about one hour and can last for several hours before internalization of the receptor occurs. This period of refractoriness is exemplified by the inability to generate a cyclic adenosine monophosphate (cAMP) second messenger response despite hormone

---

challenge (78). LH receptors become desensitized in ovarian follicles in response to the mid-cycle LH surge that promotes ovulation, and in human corpora lutea in response to elevated levels of hCG during pregnancy (85). Desensitization is followed by a decrease in intracellular cAMP levels that is functionally important for oocyte meiosis (86).

We previously examined self-association of LH receptors during desensitization using fluorescence resonance energy transfer (FRET) methods in two separate studies (96). The first experiment measured FRET between FITC- and TrITC-derived hCG bound to active or to desensitized LH receptors. Measurable energy transfer occurred between actively signaling receptors. However desensitized LH receptors exhibited a 2.4-fold increase in FRET compared to actively signaling receptors, indicating that there are more self-associated receptors in large receptor complexes formed during desensitization. Second, we examined self-association of desensitized LH receptors by measuring the energy transfer efficiency (%E) between CHO cells expressing GFP-LHR-wt and YFP-LHR-wt. Before hormone binding, there was no energy transfer between LH receptors, indicating that the receptors were not self-associated. After desensitization, the %E increased to 18% at 1 hour, and then steadily declined over the next 4 hours. Receptors were only hormone responsive again when energy transfer had reached 0%, which was not until 5 hours after desensitization. Our group also previously examined lateral diffusion of desensitized rat LH receptors coupled to green fluorescent protein (GFP-LHR-wt) using fluorescent photobleaching recovery (FPR) methods (96). After hormone binding and subsequent desensitization, LH receptors exhibited slower lateral diffusion compared to untreated receptors, and became laterally immobile within less than 1 hour. The lateral diffusion and fraction of mobile receptors

60

decreased over time, and only when receptors were again hormone responsive was the rate of lateral diffusion and the percent of mobile receptors comparable to untreated cells. Collectively, these findings suggest that hormone treatment followed by desensitization leads to LH receptor self-association and inclusion of receptors into large, laterally immobile structures. However it is not completely understood if LH receptors form dimers or oligomers following hormone binding and desensitization, or whether unoccupied receptors also dimerize prior to ligand binding.

In addition, we recently demonstrated that retention of LH receptors in membrane microdomains such as nanometer scale (129) detergent-resistant membrane rafts, or in larger membrane compartments detected by single particle tracking methods, is a characteristic of functional, hormone-occupied receptors (150). In the studies reported here, we examined whether desensitized LH receptors are also associated with membrane rafts during the time course of LH receptor desensitization. Membrane rafts are a type of specialized membrane microdomain that are enriched in cholesterol and sphingomyelin that are thought to function as signaling platforms (122). Rafts are of particular interest because they can limit the lateral movement of specific membrane proteins (122), perhaps contributing to the formation of large, slowly diffusing complexes that are found to contain desensitized receptors. We also examined, for the first time, the role of receptor confinement in micrometer scale membrane compartments (110) during desensitization as detected by single particle tracking (SPT) methods. SPT allows us to monitor the lateral diffusion of *individual* LH receptors on viable cells during desensitization. Finally, we investigated self-association of human LH receptors using a novel polarization-based FRET approach known as homo-FRET to

detect the oligomerization state of LH receptors following hormone binding and desensitization. We also present preliminary data from fluorescence correlation spectroscopy (FCS) experiments and photon counting histogram (PCH) analyses for determining the number of hLH-YFP receptors on CHO cells and detecting changes in receptor aggregation in response to increasing concentrations of hormone.

MATERIALS AND METHODS

Materials and cell culture

CHO (Chinese hamster ovary) cells were maintained in high glucose Dulbecco's Modification of Eagle's Medium (Mediatech, Inc., Manassas, VA) supplemented with 10% fetal bovine serum, 2 mM L-glutamine, 100 units of penicillin/ml, 100 µg streptomycin/ml (Gemini Bio-Products, Woodland, CA) and 1x MEM non-essential amino acid solution (Sigma-Aldrich, Inc., St. Louis, MO). All cells were grown in 5% CO_2 at 37°C in a humidified environment. Geneticin (G418 sulfate) was purchased from Mediatech, Inc. (Manassas, VA). Intact highly pure hCG antigen (Fitzgerald Industries, Inc., Concord, MA) was prepared in 1x PBS. Forskolin and the pFLAG vector were purchased from Sigma-Aldrich, Inc. (St. Louis, MO). The YFP vector was purchased from Clontech (Mountain View, CA). Monoclonal anti-FLAG antibody directed against the FLAG epitope tag was purchased from Sigma-Aldrich, Inc. (St. Louis, MO). 40 nm gold colloid was obtained from Ted Pella, Inc. (Redding, CA). Intracellular cAMP was measured using a TiterFluor Direct Cyclic AMP Enzyme Immunoassay Kit purchased from Assay Designs (Ann Arbor, MI).

Preparation and maintenance of CHO cell lines expressing FLAG or YFP tags

To determine whether LH receptors localized to membrane rafts during desensitization, stable CHO cell lines were prepared expressing human or rat LH receptor coupled to the FLAG epitope at the N-terminus of the receptor. Vectors were constructed for FLAG-tagged LH receptors as previously described (150). Selection of stable clones expressing FLAG-tagged receptors was based on the acquisition of geneticin (G418 sulfate) resistance. For FRET experiments, a stable CHO cell line expressing human LH receptors was coupled to enhanced yellow fluorescent protein (YFP) at the C-terminus as previously described (151). Clones expressing YFP were selected using fluorescence microscopy. Transfected cell lines were maintained in CHO cell medium supplemented with 400 μg/ml G418 sulfate (Mediatech, Inc., Manassas, VA).

LH receptor desensitization

We investigated LH receptor dynamics in the plasma membrane at hourly time points for 5 hours following desensitization. Desensitization can be induced *in vitro* by binding hormone and then removing it with a low pH buffer. This protocol will effectively mimic *in vivo* desensitization by uncoupling the receptor from its signal transduction machinery. It is important to note that although receptors are functionally undamaged by this treatment, are still present at the cell surface and will still bind hormone, their ability to activate the effector system has been affected (78). For experiments involving desensitization, CHO cells expressing LH receptors were incubated at 37°C for 30 minutes with 100 nM hCG and then treated as previously described for 2 to 5 minutes at 4°C with 50 mM glycine, 100 mM NaCl, pH 3.0, PBS to

63

remove bound hormone from the receptor (78). To evaluate the extent of LH receptor desensitization, levels of intracellular cAMP were assessed at 1-hour intervals following desensitization and binding of fresh hormone using a TiterFluor Direct Cyclic AMP Enzyme Immunoassay Kit (Assay Designs, Ann Arbor, MI).

Membrane preparations, raft isolation, and western blots

We investigated LH receptor interactions with membrane rafts at hourly time points for 5 hours following desensitization. To determine if there was association of LH receptors with membrane rafts, we isolated detergent-resistant membrane rafts using a discontinuous sucrose gradient and isopycnic ultracentrifugation. Approximately 50 x 10^6 CHO cells expressing LH receptor with a FLAG epitope at the N-terminus were treated with 100 nM hCG or PBS for 20 to 30 minutes at 37°C. Hormone-treated cells were then washed with fresh PBS to remove unbound hormone and subsequently treated with low pH buffer to remove bound hormone from the receptor. To isolate membrane rafts, CHO cells were washed twice with BSS and lysed for 5 minutes on ice in 1 ml of buffer containing 25 mM MES, 150 mM NaCl, 2 mM EDTA, 20% glycerol, 0.25% Triton-X 100, and protease inhibitors (Roche, Indianapolis, IN). A low-speed spin at 300 x g was performed to remove cell nuclei and large cell debris, leaving the supernatant containing the plasma membrane fragments. One ml of the supernatant was combined with 1 ml of 80% sucrose resulting in a 40% sucrose sample. A discontinuous sucrose gradient from 10% to 80% was prepared with the 40% sucrose layered in the middle. The sucrose gradient was placed into a Beckman SW-41 swinging bucket rotor and spun at 175,000 x g for 20 hours at 4°C in a Beckman Coulter Optima XL-80K Preparative

Ultracentrifuge. Eighteen equal fractions were collected from the top of the gradient downward. From each of the 18 sucrose fractions, 50 μl samples were combined with 95% SDS and 5% β-mercaptoethanol in a 1:1 ratio. SDS-PAGE was used to separate proteins from each sucrose fraction and proteins were then transferred to nitrocellulose membranes. FLAG-tagged LH receptors were identified with 30 μg of anti-FLAG M2 monoclonal antibody (Sigma-Aldrich, Inc., St. Louis, MO). The relative amount of receptor in each of the 18 fractions for all treatments was measured and quantified using a Bio-Rad GS-800 calibrated densitometer. The sucrose concentration in each fraction was determined using a Bausch and Lomb refractometer.

Single particle tracking of FLAG-tagged human LH receptors on individual CHO cells

We examined effects of desensitization on lateral dynamics and confinement of human LH receptors in the plasma membrane by tracking the movements of individual receptors with single particle tracking methods as described by Kusumi and colleagues (152). CHO cells expressing FLAG-tagged human LH receptors grown on coverslips placed in 60 mm^2 petri dishes were treated with 100 nM hCG or PBS for 30 minutes at 37°C. Cells with hormone-treated receptors were then washed with fresh PBS to remove unbound hormone and subsequently treated with low pH buffer to remove bound hormone from the receptor. To identify individual FLAG-tagged human LH receptors on CHO cells, we coupled monoclonal anti-FLAG antibody to 40 nm gold particles. Cells were labeled with gold-conjugated anti-FLAG antibody for 1 hour at 4°C. The minimal stabilizing protein concentration was determined to be 44 μg/ml and gold was conjugated

65

with the lowest possible concentration of anti-FLAG monoclonal antibody needed to stabilize the gold solution. The concentration of anti-FLAG antibody was not more than 1% of the concentration of total protein. One percent BSA in PBS was added to the solution until there were approximately 10 to 20 gold particles per cell. The binding specificity for FLAG-tagged receptors was tested by preincubating cells with a 10-fold excess of anti-FLAG antibody. After incubation with gold anti-FLAG antibody, no anti-FLAG gold particles were found on cells. Images for the appropriate controls were also taken and included unlabeled cells, untransfected CHO cells and cells labeled with gold conjugated only to the non-specific protein, BSA.

The individual gold particles were imaged by differential interference contrast with a 1.4 N.A. 63x oil objective in a Zeiss Axiovert 135 TV inverted microscope. Gold-tagged LH receptors were followed by video microscopy with a Dage IFG-300 camera and recorded for two minutes (3600 frames, 30 frames/second) at approximately 30 nm/pixel with Metamorph software from Universal Imaging. Trajectories of individual gold particles were measured over time and then sorted into various modes of motion in order to characterize the overall motion of a receptor. The trajectories for gold particles were segmented into compartments by calculation of statistical variance in particle position over time, a procedure that is similar to that developed by a number of investigators (144, 145, 153). The variance of a particle's position was calculated within windows of varying duration. These windows were translated along the particle trajectory, producing a variance plot that displays peaks indicative of inter-compartment boundaries. The results were analyzed using custom analysis programs to generate compartment size and residence time for each particle. Effective macroscopic diffusion

coefficients were calculated as the square of the compartment diagonal divided by four times the residence time in the compartment, also previously described (144).

Analysis of Polarization Homo-FRET

We investigated self-association of human LH receptors following hormone binding and subsequent desensitization using a novel FRET method termed polarization homo-FRET, or energy migration FRET (emFRET). Homo-FRET is energy transfer between identical donor and acceptor molecules, which can be assessed by imaging anisotropy, the measure of emission polarization. CHO cells stably expressing human LH receptors fused to YFP on their C-terminus were plated overnight in Willco 35 mm^2 #1.5 glass bottom petri dishes (Warner Instruments, Hamden, CT). A single cell sample was analyzed using an Olympus FV 300 confocal microscope with a polarizing beam splitter placed in front of the detection PMTs, allowing parallel and perpendicular fluorescence intensity to be recorded simultaneously. YFP was imaged with a blue argon laser and the appropriate barrier and dichroic filters were selected for 488 nm excitation. Cells that demonstrated a ring-like fluorescence at the cell's plasma membrane were selected for imaging. In addition, FRET measurements were made only on the fluorescence emitted from the ring-like image region containing LH receptors at the plasma membrane. A sequence of cell images was obtained as YFP was photobleached, with the goal of bleaching the fluorescence to about 10% of the initial average intensity within approximately 20 images. Each anisotropy measurement was taken with g-factor and background images, and imaging analysis was performed with custom analysis programs. Total intensity and fluorescence anisotropy (r) were

calculated using the following formulae: total intensity $= I_\parallel + 2I_\perp$; anisotropy $(r) = I_\parallel - I_\perp / I_\parallel + 2I_\perp$ where I is the intensity and $I_\parallel$ and $I_\perp$ are the parallel and perpendicular polarized emission components generated by excitation with linearly polarized light (148, 149).

Fluorescence Correlation Spectroscopy

We used fluorescence correlation spectroscopy (FCS) to measure the concentration of fluorophores and thereby quantify the number of YFP-tagged LH receptors per μm^2 on the stably transfected CHO hLHR YFP wt cell line used in homo-FRET experiments. CHO cells stably expressing human LH receptors fused to YFP on their C-terminus were plated overnight in Willco 35 mm^2 #1.5 glass bottom petri dishes and seeded to approximately 50% confluence. All samples were washed, treated and imaged in Tyrodes buffer with 0.2% BSA. Data was acquired using a modified Olympus microscope (T-2000 U). Sample excitation was achieved using the 514 line of an O.C. Argon Ion laser, a 520 dichroic mirror and 535LP filters. A Gaussian laser spot was positioned on the apical surface of sample cells using a 100x-oil APD's (SPCM-ARQ-14). Duel pseudo cross-correlations were calculated using an ALV-5000 correlation card and ALV software. The number of receptors per square μm was determined from the number of correlating particles in the illuminated area and the diameter of the laser beam at the cell surface.

Statistical Analysis of Data

Mean values ± S.E.M. or standard deviation are presented. Significance was assessed using the Student's t-test (unless otherwise noted) and p values are indicated ($p < 0.05$).

RESULTS

FLAG-LH receptors localize in detergent-resistant, low-density membrane rafts following desensitization

To determine whether desensitized FLAG-LH receptors associate with membrane rafts, we performed isopycnic ultracentrifugation to isolate rafts from the plasma membrane in sucrose gradients. As shown in Panel A of Figure 10, untreated human FLAG-LH receptors consistently appeared in high-density sucrose fractions 12 to 14. However over the 5 hour time course of desensitization, receptors appeared in detergent-resistant low-density sucrose fractions 5 to 10, containing sucrose concentrations ranging from approximately 21% to 39% (Figure 11). At 2 hours following desensitization, up to 70% of receptors were located in low-density sucrose fractions 1 to 10, where sucrose concentrations ranged from about 10% to 39%. As indicated in Table 1, a significant percent of human FLAG-LH receptors remained in low-density membrane fractions for several hours. Not until 5 hours later were over 90% percent of receptors found in the high-density fractions where untreated LH receptors were located. Similarly, when rat FLAG-LH receptors were examined for raft localization, there was a marked distribution of receptors in low-density sucrose fractions up to 2 hours following desensitization as shown in Figure 12. In these

experiments, desensitized rat FLAG-LH receptors primarily localized in fractions 3 to 10 containing sucrose concentrations ranging from approximately 14% to 39%.

Binding of hCG to FLAG-hLH receptors desensitizes the receptor for several hours

To evaluate the extent of LH receptor signaling during desensitization, levels of intracellular cAMP were assessed at 1-hour intervals following desensitization and brief hormone challenge. CHO cells expressing human FLAG-LH receptors were incubated with 100 nM hCG for 30 minutes at 37°C and then washed with a low pH buffer to remove the bound hormone as described in the Materials and Methods. At 1-hour intervals following removal of hormone, cells were challenged with 100 nM hCG for an additional 30 minutes at 37°C. As shown in Table 2, there was a 2- to 3-fold increase in cAMP in response to treatment with 100 nM hCG or 20 nM forskolin. However removal of the desensitizing hormone followed by brief hormone challenge resulted in no increase in cAMP over basal levels for 4 hours. After 5 hours, a response to hCG resulted in an increase in cAMP comparable to the cAMP response observed after initial exposure to hCG.

Single particle tracking of desensitized human FLAG-LH receptors demonstrates confinement of receptors in small membrane compartments

To assess the lateral dynamics of LH receptors during desensitization, we used single particle tracking methods to track the movements of single LH receptors on the plasma membrane of viable CHO cells. Representative trajectories from FLAG-tagged human LH receptors recorded for two minutes are presented in Figure 13. Receptors

desensitized by hCG became confined in small membrane compartments with an average diameter of 84 ± 12 nm. These compartments are significantly smaller than the 199 ± 17 nm diameter regions occupied by untreated receptors (Table 3). Desensitized receptors remained confined in small diameter compartments exhibiting slow lateral diffusion for 3 hours. In general, as receptors accessed increasingly larger compartments, their rate of diffusion (D) also increased (Figure 14). The average residence time of receptors within compartments and the number of compartments accessed by the receptor in two minutes did not significantly differ for untreated and desensitized receptors. However the rate of diffusion (D) for an individual receptor within each compartment was reduced by a factor of five for desensitized receptors.

Figure 15 displays the distribution of compartment sizes accessed by LH receptors at hourly time points of desensitization. Seventy two percent of desensitized LH receptors were confined in small compartments with a diameter of less than 100 nm at 1 hour following hormone treatment (Table 4). By 5 hours following hormone treatment, the majority of LH receptors exhibited unconfined lateral diffusion in large compartments typical of untreated cells.

Human LH receptors self-associate in response to hormone treatment and receptor desensitization

To analyze the self-association or aggregation state of human LH receptors in response to hormone treatment and initial desensitization, we performed homo-FRET experiments on CHO cells stably expressing human YFP-LH receptors. Homo-FRET was assessed by imaging anisotropy (r), a measure of emission polarization (Figure 16).

71

Photobleaching YFP irreversibly reduced the concentration of fluorophores capable of acting as acceptors, therefore energy transfer was indicated by a rise in FRET as bleaching proceeded (148). If receptors were associated, indicating energy transfer, then acceptor molecules were oriented different than donor molecules and anisotropy subsequently increased.

The data presented here indicates that desensitized LH receptors following 1 hour of hormone treatment exhibited a higher level of self-association than untreated LH receptors. As shown in Table 5, the difference in mean anisotropy for 10 cells following desensitization (0.0455) was larger than the difference in mean anisotropy for 10 untreated cells (0.0208), indicating a higher degree of aggregation of the desensitized receptors. Additionally, LH receptors exposed to 100 nM hCG for 30 minutes at 37°C exhibited a difference in mean anisotropy (0.0899) that was significantly different when compared to untreated receptors, and even greater than desensitized LH receptors.

In addition, FCS experiments were performed on the stably transfected CHO hLHR YFP cell line that was used in homo-FRET experiments. Figure 17 presents the number of CHO cells expressing varying numbers of receptors per μm^2. Importantly, the receptor numbers per cell were low, and overexpression of hLH-YFP receptors was not evident. Receptor overexpression is a potential problem in biophysical techniques used to assess receptor aggregation because artificial levels of receptor may induce interactions that would normally not occur in a physiological environment (54). A complementary method, a photon counting histogram (PCH) analysis, was also used to differentiate between species of similar diffusion coefficient through their molecular brightness. The PCH is particularly useful here because it can also resolve aggregation

through molecular species brightness levels. As shown in Figure 18, with increasing concentrations of hCG, molecular brightness increases, indicating further aggregation of human LH-YFP receptors.

DISCUSSION

In this work, we used biophysical methods to shed light on the nature of LH receptor desensitization, specifically examining the membrane organization during desensitization. We investigated the role of the plasma membrane in contributing to LH receptor desensitization – specifically whether receptor aggregation, confinement in small membrane compartments, and association with membrane rafts accompany desensitization. We found that individual human LH receptors are confined in small membrane compartments and localize in membrane rafts after desensitization. These receptors do not demonstrate signaling via cAMP while they are confined, suggesting that the microenvironment within these compartments may be different for desensitized versus actively signaling receptors. In addition, LH receptors appear to exhibit increased self-association following desensitization, either by transitioning from monomers to dimers/oligomers, or by forming larger aggregates of receptors. Membrane microdomains such as membrane rafts and the compartments detected by SPT may be important in allowing LH receptor self-association in areas where β-arrestin-1 and other proteins such as ARF6 and ARNO are found. These events could facilitate the function of LH receptor desensitization by helping to dampen the cAMP response at the plasma membrane.

Receptor desensitization is a common feature of GPCRs. However it is becoming increasingly clear that the diversity of GPCR structure and function results in different patterns of intracellular signaling, including different mechanisms of desensitization (79). The β_2-adrenergic receptor (β_2-AR) has served as a model for GPCR desensitization and its signal transduction mechanisms are well-studied. It is known that the β_2-AR is desensitized within seconds to minutes and, after removal of ligand, the receptor recovers from the desensitized state in about 20 minutes (83). Like many GPCRs, desensitization of the β_2-AR depends on phosphorylation of the C-terminal domain and/or 3rd intracellular loop by two different classes of serine/threonine kinases, the second messenger dependent kinases such as PKA, and the G protein-coupled receptor kinases (GRK) (84). It is well-documented in a number of GPCRs that phosphorylation of these residues promotes interaction of the receptor with regulatory molecules like β-arrestin that leads to desensitization of the receptor (79).

However LH receptor desensitization appears to have different mechanisms from other GPCRs. Of note, work by Hunzicker-Dunn and colleagues has shown that phosphorylation of the LH receptor is not necessary for receptor desensitization (89). In addition, aggregation of LH receptors following binding of hormone has been widely reported. Early studies by Luborsky and colleagues using electron microscopy demonstrated the presence of small groups or microaggregates of LH receptors on the surface of rat luteal cells following exposure to high concentrations of ovine LH (94). In addition, immunofluorescence studies of the LH receptor on rat granulosa cells by Amsterdam et al. demonstrated the formation of large, punctate structures on the cell membrane following hCG treatment (95). Interestingly, larger clusters of LH receptors

were observed on the cell surface following prolonged exposure to hCG (up to 4 hours) that coincided with a diminished cAMP response after the addition of fresh hormone. A number of biophysical studies investigating the organization of LH receptors in the plasma membrane during desensitization have revealed similar findings. Using time-resolved phosphorescence anisotropy (TPA) on porcine follicular membranes, Hunzicker-Dunn and colleagues observed that desensitized LH receptors organize into large complexes that exhibit rotational correlation times about 3-fold slower than actively signaling LH receptors (90), suggesting that desensitized receptors are present in even larger molecular complexes than active receptors. Conclusions from these studies indicate that organization of LH receptors into large clusters or aggregates in the plasma membrane may inactivate hormone-receptor complexes, thereby desensitizing the cell by interfering with receptor coupling to adenylate cyclase.

For the first time, we monitored the motions of individual desensitized LH receptors presumably located in large, microscopically-visible complexes containing multiple copies of receptors on the plasma membrane. The single particle tracking methods used here reveal that desensitized LH receptors display short-termed confined diffusion within membrane compartments, suggesting that the cytoskeleton plays a role in confining LH receptor movement according to Kusumi's membrane skeleton fence model (128). This idea, taken together with data from FRET experiments on desensitized LH receptors, suggests that oligomers of LH receptors may form a molecular complex that inevitably becomes temporarily immobilized (128). The 5-fold decrease in macroscopic diffusion coefficients that we observed between untreated and desensitized LH receptors reflects this proposed immobility. Oligomerization-induced trapping might be an

important regulatory mechanism in the desensitization of LH receptors. Temporarily confining LH receptors could potentially prevent receptors from associating with, or becoming segregated from, other signaling molecules in membrane microdomains (128). Furthermore, the microenvironment could promote desensitized LH receptors to interact with proteins involved in desensitization like β-arrestin-1, as well as small G protein-associated molecules like ARF6 and ARNO that are directly involved in regulating the release of β-arrestin-1 from the plasma membrane.

It is unknown whether desensitized LH receptors transition from monomers to dimers/oligomers, or alternatively, whether clusters of desensitized LH receptors form large aggregates of receptors on the cell surface. The homo-FRET results presented here are in agreement with those of our previous studies of desensitized LH receptors using conventional hetero-FRET methods, in which significant energy transfer occurred between desensitized LH receptors compared to untreated receptors (96). However, Segaloff and colleagues recently reported that transiently transfected human LH receptors constitutively self-associate in living cells using bioluminescence resonance energy transfer (BRET) techniques (154). Their data also suggests that human LH receptor dimers/oligomers are formed early in the biosynthetic pathway in the endoplasmic reticulum, and that they are not affected by hCG treatment. Here we have addressed these issues with homo-FRET and FCS techniques, in which we have shown that a stably transfected cell line consists of low levels of receptors per cell. The observed change in anisotropy with increasing hCG concentrations suggests receptor rearrangement, and the observed change in intensity of PCH from FCS studies suggests further aggregation of LH receptors in response to hormone.

Novel biophysical techniques such as single particle tracking (SPT) and polarization homo-FRET have served as powerful tools in the study of molecular interactions on the plasma membrane. These techniques can be widely applied to studying the desensitization of G protein-coupled receptors like the LH receptor. Future studies could include further investigating GPCR desensitization by using SPT on other GPCRs with unique characteristics such as another member of the rhodopsin class of GPCR, the GnRH receptor, which has a short 1 to 2 amino acid C-terminal tail and appears to be resistant to arrestin-dependent internalization and desensitization. The desensitization of GPCRs like the LH receptor is an important physiological feedback mechanism in many systems in addition to reproduction which protects against overstimulation of the receptor (79). Therefore it is essential to understand the molecular mechanisms of desensitization because of its contribution to the regulation of GPCR signaling. A better understanding of the mechanisms involved in signal transduction of GPCRs may lead to treatments for disease pathologies where receptor-mediated signal transduction is compromised.

Table 1: Distribution of human FLAG-LH receptors on CHO cells present in low- and high-density membrane fractions. Data shown are the mean ± S.E.M.

Treatment(s)	10.01-38.78% Sucrose (Fractions 1-10)	43.49-79.66% Sucrose (Fractions 11-18)	n
None	4 ± 1^a	96 ± 1	5
100 nM hCG, low pH buffer, 1 hour	46 ± 5^b	54 ± 5	5
100 nM hCG, low pH buffer, 2 hours	70 ± 17^b	30 ± 17	3
100 nM hCG, low pH buffer, 3 hours	48 ± 14^b	52 ± 14	3
100 nM hCG, low pH buffer, 4 hours	46 ± 3^b	54 ± 3	3
100 nM hCG, low pH buffer, 5 hours	9 ± 2^b	91 ± 2	4

a,b Values with different superscripts differ significantly ($p < 0.05$).

Table 2: cAMP responsiveness of cells expressing human FLAG-LH receptors. Data shown are the mean ± S.E.M for at least 2 experiments performed in triplicate.

Cell line	Treatment(s)	Fold increase over basal cAMP levels	cAMP conc (pmol/mL)	n
CHO hLHR FLAG	None	1.0^a	14 ± 2.7	8
CHO hLHR FLAG	100 nM hCG	2.2 ± 0.7^b	33 ± 14	5
CHO hLHR FLAG	20 nM forskolin	3.1 ± 0.5^b	49 ± 18	5
CHO hLHR FLAG	100 nM hCG, low pH buffer, 1 hour	1.0 ± 0.2^a	11 ± 2.4	6
CHO hLHR FLAG	100 nM hCG, low pH buffer, 2 hours	1.2 ± 0.4^a	6.9 ± 2.9	2
CHO hLHR FLAG	100 nM hCG, low pH buffer, 3 hours	0.4 ± 0.3^a	3.0 ± 0.7	3
CHO hLHR FLAG	100 nM hCG, low pH buffer, 4 hours	0.8 ± 0.7^a	3.6 ± 0.1	2
CHO hLHR FLAG	100 nM hCG, low pH buffer, 5 hours	2.6 ± 2.2^a	49 ± 46	6

a,b Values with different superscripts differ significantly ($p < 0.05$).

Table 3: Single particle tracking of human FLAG-LH receptors on individual CHO cells labeled with gold-conjugated anti-FLAG antibody. Data shown are the mean ± standard deviation; Compartment diameter is mean ± S.E.M.; a,b differ significantly (p<0.05).

Cell line	Treatment(s)	Number of of particles analyzed	Number of compartments/ 2 min trajectory	D_{0-1}[1] $(10^{-11}cm^2sec^{-1})$	$D = L_r^2/4t$ [2] $(10^{-11}cm^2sec^{-1})$	Time [3] (t) (sec)	Compartment [4] diameter (L_r) (nm)
CHO hLHR FLAG	None	20	5 ± 2	6.2 ± 2.6	0.87 ± 1.2	22 ± 15	199 ± 17[a]
CHO hLHR FLAG	100 nM hCG, low pH buffer, 1 hour	10	5 ± 2	2.2 ± 0.96	0.17 ± 0.18	19 ± 15	84 ± 12[b]
CHO hLHR FLAG	100 nM hCG, low pH buffer, 2 hours	10	6 ± 2	3.5 ± 1.5	0.22 ± 0.20	19 ± 12	97 ± 13[b]
CHO hLHR FLAG	100 nM hCG, low pH buffer, 3 hours	20	6 ± 2	3.4 ± 2.4	0.30 ± 0.35	18 ± 11	118 ± 13[b]
CHO hLHR FLAG	100nM hCG, low pH buffer, 4 hours	20	4 ± 2	3.6 ± 1.7	0.48 ± 0.71	23 ± 14	153 ± 15[b]
CHO hLHR FLAG	100nM hCG, low pH buffer, 5 hours	10	5 ± 2	4.0 ± 1.9	0.59 ± 0.78	20 ± 12	169 ± 22[a]

[1] D_{0-1}: Diffusion coefficient within compartment calculated from the first two points of MSD vs. time plot as described by Daumas et al. (145).
[2] D represents the diffusion coefficient within a compartment as calculated from compartment size (L_r) and particle residence time (t) as $D = L_r^2/4t$ as described by Saxton (144).
[3] Average particle residence time for residence within a compartment.
[4] The average diameter of an individual compartment was calculated as described by Daumas et al. (145) and Murase et al. (153).

Table 4: Percent of human FLAG-LH receptors present in membrane compartments of less than 100 nm and greater than 100 nm on CHO cells. Data shown are the mean ± standard deviation.

Treatment(s)	% hLHR in less than 100 nm compartments	% hLHR in greater than 100 nm compartments	n
None	12 ± 6^a	88 ± 6	20
100 nM hCG, low pH buffer, 1 hr	72 ± 8^b	28 ± 8	10
100 nM hCG, low pH buffer, 2 hrs	58 ± 10^b	42 ± 10	10
100 nM hCG, low pH buffer, 3 hrs	45 ± 9^b	55 ± 9	20
100 nM hCG, low pH buffer, 4 hrs	21 ± 8^b	79 ± 8	20
100 nM hCG, low pH buffer, 5 hrs	13 ± 7^a	87 ± 7	10

a,b Values with different superscripts differ significantly ($p < 0.05$).

Table 5: Homo-FRET summary of hormone-treated and desensitized human YFP-LH receptors expressed on CHO cells. Data shown are the mean ± S.E.M.

| Cell line | Treatment(s) | n | Mean Anisotropy | | |
			Before (r initial)	After (r final)	Difference (r final – r initial)
CHO hLHR YFP wt	None	10	0.188	0.208	0.0208 ± 0.005^a
CHO hLHR YFP wt	100 nM hCG	10	0.166	0.255	0.0899 ± 0.014^b
CHO hLHR YFP wt	100 nM hCG low pH buffer, 1 hr	10	0.179	0.224	0.0455 ± 0.014^a

a,b Values with different superscripts differ significantly ($p<0.05$).

A. human FLAG-LH receptor
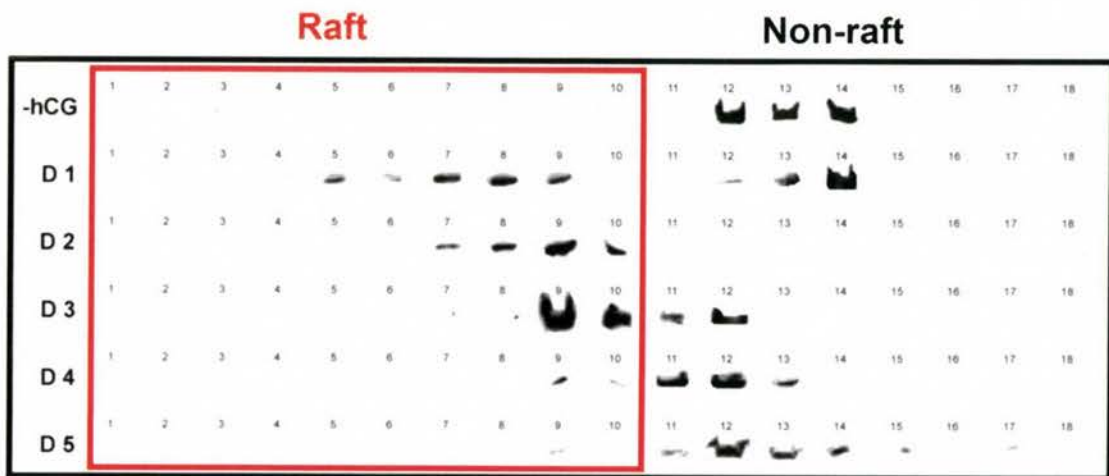
B. rat FLAG-LH receptor
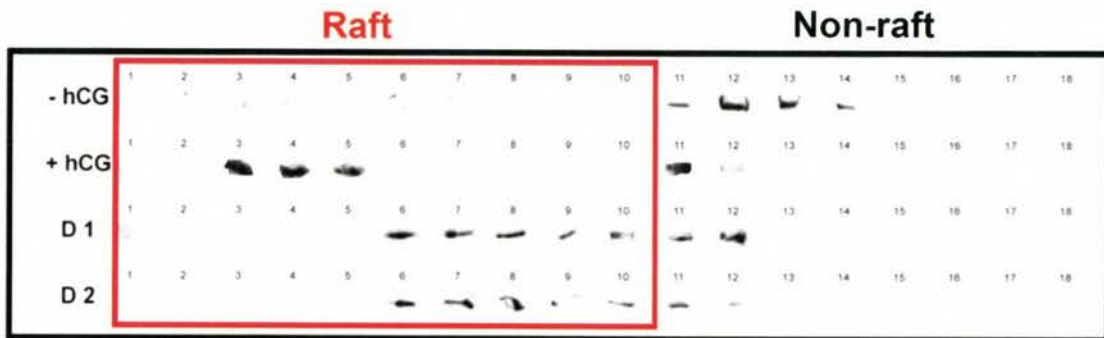
Figure 10: Representative western blots from CHO cells expressing human FLAG-LH receptors (Panel A) and rat FLAG-LH receptors (Panel B) after ultracentrifugation. Untreated LH receptors (- hCG), receptors treated with 100 nM hCG (+ hCG) and desensitized receptors examined at hourly time points (D1, D2, D3, D4, D5) are presented. Raft fractions are indicated as fractions 1 to 10 and contain sucrose concentrations of 10.01% to 38.78%. Non-raft fractions are indicated as fractions 11 to 18 and contain sucrose concentrations of 43.49% to 79.66%.
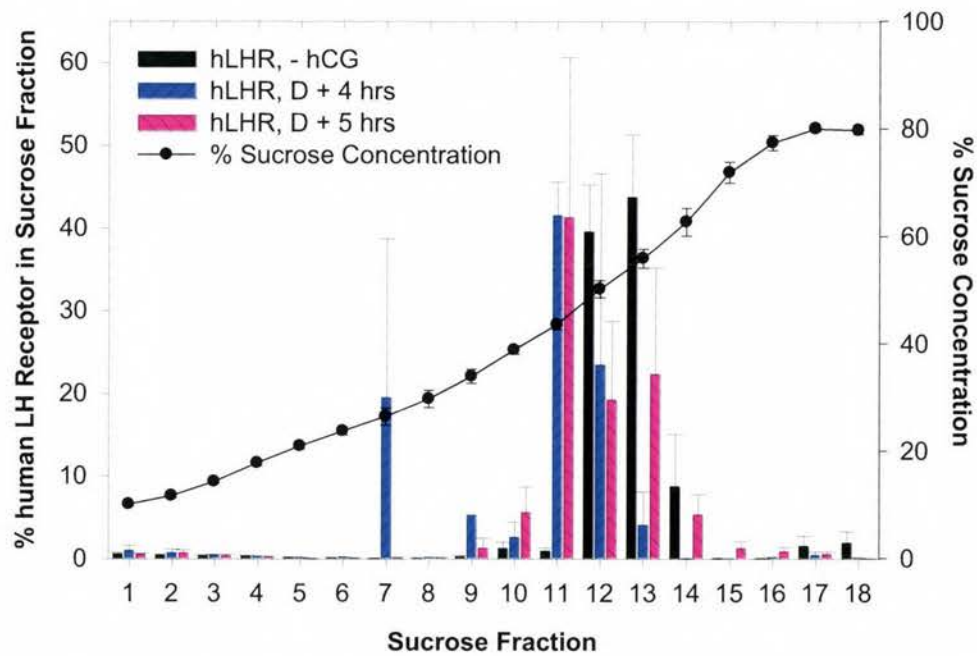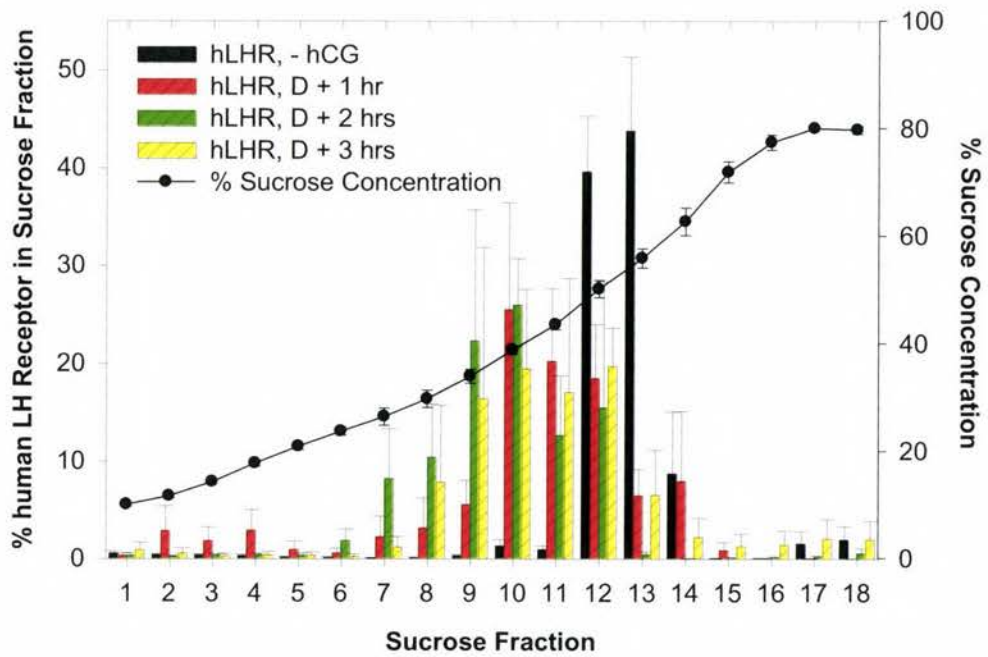
Figure 11: Analysis of western blots by densitometry. Data shown are the mean ± S.E.M. for at least 3 separate experiments examining raft association of human FLAG-LH receptors.
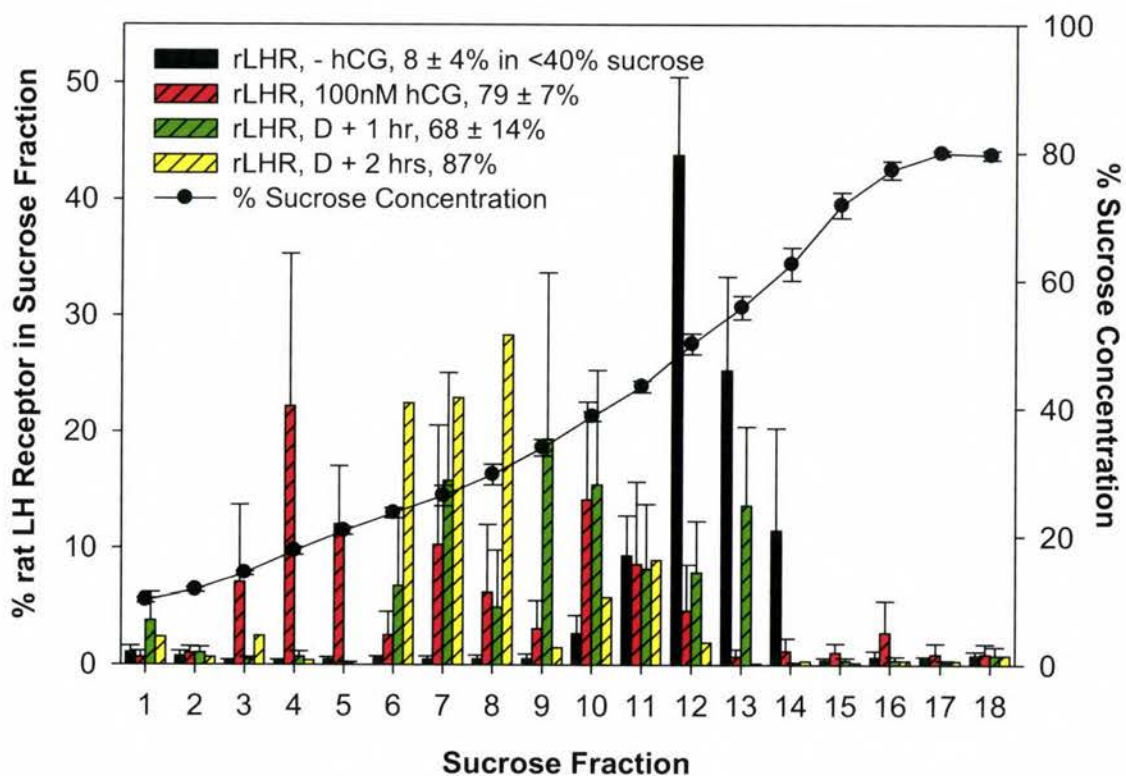
Figure 12: Analysis of western blots by densitometry for rat FLAG-LH receptors.

Data shown are the mean ± S.E.M for a minimum of 3 experiments (except D + 2 hrs, which indicates desensitized LH receptors analyzed at 2 hours following desensitization).
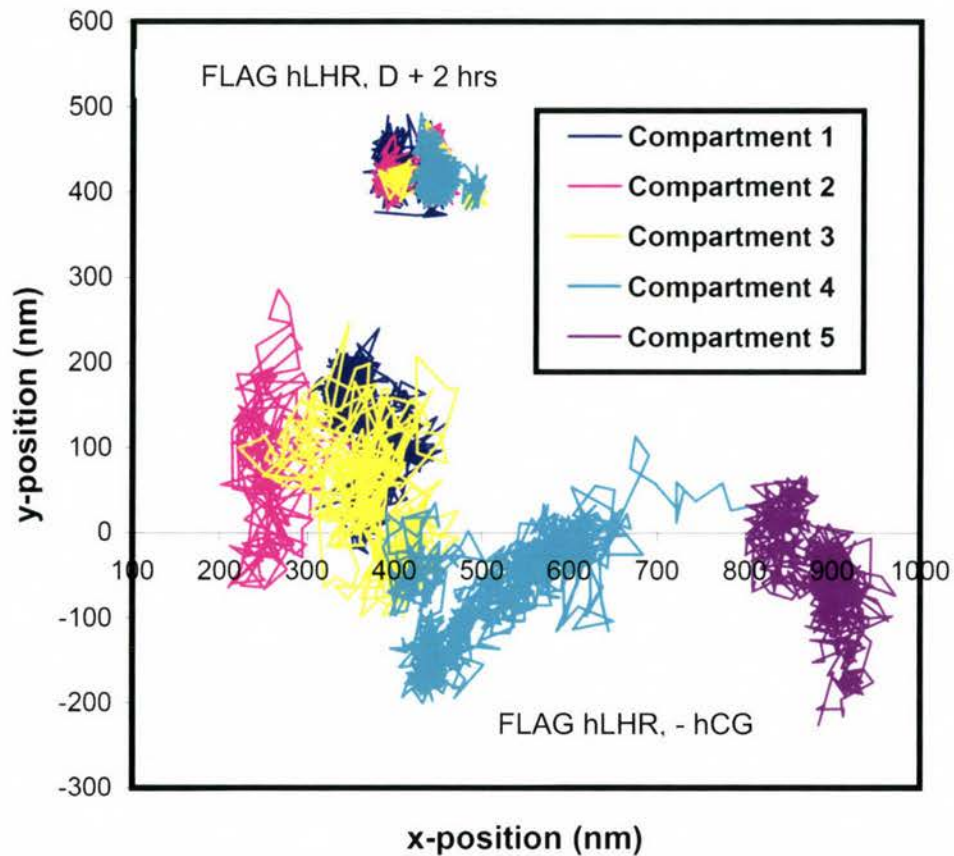
Figure 13: Representative trajectories for human FLAG-tagged LH receptors stably expressed on CHO cells, where (- hCG) indicates an untreated receptor and (D + 2 hrs) indicates a receptor analyzed at two hours following desensitization. Trajectories were segemented into compartments, each indicated by a different color. The average compartment diameter of the desensitized LH receptor (D + 2 hrs) is significantly smaller than the average compartment diameter of the untreated receptor. Analysis of the size of a compartment and the particle residence time provides an estimate of the diffusion coefficient expected for the receptor.
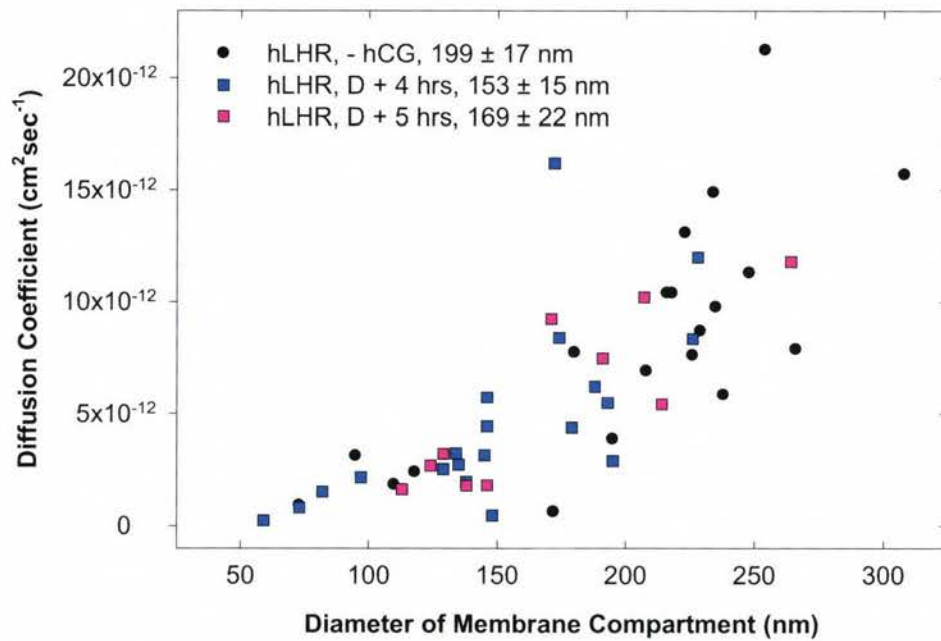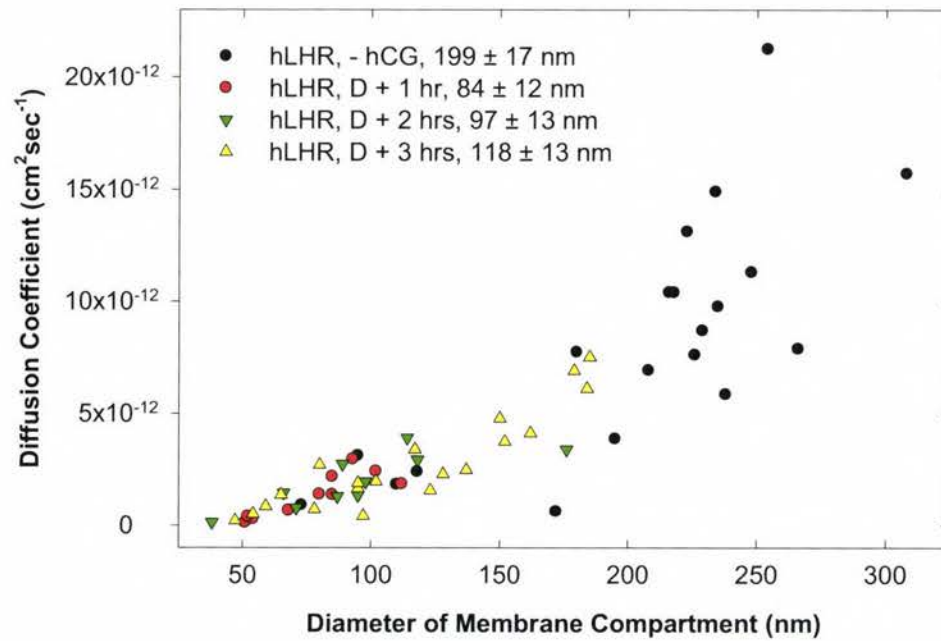
Figure 14: Single particle tracking studies of human FLAG-LH receptors. Desensitized receptors appeared in significantly smaller compartments and exhibited slower diffusion rates for several hours when compared to untreated receptors.
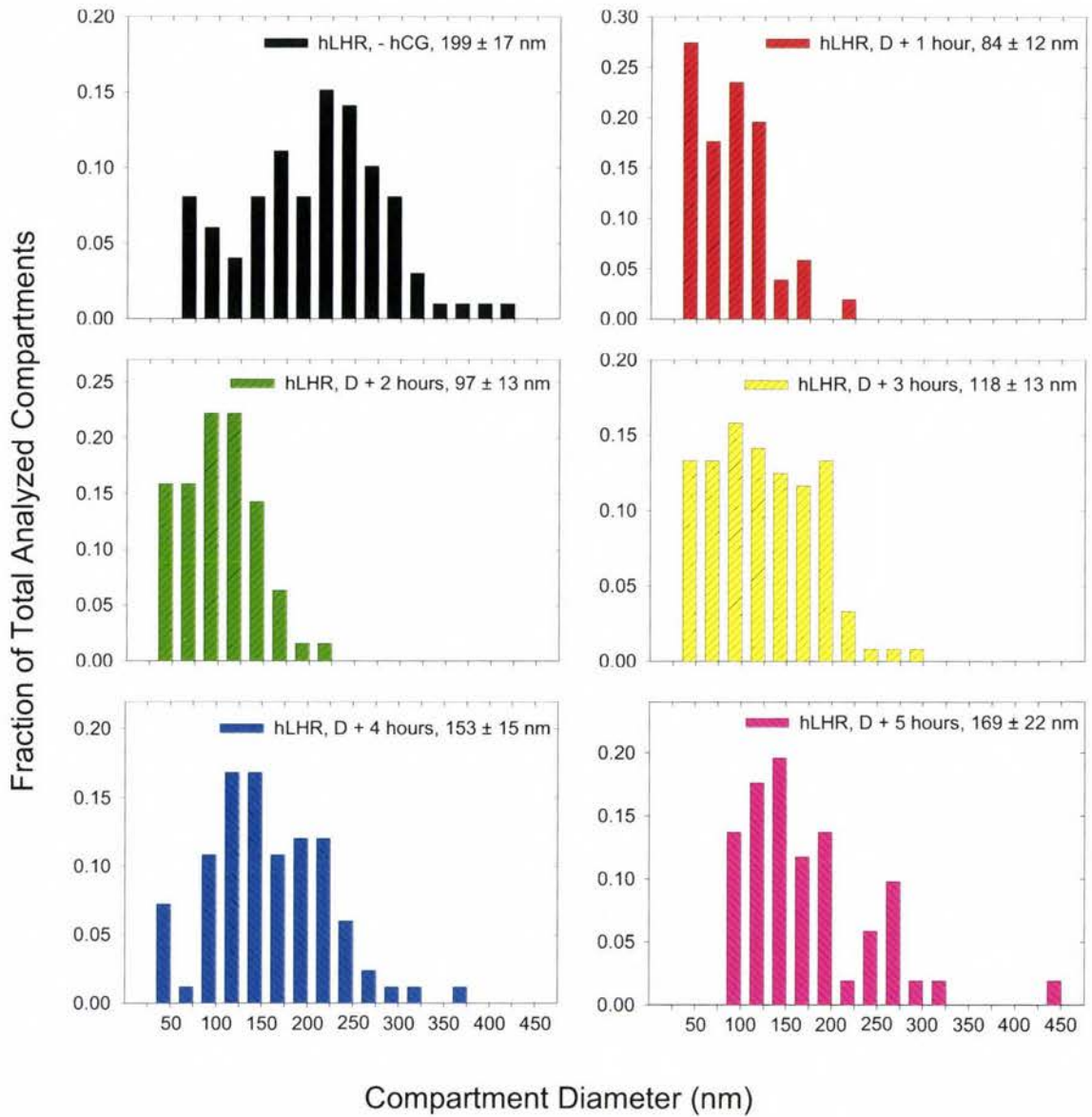
Figure 15: Distribution of compartment sizes from single particle tracking studies of human FLAG-LH receptors. Desensitized receptors became transiently confined in small membrane compartments with diameters of less than 100 nm for several hours.
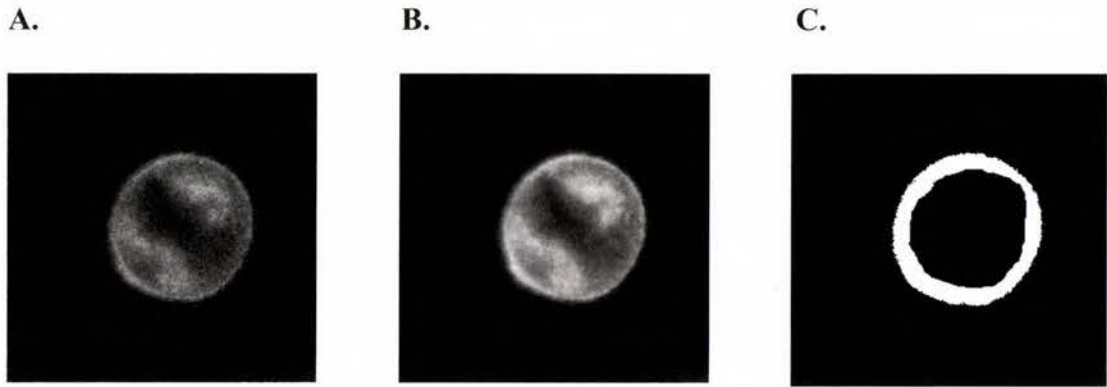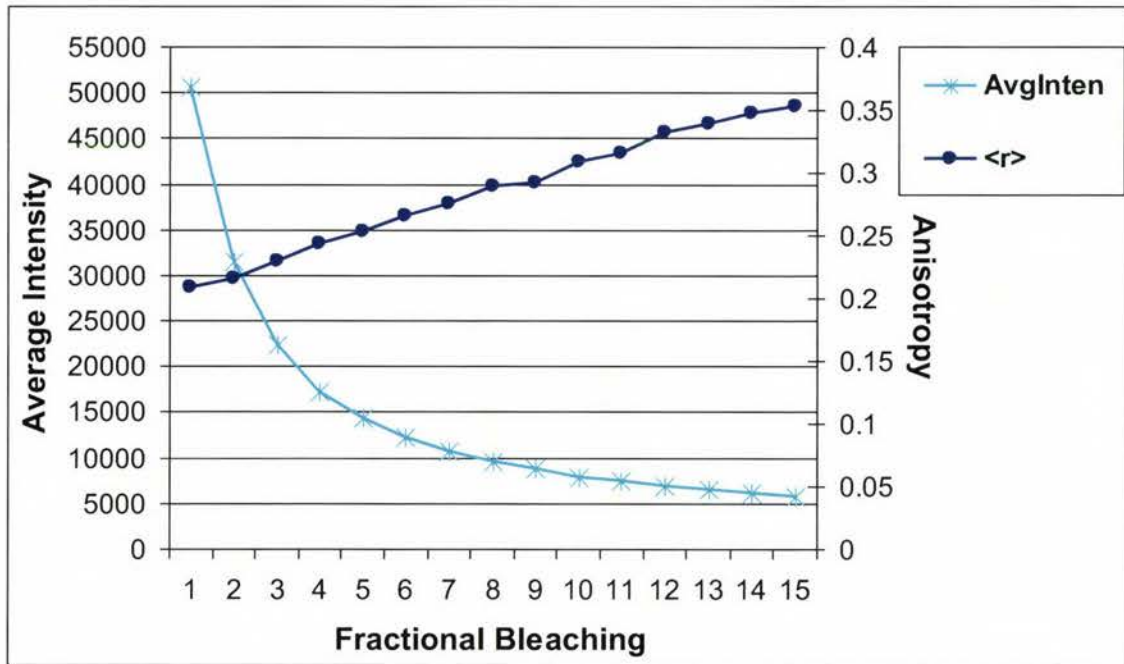
Figure 16: Images of a representative CHO cell stably expressing human LH-YFP receptors used in a homo-FRET experiment. Panel (A) is channel 1 (horizontal, perpendicular), Panel (B) is channel 2 (vertical, parallel) and Panel C shows the masked image indicating that FRET was measured only at the outer membrane. Panel (D): Decay of fluorescence average intensity (AvgInten) occurs with photobleaching of YFP that is accompanied by a rise in anisotropy <r>.
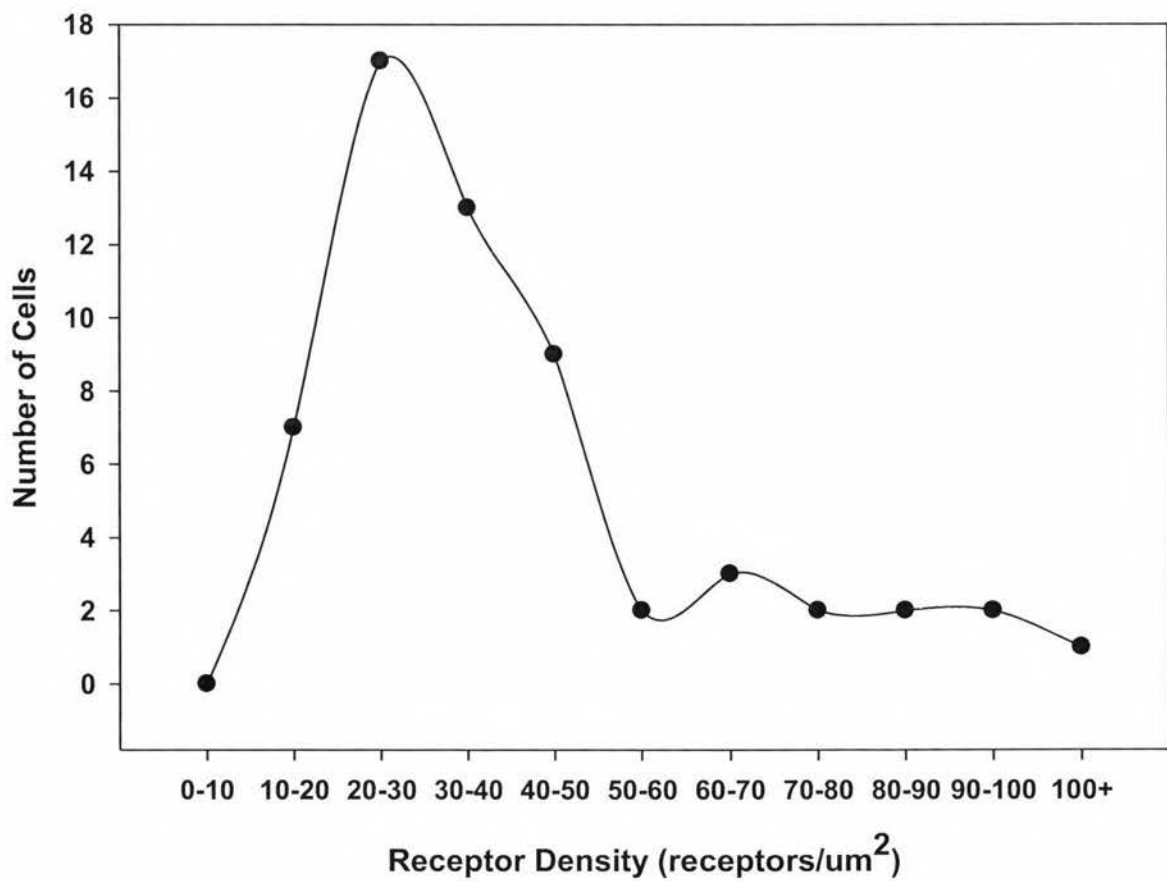
Figure 17: Data from FCS experiments used to determine the number of receptors per μm^2 on stably transfected CHO hLHR YFP cells. Surface area was calculated as 1100 μm^2 and the average number of receptors per cell was determined to be 33,400 receptors.
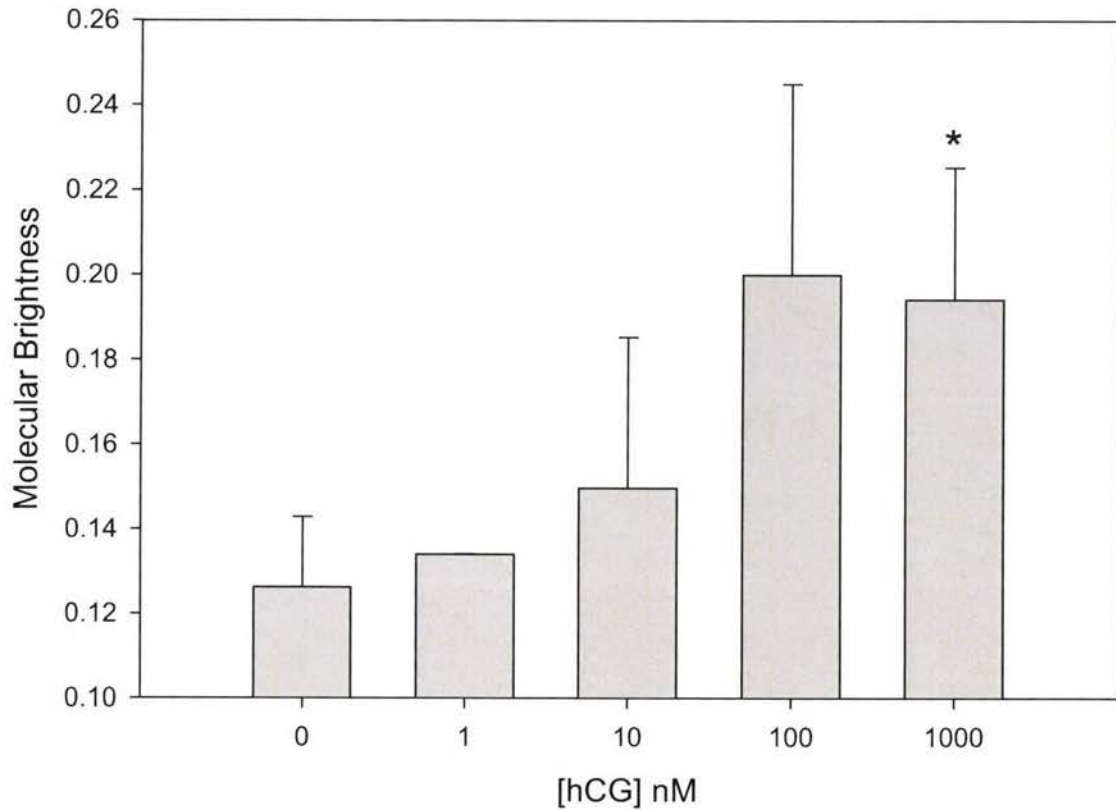
Figure 18: A photon counting histogram (PCH) analysis to study the monomer-dimer dynamics of human LH-YFP receptors on CHO cells in response to increasing concentrations of hCG. An increase in molecular brightness indicates further aggregation of receptors. Data shown are the mean ± S.E.M. for a minimum of 4 experiments. Significance was assessed compared to 0 nM hCG using the two tailed paired t-test with unequal variance ($p < 0.05$).

CHAPTER III[2]

MEMBRANE COMPARTMENTALIZATION OF LUTEINIZING HORMONE

RECEPTORS DEPENDS ON HORMONE, AN INTACT CYTOSKELETON AND

RECEPTOR PALMITOYLATION

INTRODUCTION

Luteinizing hormone (LH) receptors undergo substantial changes in lateral and rotational dynamics as well as translocation to membrane rafts upon treatment with receptor-saturating concentrations of either luteinizing hormone (LH) or human chorionic gonadotropin (hCG) (81). Hormone-treated receptors are also self-associated into dimers/oligomers as evaluated using various techniques for measuring fluorescence resonance energy transfer between receptors (37). Although previous experimental strategies have examined changes in receptor motions on single cells or collections of cells, it is now possible to examine confinement of *individual* receptors in membrane microdomains using the microscope-based technique of single particle tracking (SPT) (152). This technique examines motions of individual LH receptors tagged on the N-

---

[2]This chapter is adapted from a manuscript in preparation to be submitted to *Biology of Reproduction.* Jingjing Liu, Amber L. Wolf-Ringwall, Peter W. Winter, Ying Lei, Steven M.L. Smith, Alan K. Van Orden, B. George Barisas, and Deborah A. Roess (2010) Membrane Compartmentalization of Luteinizing Hormone Receptors Depends on Hormone, an Intact Cytoskeleton and Receptor Palmitoylation.

terminus with the FLAG epitope and visualized using anti-FLAG antibodies coupled to 40 nm gold (Au) particles. The centroid for the gold particles is determined from video images and the particle trajectory is analyzed over time. We have previously shown that gold particles bound to individual FLAG-LHR-wt exhibited distinctive motions in the absence and presence of 100 nM hCG (150). hCG treatment reduced the size of compartments containing FLAG-LHR-wt from 230 ± 79 nm to 86 ± 36 nm. Although the average residence time for receptors within compartments and the number of compartments accessed by FLAG-LHR-wt over two minutes did not differ significantly for untreated and hCG-treated cells, an individual receptor's rate of diffusion D within each compartment was reduced by a factor of ten following hCG treatment. Methyl-β-cyclodextrin (MβCD) extraction of membrane cholesterol largely reversed the effects of hCG on compartment size and receptor lateral diffusion.

Although the mechanism involved in targeting of hCG-occupied LH receptors to small compartments is not clear, previous single particle tracking studies provide some insight into the nature of LH receptor-containing structures. Exposure to high concentrations of hCG results in LH-wt receptors that are largely confined within small compartments, remain within these compartments for comparatively long times, and appear to diffuse pseudo-randomly before being captured within another compartment of similar size (150). Similar behavior has been described and analyzed by Kusumi and coworkers (153) for selected phospholipids and for transferrin receptor (130) and by Daumas et al. (145) for the μ opioid receptor, a G protein-coupled receptor involved in pain responses. Daumas argues that μ opioid receptor motions reflect its diffusion within the bulk membrane followed by confinement within a microdomain that itself diffuses

slowly and suggests that this confinement is due to interactions with the confining molecules. Alternatively, Ritchie et al. (155) suggest that particles may be confined by proteins forming a barrier that is either continuous (fence) or discontinuous (pickets). Fences or pickets can confine and limit receptor diffusion within small membrane regions while still permitting intermittent escape from a compartment followed by faster diffusion in the bulk membrane. Our previous studies of LH receptor lateral diffusion using fluorescence photobleaching recovery methods suggest that actin microfilaments may provide fences or organizing structures for pickets that restrict the lateral motions of the receptor (156).

Confinement within small compartments may be affected by a number of factors, the effects of which we have examined here using single particle tracking methods. Because hormone binding to the receptor may be necessary for receptor compartmentalization, we have, for the first time, examined the effects of lower hormone concentrations on receptor motions. In addition, we have investigated the effects of increasing hormone concentrations on *native* LH receptors expressed on KGN human granulosa-like tumor cells tagged using a form of hCG that lacks glycosylation. We have also explored whether point mutations to palmitoylation sites on the LH receptor C-terminus known to eliminate LH-wt receptor translocation into membrane rafts (157) also affect receptor confinement in small compartments, and whether an intact cytoskeleton is necessary to restrict LH receptor motions, presumably within cytoskeletally-defined compartments, as has been suggested by studies of receptor lateral and rotational dynamics (38). Finally, because slower lateral diffusion can result from self-association of human LH receptors on CHO cells, we used a novel polarization-based FRET

approach known as homo-FRET to detect the oligomerization state of LH receptors in response to increasing concentrations of hormone, and fluorescence correlation spectroscopy (FCS) to determine the number of YFP-tagged human LH receptors stably transfected in the CHO cell line. FCS studies also serve as an alternative method in assessing receptor aggregation in response to increasing concentrations of hormone by photon counting histogram (PCH) analyses.

MATERIALS AND METHODS

Materials

CHO cells were maintained in high glucose Dulbecco's Modification of Eagle's Medium (DMEM) (Mediatech, Inc., Manassas, VA) supplemented with 10% fetal bovine serum (FBS), 2 mM L-glutamine, 100 units of penicillin/ml, 100 μg streptomycin/ml (Gemini Bio-Products, Woodland, CA) and 1x MEM non-essential amino acid solution (Sigma-Aldrich, Inc., St. Louis, MO). The steroidogenic KGN human granulosa-like tumor cell line developed by Dr. Yoshihiro Nishi and Dr. Toshihiko Yanase at Kyusyu University (158) was kindly provided by Dr. James Dias at the Wadsworth Center. KGN cells were maintained in DMEM/Ham's F12 medium supplemented with 10% FBS, 2 mM L-glutamine and 100 units of penicillin/ml as previously described (158). All cells were grown in 5% CO_2 at 37°C in a humidified environment. Geneticin (G418 sulfate) was purchased from Mediatech, Inc. (Manassas, VA). The YFP vector was purchased from Clontech (Mountain View, CA). Monoclonal anti-FLAG antibody directed against the FLAG epitope tag and methyl-β-cyclodextrin (MβCD) were purchased from Sigma-Aldrich, Inc. (St. Louis, MO). 40 nm gold colloid was obtained from Ted Pella, Inc.

(Redding, CA). Intact highly pure hCG antigen (Fitzgerald Industries, Inc., Concord, MA) was prepared in 1x PBS. Dr. George Bousfield of Wichita State University kindly provided the chemically deglycosylated hCG used in single particle tracking studies on KGN cells.

Preparation and maintenance of CHO cell lines expressing FLAG or YFP tags

To test whether rat LH receptors are confined in small membrane compartments following binding of ligand, we generated stable cell lines expressing the FLAG-tagged LH receptor. Dr. K.J. Menon from the University of Michigan kindly provided us with N-terminal FLAG-tagged LHR subcloned into the pFLAG vector (Sigma-Aldrich, Inc., St. Louis, MO). All cell lines were prepared by Dr. Ying Lei. To examine palmitoylation-deficient receptors, we mutated cysteines in LHR at positions 621 and 622 to serines using the QuikChange site-directed mutagenesis kit from Stratagene according to Manufacturer's instructions. For FRET and FCS experiments, a stable CHO cell line expressing human LH receptors was coupled to enhanced yellow fluorescent protein (YFP) at the C-terminus as previously described (151). Clones expressing YFP were selected using fluorescence microscopy. Selection of stable clones expressing the FLAG-tagged receptors was based on the acquisition of geneticin (G418) resistance.

Single particle tracking of LH receptors on individual cells

Lateral dynamics and the size of compartments accessed by individual rat FLAG-LH-wt receptors were evaluated using single particle tracking methods as described by Kusumi and coworkers (132). To identify rat FLAG-tagged LH receptors on CHO cells,

40 nm nanogold particles were conjugated with a mixture of anti-FLAG monoclonal antibody and BSA at the lowest possible total protein concentration, typically 40 μg/mL, needed to stabilize the gold solution. The ratio of antibody to BSA, typically 1:100 by weight, was selected to give 10 to 20 particles bound per cell. This binding was specific for FLAG-tagged receptors; when cells were preincubated with a 10-fold excess of anti-FLAG antibody, no anti-FLAG-gold particles were detected on cells. In some experiments, cells were treated with 0.1, 1 or 100 nM hCG for 1 hour after labeling of receptors with gold-conjugated anti-FLAG antibody, or were pre-treated with 40 μg/mL cytochalasin D for 1 hour prior to labeling with gold-conjugated anti-FLAG antibody.

To track native human LH receptors expressed on KGN granulosa cells, we coupled 40 nm gold particles to hCG or deglycosylated hCG (DG-hCG), also as a mixture with BSA at the lowest possible total protein concentration. For this set of experiments, some KGN cells were treated with 0.1, 1 or 100 nM hCG for 1 hour after labeling receptors with hCG or DG-hCG conjugated gold particles.

Individual nanoparticles were imaged by differential interference contrast using a 1.4 N.A. 63x oil objective in a Zeiss Axiovert 135 microscope. Images were acquired using a Dage IFG-300 camera and were recorded for two minutes (3600 frames) at approximately 30 nm/pixel under the control of Metamorph software (Molecular Devices Corp.). The trajectories for individual gold particles were segmented into compartments by calculation of statistical variance in particle position over specific time windows using a procedure similar to that developed by a number of investigators (144, 145, 153). The variance of a particle's position was calculated within windows of varying duration. These windows were translated along the particle trajectory, producing a variance plot

that exhibits peaks that indicated inter-compartment boundaries. These results were analyzed to yield the compartment size and residence time for each particle. Effective macroscopic diffusion coefficients were calculated as the square of the compartment diagonal divided by four times the residence time in the compartment as previously described (144).

Analysis of Polarization Homo-FRET

We investigated self-association of human LH receptors in response to increasing concentrations of hCG, 0.1, 1 and 100 nM, using a novel FRET method termed polarization homo-FRET, or energy migration FRET (emFRET). Homo-FRET is energy transfer between identical donor and acceptor molecules, which can be assessed by imaging anisotropy, the measure of emission polarization. CHO cells stably expressing human LH receptors fused to YFP on their C-terminus were plated overnight in Willco 35 mm^2 #1.5 glass bottom petri dishes (Warner Instruments, Hamden, CT). A single cell sample was analyzed using an Olympus FV 300 confocal microscope with a polarizing beam splitter placed in front of the detection PMTs, allowing parallel and perpendicular fluorescence intensity to be recorded simultaneously. YFP was imaged with a blue argon laser and the appropriate barrier and dichroic filters were selected for 488 nm excitation. Cells that demonstrated a ring-like fluorescence at the cell's plasma membrane were selected for imaging. In addition, FRET measurements were made only on the fluorescence emitted from the ring-like image region containing LH receptors at the plasma membrane. A sequence of cell images was obtained as YFP was photobleached, with the goal of bleaching the fluorescence to about 10% of the initial

average intensity within approximately 20 images. Each anisotropy measurement was taken with g-factor and background images, and imaging analysis was performed with custom analysis programs. Total intensity and fluorescence anisotropy (r) were calculated using the following formulae: total intensity = $I_{\parallel} + 2I_{\perp}$; anisotropy (r) = $I_{\parallel} - I_{\perp} / I_{\parallel} + 2I_{\perp}$ where I is the intensity and $I_{\parallel}$ and $I_{\perp}$ are the parallel and perpendicular polarized emission components generated by excitation with linearly polarized light (148, 149).

Fluorescence Correlation Spectroscopy

We used fluorescence correlation spectroscopy (FCS) to measure the concentration of fluorophores and thereby quantify the number of YFP-tagged LH receptors per μm^2 on the stably transfected CHO hLHR YFP wt cell line used in homo-FRET experiments. CHO cells stably expressing human LH receptors fused to YFP on their C-terminus were plated overnight in Willco 35 mm^2 #1.5 glass bottom petri dishes and seeded to approximately 50% confluence. All samples were washed, treated and imaged in Tyrodes buffer with 0.2% BSA. Data was acquired using a modified Olympus microscope (T-2000 U). Sample excitation was achieved using the 514 line of an O.C. Argon Ion laser, a 520 dichroic mirror and 535LP filters. A Gaussian laser spot was positioned on the apical surface of sample cells using a 100x-oil APD's (SPCM-ARQ-14). Duel pseudo cross-correlations were calculated using an ALV-5000 correlation card and ALV software. The number of receptors per square μm was determined from the number of correlating particles in the illuminated area and the diameter of the laser beam at the cell surface.

Statistical Analysis of Data

Mean values ± S.E.M. or standard deviation are presented. Significance was assessed using the Student's t-test (unless otherwise noted) and p values are indicated ($p < 0.05$).

RESULTS AND DISCUSSION

FLAG-tagged LH receptors on CHO cells demonstrate confinement in small membrane compartments in response to increasing concentrations of hCG

Binding of 100 nM hCG to rat LH-wt receptors, a hormone concentration sufficient to saturate available LH receptors, results in redistribution of essentially all LH receptors to membrane rafts (150) and, in fluorescence photobleaching recovery measurements of LH receptor lateral diffusion, a marked reduction in the fraction of mobile LH receptors (96). Single particle tracking techniques, in contrast to fluorescence photobleaching recovery measurements, probe the lateral dynamics of *individual* molecules rather than a large population of molecules and so permit analysis of the relative number of receptors exhibiting particular diffusive properties. For LH receptors, we were interested to know whether low concentrations of hormone immobilized a fraction of available receptors or whether binding of hormone, perhaps only to a small subpopulation of available receptors, resulted in immobilization of all available receptors.

As shown in Figure 19, treating cells with 0.1 nM hCG resulted in the appearance of a subset of receptors that exhibited slow lateral diffusion and were confined in small compartments. Increasing hCG to 1 nM and 100 nM, respectively, reduced the average diffusion coefficient for the LH-wt receptors (Table 6) and increased

the number of particles appearing in compartments of less than 100 nm diameter to 62% and 91%. This produced two receptor populations that included slowly diffusing receptors in small compartments and receptors with faster diffusion that accessed significantly larger compartments (Figure 19). When cells were treated with 100 nM hCG, a hormone concentration that saturates all available membrane LH receptors and, in fluorescence photobleaching recovery studies, produces laterally immobile receptors, the average diffusion coefficient was approximately 10^{-12}cm^{2}sec^{-1} (Table 6). Thus, LH receptors are laterally immobile when it is likely that available LH receptors have bound ligand. Although we cannot determine from these results whether slowly diffusing receptors have bound hCG, these data suggest that hormone occupancy may be related to LH receptor retention in small compartments where the particle exhibits slow diffusion. These compartments are distinct from membrane rafts (110) which appear to be smaller, transiently organized microdomains within the membrane.

Single particle tracking of native hormone-occupied LH receptors on KGN cells demonstrate confinement of receptors in small membrane compartments

To assess the lateral dynamics of hCG-occupied LH receptors, we used single particle tracking methods to track the movements of LH receptors on the plasma membrane of viable KGN granulosa-like tumor cells. As shown in Table 7, hCG-bound LH receptors occupied membrane compartments with an average diameter of 186 ± 21 nm. With increasing concentrations of hCG, more receptors were confined in small membrane compartments, although not to the extent that we observed with FLAG-tagged LH receptors on CHO cells. Receptors exposed to saturating concentrations of hCG were

found in compartments with an average diameter of 108 ± 11 nm. These compartments are significantly smaller than the 217 ± 27 nm diameter regions occupied by untreated, non-functional LH receptors that were labeled with only gold-conjugated degylcosylated hCG, thereby representing non-functional hormone-receptor complexes.

As observed in previous SPT studies of FLAG-tagged LH receptors on CHO cells, the average residence time of native LH receptors within compartments and the number of compartments accessed by the receptor in two minutes did not significantly differ between untreated and hormone-treated receptors, or between hCG and DG-hCG-bound receptors (Table 7). However the rate of diffusion (D) for an individual receptor within each compartment was reduced for hCG-occupied receptors when compared to DG-hCG-occupied receptors, suggesting that only functional hormone-receptors exhibit slower lateral diffusion. Figure 20 illustrates the dose-dependent distribution of compartment sizes accessed by hCG-occupied LH receptors in response to increasing concentrations of hCG. Following a low dose of 0.1 nM hCG, only 16% of hCG-occupied LH receptors were confined in small compartments with a diameter of less than 100 nm. This number increased to 48% when cells were exposed to saturating concentrations of 100 nM hCG (Table 8).

Interestingly, we also observed confinement of DG-hCG-occupied LH receptors when KGN cells were exposed to saturating concentrations of hCG (100 nM), as shown in Figure 21. This suggests that some non-functional hormone-receptor complexes also redistribute to small membrane compartments in response to hormone. Future studies examining the possible interactions between functional and non-functional LH receptors during signal transduction would be helpful to better understand these findings. For

example, FRET experiments using fluorescent functional and non-functional ligands may help to resolve receptor-receptor interactions in small membrane compartments during signal transduction.

The cytoskeleton appears to play a role in restricting hormone-treated receptors within small compartments

FLAG-tagged LH receptors on CHO cells treated with 40 μg/mL cytochalasin D, a microfilament disruptor, exhibit fast lateral diffusion within large compartments both before and after exposure to 100 nM hCG (Table 9). There was no effect of hCG treatment on the average diffusion coefficient or the average compartment diameter accessed by LHR-wt in the absence of an intact cytoskeleton and these values were similar to LHR-wt in the absence of hormone on cells with an intact cytoskeleton. Possible membrane models to explain this behavior include disruption of protein compartments defined by cytoskeletally-anchored proteins that serve as protein fences (155).

Palmitoylation sites on LH receptors may also play a role in compartmentalization of hCG-treated receptors

We examined receptors where cysteine was mutated to serine at positions 621 and 622 (LHR-C621,622S) which have been previously described as palmitoylation sites for the LH receptor (63, 159). The average values for the compartment diameters accessed by either untreated or hCG-treated LHR-C621,622S are approximately 200 nm (Table 10). Individual LHR-C621,622S are generally not confined in small

compartments although their diffusion coefficients are slower than those of either untreated wild type receptors or receptors on cells treated with cytochalasin D (Tables 9 and 10). Interestingly, these mutant receptors retain their ability to signal via cAMP (63, 159) as do dopamine D1 (160) and serotonin 4a (161) receptors with similar mutations. Thus, prolonged compartmentalization may not be necessary for LH receptor signal transduction. These experiments, however, do not eliminate the possibility that the interactions of mutant receptors with the molecular contents of small compartments are more short-lived than for wild type receptors.

Together, these studies suggest that compartmentalization of LH receptors occurs following binding of ligand and that this process requires an intact cytoskeleton. It has been suggested by Kusumi and colleagues that ligand-induced receptor conformational changes increase receptor interactions with signaling molecules on the membrane's cytoplasmic face and so increase the likelihood of receptor interactions with the membrane cytoskeleton. Given the dynamic nature of the cytoskeleton, such molecular complexes can be expected to generate apparent compartmentalization of receptor motions over a variety of time and distance scales. Presumably, hCG-induced formation of larger receptor complexes with signaling molecules or other cytoplasmic proteins enhances receptor sensitivity to the presence of cytoskeletal elements and so reduces the size of apparent compartments confining the receptor. The role for LH receptor palmitoylation in receptor-mediated signaling (162) and receptor compartmentalization and raft localization is generally unclear and may prove ultimately to be receptor-specific.

Human LH receptors self-associate in response to increasing concentrations of hCG

To analyze the self-association or aggregation state of LH receptors in response to hormone treatment, we performed homo-FRET experiments on CHO cells stably expressing human LH-YFP receptors. Homo-FRET was assessed by imaging anisotropy (r), a measure of emission polarization. Photobleaching YFP irreversibly reduced the concentration of fluorophores capable of acting as acceptors, therefore energy transfer was indicated by a rise in FRET as bleaching proceeded (148). If receptors were associated, indicating energy transfer, then acceptor molecules were oriented different than donor molecules and anisotropy subsequently increased.

The data presented here indicates that hormone-treated LH receptors exhibited a higher level of self-association than untreated LH receptors. As shown in Table 11, the difference in mean anisotropy for 10 cells following 100 nM hCG treatment (0.0899) was larger and significantly different than the difference in mean anisotropy for 10 untreated cells (0.0208), indicating a higher degree of aggregation of hormone-treated receptors. In addition, the difference in mean anisotropy appears to increase with increasing concentrations of hCG, indicating a higher degree of receptor self-association from 0.1 nM to 100 nM hCG-treated cells (Figure 22). These results are in agreement with those of our previous study of hormone-treated LH receptors using conventional hetero-FRET methods, in which significant energy transfer occurred between hormone-treated LH receptors compared to untreated receptors (151).

Additionally, FCS studies performed on stably transfected CHO hLHR YFP cells reveal LH receptor aggregation with increasing concentrations of hCG. Figure 23 presents the number of cells with relatively low numbers of receptors per μm^2. A photon

counting histogram (PCH) analysis was also used to differentiate between species of similar diffusion coefficient through their molecular brightness. A PCH is particularly useful here because it can also resolve aggregation through molecular species brightness levels. As shown in Figure 24, with increasing concentrations of hCG, molecular brightness increases, indicating further aggregation of human LH-YFP receptors.

Table 6: Dose-dependent effects of hCG on individual rat FLAG-LH-wt receptors on individual CHO cells assessed by single particle tracking. Data shown are the mean ± standard deviation; a,b differ significantly (p<0.05).

Cell line	Treatment [hCG]	Number of of particles analyzed	Number of compartments/ 2 min trajectory	D_{0-1} [1] $(10^{-11}cm^2sec^{-1})$	$D = L_r^2/4t$ [2] $(10^{-11}cm^2sec^{-1})$	Time [3] (t) (sec)	Compartment [4] diameter (L_r) (nm)
CHO rLHR FLAG wt	None	20	6 ± 2	6.8 ± 3.8	1.2 ± 0.8	16 ± 13	230 ± 79[a]
CHO rLHR FLAG wt	0.1	20	3 ± 1	4.1 ± 5.0	1.4 ± 1.4	30 ± 18	211 ± 114[a]
CHO rLHR FLAG wt	1	20	4 ± 1	3.5 ± 2.2	0.9 ± 1.5	29 ± 16	122 ± 72[b]
CHO rLHR FLAG wt	100	20	5 ± 2	2.9 ± 1.1	0.1 ± 1.8	20 ± 11	86 ± 36[b]

[1] D_{0-1}: Diffusion coefficient within compartment calculated from the first two points of MSD vs. time plot as described by Daumas et al. (145).

[2] D represents the diffusion coefficient within a compartment as calculated from compartment size (L_r) and particle residence time (t)

as $D = L_r^2/4t$ as described by Saxton (144).

[3] Average particle residence time for residence within a compartment.

[4] The average diameter of an individual compartment was calculated as described by Daumas et al. (145) and Murase et al. (153).

Table 7: Single particle tracking of human LH receptors on individual KGN cells labeled with gold-conjugated hCG or deglycosylated hCG. Data shown are the mean ± standard deviation; Compartment diameter is mean ± S.E.M.; a,b differ significantly (p<0.05).

Cell line	Au probe	Treatment [hCG]	Number of particles analyzed	Number of compartments/ 2 min trajectory	D_{0-1}[1] $(10^{-11} cm^2 sec^{-1})$	$D = L_r^2/4t$ [2] $(10^{-11} cm^2 sec^{-1})$	Time [3] (t) (sec)	Compartment [4] diameter (L_r) (nm)
KGN hLHR	Au-hCG	None	20	5 ± 2	2.8 ± 1.3	0.70 ± 1.0	24 ± 21	186 ± 21[a]
KGN hLHR	Au-hCG	0.1	20	5 ± 2	2.2 ± 0.77	0.48 ± 0.64	24 ± 20	156 ± 17[a]
KGN hLHR	Au-hCG	1	20	6 ± 2	2.4 ± 0.93	0.62 ± 1.1	21 ± 17	148 ± 16[b]
KGN hLHR	Au-hCG	100	20	6 ± 2	2.0 ± 0.73	0.27 ± 0.49	20 ± 13	108 ± 11[b]
KGN hLHR	Au-DG-hCG	None	20	4 ± 2	2.0 ± 0.74	1.6 ± 4.1	27 ± 26	217 ± 27[a]
KGN hLHR	Au-DG-hCG	100	20	5 ± 1	2.1 ± 0.70	0.46 ± 0.79	25 ± 18	145 ± 20[b]

[1] D_{0-1}: Diffusion coefficient within compartment calculated from the first two points of MSD vs. time plot as described by Daumas et al. (145).

[2] D represents the diffusion coefficient within a compartment as calculated from compartment size (L_r) and particle residence time (t)

as $D = L_r^2/4t$ as described by Saxton (144).

[3] Average particle residence time for residence within a compartment.

[4] The average diameter of an individual compartment was calculated as described by Daumas et al. (145) and Murase et al. (153).

Table 8: Percent of human LH receptors on KGN cells present in membrane compartments of less than 100 nm and greater than 100 nm. Data shown are the mean ± S.E.M.

Treatment	% hLHR in less than 100 nm compartments	% hLHR in greater than 100 nm compartments	n
Au-hCG probe, 0 nM hCG	15 ± 5^a	85 ± 5	20
Au-hCG probe, 0.1 nM hCG	16 ± 6^a	84 ± 6	20
Au-hCG probe, 1 nM hCG	31 ± 8^a	69 ± 8	20
Au-hCG probe, 100 nM hCG	48 ± 7^b	52 ± 7	20
Au-DG-hCG probe, 0 nM hCG	12 ± 6^a	88 ± 6	20
Au-DG-hCG probe, 100 nM hCG	34 ± 8^b	66 ± 8	20

a,b Values with different superscripts differ significantly ($p < 0.05$).

Table 9: Effect of cytochalasin D on rat FLAG-LH-wt receptor lateral diffusion assessed by single particle tracking. Data shown are the mean ± standard deviation; a,b differ significantly (p<0.05).

Cell line	Pre-Treatment, then Hormone Treatment	Number of of particles analyzed	Number of compartments/ 2 min trajectory	D_{0-1} [1] $(10^{-11}cm^2sec^{-1})$	$D = L_r^2/4t$ [2] $(10^{-11}cm^2sec^{-1})$	Time [3] (t) (sec)	Compartment [4] diameter (L_r) (nm)
CHO rLHR FLAG wt	Cytochalasin D, None	20	2 ± 1	3.6 ± 3.9	2.8 ± 2.4	25 ± 18	221 ± 80[a]
CHO rLHR FLAG wt	Cytochalasin D, 100 nM hCG	20	2 ± 1	2.8 ± 1.8	2.2 ± 1.7	29 ± 14	204 ± 66[a]
CHO rLHR FLAG wt	None, None	20	6 ± 2	6.8 ± 3.8	1.2 ± 0.8	16 ± 13	230 ± 79[a]
CHO rLHR FLAG wt	None, 100 nM hCG	20	5 ± 2	2.9 ± 1.1	0.1 ± 1.8	20 ± 11	86 ± 36[b]

[1] D_{0-1}: Diffusion coefficient within compartment calculated from the first two points of MSD vs. time plot as described by Daumas et al. (145).

[2] D represents the diffusion coefficient within a compartment as calculated from compartment size (L_r) and particle residence time (t)

as $D = L_r^2/4t$ as described by Saxton (144).

[3] Average particle residence time for residence within a compartment.

[4] The average diameter of an individual compartment was calculated as described by Daumas et al. (145) and Murase et al. (153).

Table 10: FLAG-tagged LHR-C621,622S did not appear in small compartments following binding of hormone. Data shown are the mean ± standard deviation; a,b differ significantly ($p < 0.05$).

Cell line	Treatment	Number of of particles analyzed	Number of compartments/ 2 min trajectory	D_{0-1}[1] (10^{-11}cm^{2}sec^{-1})	$D = L_r^2/4t$[2] (10^{-11}cm^{2}sec^{-1})	Time[3] (t) (sec)	Compartment[4] diameter (L_r) (nm)
CHO rLHR FLAG-621,622S	None	10	3 ± 1	1.1 ± 0.3	0.4 ± 0.6	29 ± 12	204 ± 74[a]
CHO rLHR FLAG-621,622S	100 nM hCG	10	3 ± 1	1.0 ± 1.0	0.1 ± 0.2	32 ± 11	195 ± 47[a]
CHO rLHR FLAG wt	None	20	6 ± 2	6.8 ± 3.8	1.2 ± 0.8	16 ± 13	230 ± 79[a]
CHO rLHR FLAG wt	100 nM hCG	20	5 ± 2	2.9 ± 1.1	0.1 ± 1.8	20 ± 11	86 ± 36[b]

[1] D_{0-1}: Diffusion coefficient within compartment calculated from the first two points of MSD vs. time plot as described by Daumas et al. (145).

[2] D represents the diffusion coefficient within a compartment as calculated from compartment size (L_r) and particle residence time (t)

as $D = L_r^2/4t$ as described by Saxton (144).

[3] Average particle residence time for residence within a compartment.

[4] The average diameter of an individual compartment was calculated as described by Daumas et al. (145) and Murase et al. (153).

Table 11: Homo-FRET summary of untreated and hormone-treated human LH-YFP receptors expressed on CHO cells. Data shown are the mean ± S.E.M.

| Cell line | Treatment hCG (nM) | n | Mean Anisotropy | | |
			Before (r initial)	After (r final)	Difference (r final – r initial)
CHO hLHR YFP wt	None	10	0.188	0.208	0.0208 ± 0.005^a
CHO hLHR YFP wt	0.1	10	0.158	0.203	0.0447 ± 0.013^a
CHO hLHR YFP wt	1	10	0.186	0.252	0.0659 ± 0.013^b
CHO hLHR YFP wt	100	10	0.166	0.255	0.0899 ± 0.014^b

a,b Values with different superscripts differ significantly ($p<0.05$).
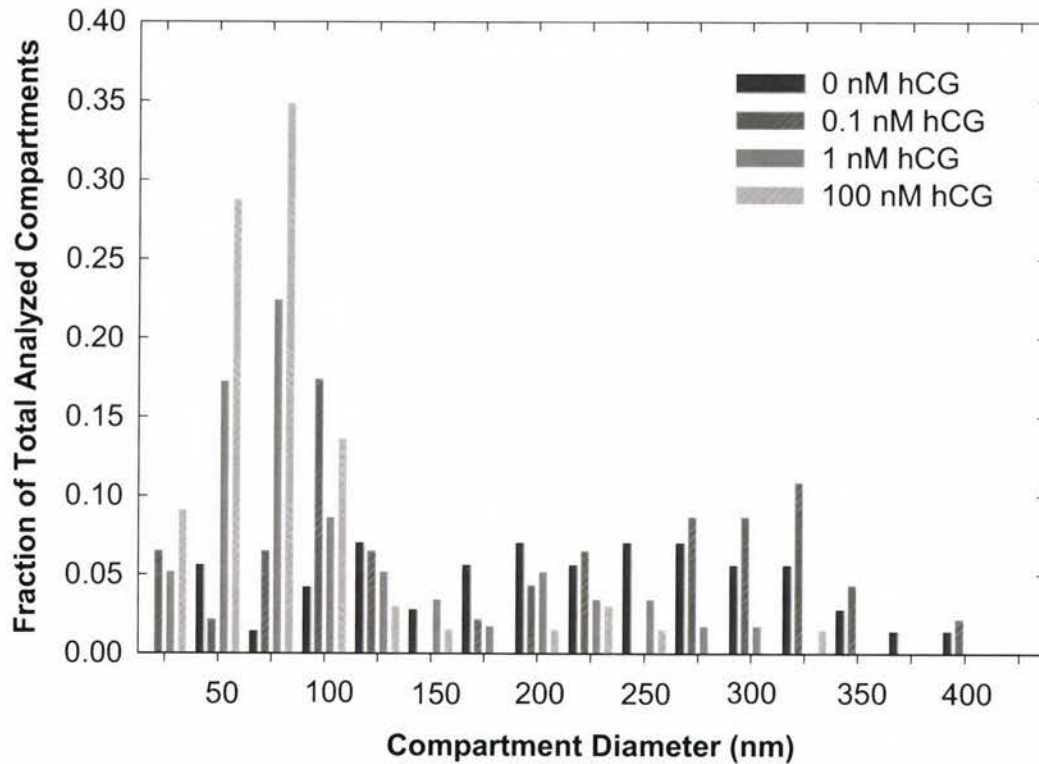
Figure 19: Dose-dependent LH receptor movement into small compartments. CHO cells expressing rat FLAG-LH receptors were treated with hormone concentrations ranging from 0.1 nM to 100 nM. After treatment with 1 nM and 100 nM hCG, 62% and 91% of the receptors were confined in small compartments with a diameter of less than 100 nm. The remaining receptors exhibited unconfined lateral diffusion in large compartments typical of untreated cells.
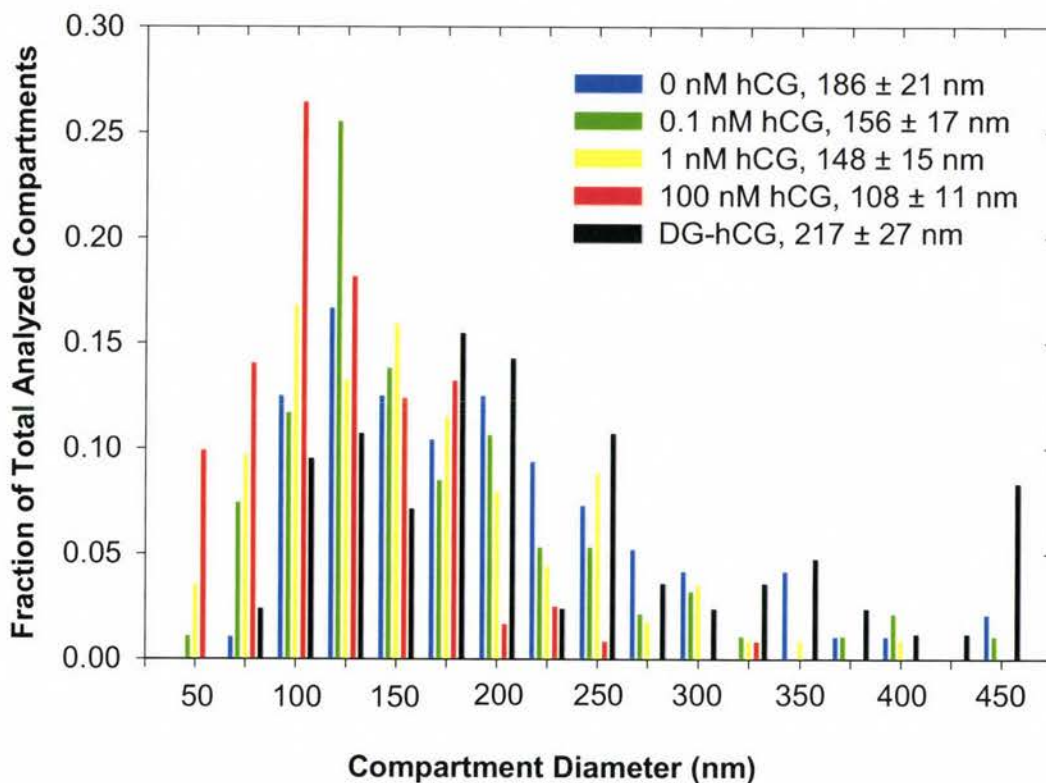
Figure 20: Single particle tracking studies of hCG-occupied LH receptors on KGN granulosa cells treated with increasing concentrations of hCG. A dose-dependent effect is observed as more LH receptors moved into small membrane compartments with diameters of less than 100 nm. In contrast, DG-hCG-occupied LH receptors were more broadly distributed in varying diameter compartments with an average compartment size of 217 ± 27 nm.
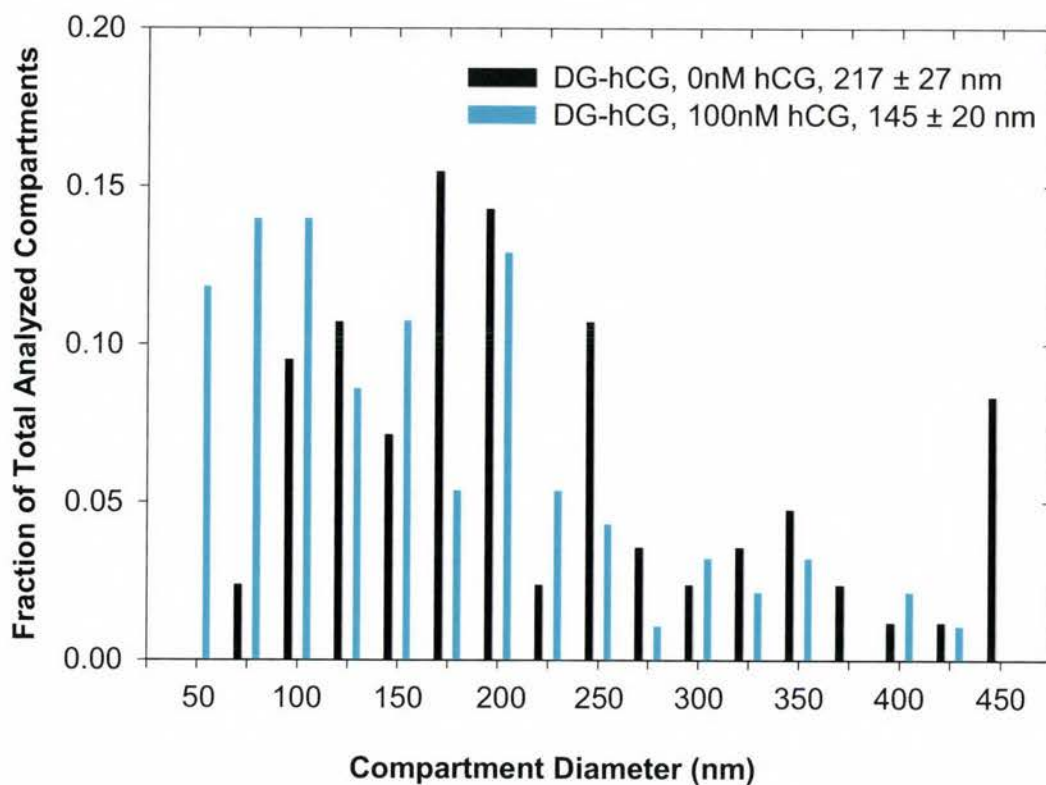
Figure 21: A comparison between DG-hCG-occupied LH receptors on KGN cells with and without additional hormone treatment. Although all receptors examined were bound with non-functional hormone, more of these receptors were confined in small membrane compartments when cells were treated with saturating concentrations of hCG (100 nM).
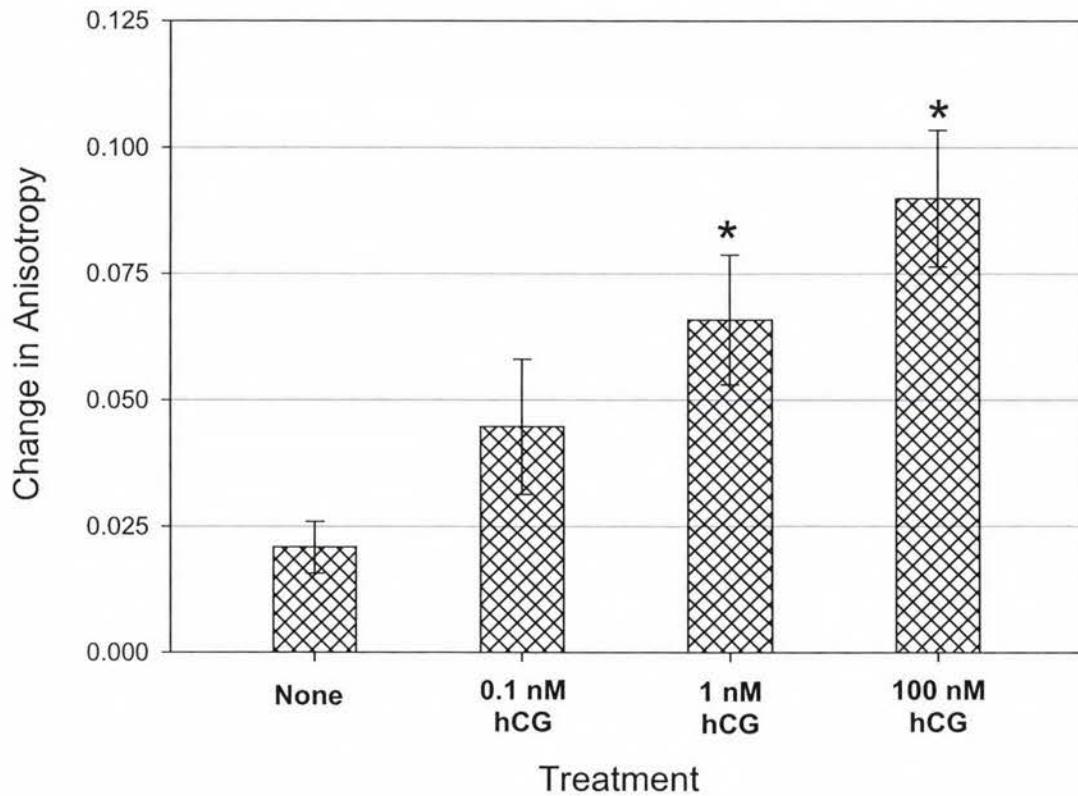
Figure 22: Homo-FRET experiments performed on CHO hLHR YFP wt cells demonstrate changes in anisotropy that increase with increasing concentrations of hCG. The mean change in anisotropy for cells treated with 1 nM and 100 nM hCG are significantly different when compared to the mean change in anisotropy for the same number of untreated cells.
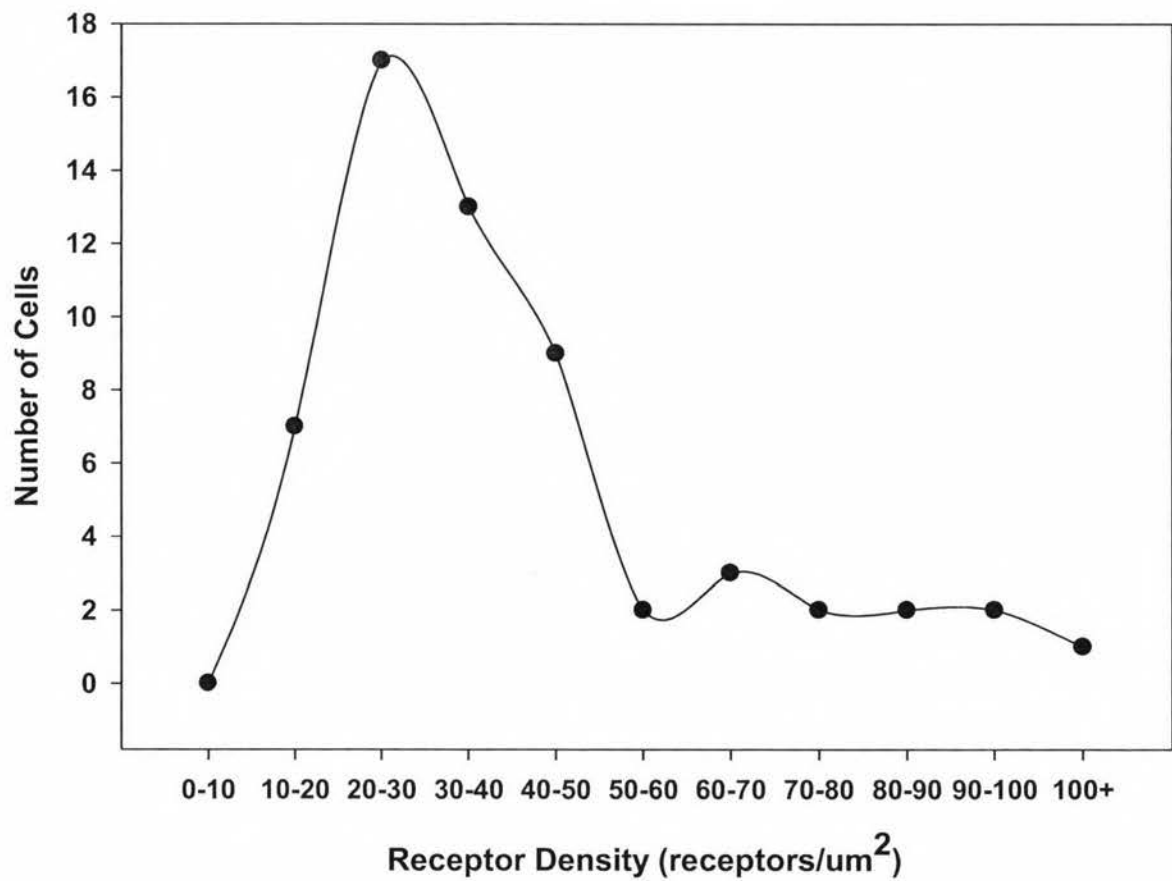
Figure 23: Data from FCS experiments used to determine the number of receptors per μm^2 on stably transfected CHO hLHR YFP cells. Surface area was calculated as 1100 μm^2 and the average number of receptors per cell was determined to be 33,400 receptors.
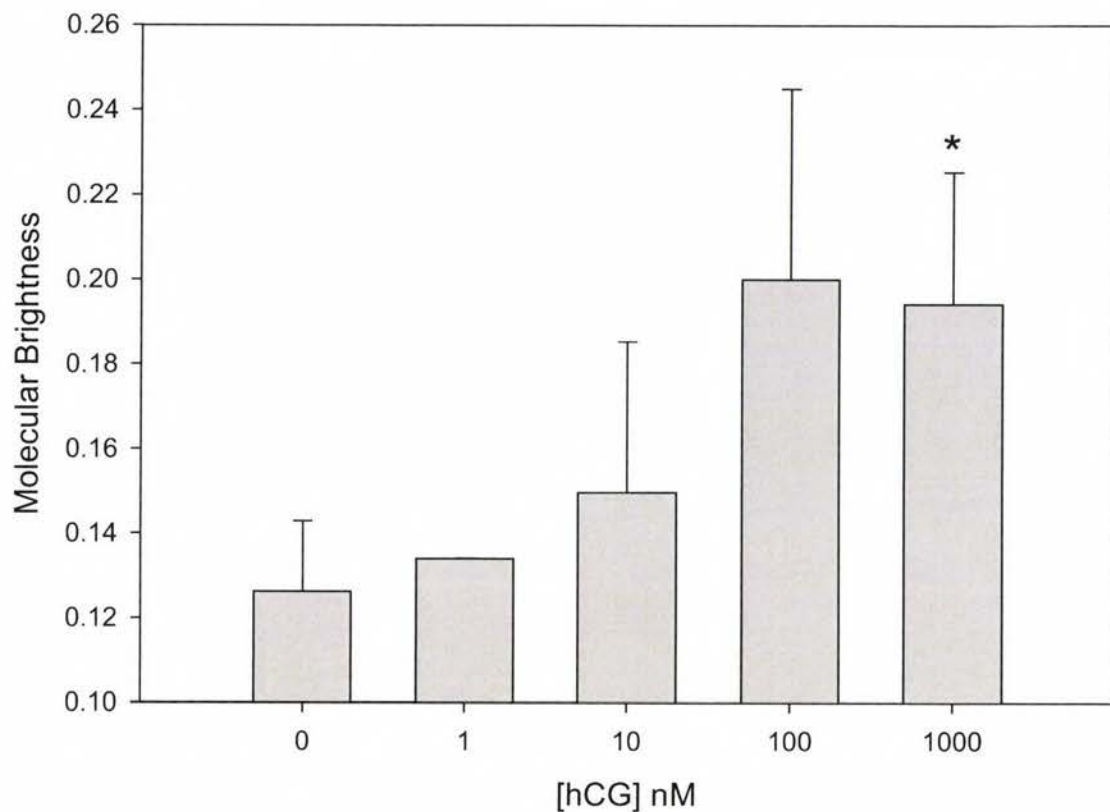
Figure 24: A photon counting histogram (PCH) analysis to study the monomer-dimer dynamics of human LH-YFP receptors on CHO cells in response to increasing concentrations of hCG. An increase in molecular brightness indicates further aggregation of receptors and appears to occur in a dose-dependent manner. Data shown are the mean ± S.E.M. for a minimum of 4 experiments. Significance was assessed compared to 0 nM hCG using the two tailed paired t-test with unequal variance ($p<0.05$).

CHAPTER IV[3]

EFFECTS OF hCG CONCENTRATION AND PULSATILE HORMONE EXPOSURE ON THE COMPARTMENTALIZATION OF LUTEINIZING HORMONE RECEPTORS ON M17 NEUROBLASTOMA CELLS

AND

A PROSPECTIVE STUDY EXAMINING REAL-TIME CHANGES IN cAMP

INTRODUCTION

Luteinizing hormone (LH) is a gonadotropin that is released from the anterior pituitary in pulsatile fashion. The amplitude of LH pulses has been shown to increase with age, particularly in postmenopausal women (4). Recently it has been suggested that an increase in overall LH levels can contribute to the development of Alzheimer's Disease by activating LH receptors in the postmenopausal brain, possibly contributing to neurodegenerative processes such as increases in cell synthesis and in the secretion of amyloid-β. Thus the increasing levels of LH associated with aging may play a role in the development and progression of Alzheimer's Disease.

---

[3]This chapter was adapted from an abstract presented at the 2009 Annual University Research Colloquium by Amber Wolf-Ringwall entitled "Effects of Dose Response and Pulsatile Hormone Exposure on the Compartmentalization of Luteinizing Hormone Receptors on M17 Neuroblastoma Cells."

We are interested in studying LH receptor-mediated signaling events using microscope-based methods on live cells. With single particle tracking methods, we have shown that LH receptors treated with human chorionic gonadotropin (hCG) on Chinese hamster ovary cells exhibit confined diffusion in small membrane compartments (150). With increasing hormone concentrations, more receptors were found in small diameter compartments where they exhibited slower diffusion. In addition, receptors exposed to continuous hormone became desensitized and remained confined in small compartments for several hours.

In the aging brain, it is likely that the LH pulsatility observed in postmenopausal women translates to pulsatile, transient signaling. Here, we consider what effects hormone concentration and pulsatile hormone exposure have on LH receptor-mediated signaling. We investigated, for the first time, whether extragonadal LH receptors endogenously expressed on a neuron-like cell line, M17 neuroblastoma cells, become confined within small membrane compartments following exposure to increasing concentrations of hormone. We also examined the effect of low amplitude hormone pulses typically seen in younger, premenopausal women on LH receptor compartmentalization. Importantly, we performed these experiments while assessing cAMP levels. Additionally, we discuss a prospective study analyzing *real-time* changes in cAMP levels in M17 cells using a novel biophysical method, fluorescence resonance energy transfer (FRET) and a FRET reporter protein called ICUE1 (*indicator of cAMP using Epac*). ICUE1 allows real-time evaluation of cAMP levels as LH receptor-mediated signaling occurs. This work contributes to a better understanding of the events involved in LH receptor-mediated signaling in the aging brain, which may help to

elucidate a possible mechanism for LH in the development of Alzheimer's Disease, and attempt to explain a role for LH in extragonadal tissues.

MATERIALS AND METHODS

Materials and cell culture

BE(2)-M17 human neuroblastoma cells were purchased from ATCC (Manassas, VA) and maintained in Minimum Eagle's Medium (MEM)/Ham's F12 medium (Mediatech, Inc., Manassas, VA) supplemented with 10% fetal bovine serum, 1 mM L-glutamine, 100 units of penicillin/ml, 100 μg streptomycin/ml (Gemini Bio-Products, Woodland, CA), sodium bicarbonate, sodium pyruvate and 1x MEM non-essential amino acid solution (Sigma-Aldrich, Inc., St. Louis, MO). Cells were grown in 5% CO_2 at 37°C in a humidified environment. Intact highly pure hCG antigen (Fitzgerald Industries, Inc., Concord, MA) was prepared in 1x PBS. Dr. George Bousfield of Wichita State University kindly provided the chemically deglycosylated hCG. Forskolin and ELISA kits detecting amyloid-β were purchased from Sigma-Aldrich, Inc. (St. Louis, MO). 40 nm gold (Au) colloid was obtained from Ted Pella, Inc. (Redding, CA). Intracellular cAMP was measured using a TiterFluor Direct Cyclic AMP Enzyme Immunoassay Kit purchased from Assay Designs (Ann Arbor, MI). The DNA for ICUE1 cloned in pcDNA 3 was a gift from Dr. Jin Zhang at The Johns Hopkins University School of Medicine.

Hormone treatments and cAMP analysis

M17 cells expressing human LH receptors were incubated with 0.1, 1 or 100 nM hCG for 30 minutes at 37°C. Additionally, some M17 cells were exposed to 2 x 0.1 nM or 2 x 1 nM pulses of hCG that are characteristic of low dose hormone pulses found in premenopausal women. The second pulse of hCG was administered 15 minutes after the first hCG incubation time of 30 minutes. To monitor the extent of LH receptor signaling, levels of intracellular cAMP were assessed following exposure to hCG and in response to low dose pulses of hCG using a TiterFluor Direct Cyclic AMP Enzyme Immunoassay Kit (Assay Designs, Ann Arbor, MI). In addition, 20 nM forskolin, used as a positive control to maximally stimulate adenylate cyclase, was given to M17 cells for 30 minutes at 37°C prior to cell lysis.

Single particle tracking of native LH receptors on individual M17 human neuroblastoma cells

We examined effects of increasing hCG concentration and low dose hormone pulses on the lateral dynamics and confinement of human LH receptors in the plasma membrane by tracking the movements of individual receptors with single particle tracking methods as described by Kusumi and colleagues (132). M17 cells expressing endogenous human LH receptors grown on coverslips placed in 60 mm^2 petri dishes were treated with 0.1, 1 or 100 nM hCG or PBS for 30 minutes at 37°C. In addition, some M17 cells were exposed to 2 x 1 nM pulses of hCG.

To identify individual LH receptors on M17 cells, we coupled hCG or deglycosylated hCG (DG-hCG) to 40 nm gold particles. To identify hormone-activated

and inactivated LH receptors, cells were labeled with gold-conjugated hCG or DG-hCG, respectively, for 1 hour at 4°C. The minimal stabilizing protein concentration was determined to be 44 µg/ml and gold was conjugated with the lowest possible concentration of hCG or DG-hCG needed to stabilize the gold solution. The concentration of hCG or DG-hCG was not more than 1% of the concentration of total protein. One percent bovine serum albumin (BSA) in PBS was added to the solution until there were approximately 10 to 20 gold particles per cell. The binding specificity for LH receptors was tested by preincubating cells with a 10-fold excess of hCG or DG-hCG. After incubation with gold-conjugated hCG or DG-hCG, no gold particles were found on cells. Images for the appropriate controls were also taken and included unlabeled cells and cells labeled with gold conjugated only to BSA.

The individual gold particles were imaged by differential interference contrast with a 1.4 N.A. 63x oil objective in a Zeiss Axiovert 135 TV inverted microscope. Gold-labeled LH receptors were followed by video microscopy with a Dage IFG-300 camera and recorded for two minutes (3600 frames, 30 frames/second) at approximately 30 nm/pixel with Metamorph software from Universal Imaging. Trajectories of individual gold particles were measured over time and then sorted into various modes of motion in order to characterize the overall motion of a receptor. The trajectories for gold particles were segmented into compartments by calculation of statistical variance in particle position over time, a procedure that is similar to that developed by a number of investigators (144, 145, 153). The variance of a particle's position was calculated within windows of varying duration. These windows were translated along the particle trajectory, producing a variance plot that displays peaks indicative of inter-compartment

123

boundaries. The results were analyzed using custom analysis programs to generate compartment size and residence time for each particle. Effective macroscopic diffusion coefficients were calculated as the square of the compartment diagonal divided by four times the residence time in the compartment also previously described (144).

Statistical Analysis of Data

Mean values ± S.E.M. or standard deviation are presented. Significance was assessed using the Student's t-test and p values are indicated ($p < 0.05$).

RESULTS AND DISCUSSION

To assess the lateral dynamics of LH receptors in response to increasing concentrations of hormone and low dose hormone pulses, we used single particle tracking methods to track the movements of single LH receptors on the plasma membrane of viable M17 cells. hCG-occupied LH receptors exposed to a single, high dose of hCG (100 nM) that saturated all available membrane receptors moved into small compartments with an average diameter of 131 ± 18 nm. These compartments are significantly smaller than the 301 ± 55 nm diameter regions occupied by non-functional hormone-receptor complexes (DG-hCG occupied receptors). As receptors accessed increasingly larger membrane compartments, their rate of diffusion (D) also increased, as shown in Figure 25. Overall, the rate of diffusion (D) for an individual receptor within each compartment was reduced for receptors treated with higher concentrations of hCG.

For the low dose hormone treatments of 0.1 nM, 1 nM and 2 x 1 nM hCG pulses, a subset of receptors accessed small membrane compartments and this number increased

with increasing concentrations of hCG. After treatment with 2 x 1 nM pulses of hCG and a single high dose of 100 nM hCG, 19% and 32% of LH receptors were confined in small compartments with a diameter of less than 100 nm (Table 14). In addition, Figure 26 displays the distribution of compartment sizes accessed by LH receptors in response to a single, high dose of hCG (100 nM) compared to hCG-bound receptors only and DG-hCG-bound receptors only.

To assess LH-receptor mediated signaling, levels of intracellular cAMP were measured following exposure to increasing concentrations of hCG, and after low dose pulses of hCG. As shown in Table 12, there was approximately a 2-fold increase in cAMP response to treatment with 100 nM hCG or 20 nM forskolin. However, low dose hormone and pulses of 1 nM hCG resulted in no increase in cAMP over basal levels. Because only forskolin-treated cells showed a significant increase in cAMP accumulation, and a small percentage of hCG-occupied LH receptors accessed small membrane compartments, perhaps another cell line similar to a neuron expressing LH receptors would be beneficial in these experiments. Assaying cAMP levels with a colorimetric cAMP assay kit requires lysing a large number of cells, typically 1 to 1.5 x 10^6 cells per well, to determine the concentration of cAMP in the cytoplasm. We demonstrated that this method used to determine cAMP changes in response to hormone pulses and increasing hormone concentrations does not appear to be sensitive enough for use in the M17 cell line, as changes in cAMP did not increase significantly in response to saturating concentrations of hormone. Alternatively, a live-cell imaging technique utilizing hetero-FRET with a FRET reporter protein, ICUE1, will allow constant, consistent monitoring of cAMP changes in single M17 cells.

Thus far, we determined that endogenous LH receptors expressed in M17 human neuroblastoma cells appear to become transiently confined in small membrane compartments in response to hormone treatment, although not to the extent seen in our previous studies of FLAG-tagged LH receptors stably transfected on CHO cells. With increasing hCG concentrations, the number of LH receptors confined in small membrane compartments increases, as does the level of the second messenger molecule cAMP, to some degree. This suggests that higher circulating levels of LH in postmenopausal women could result in an increase in LH receptor-mediated signaling in the brain. The effect of a non-functional hormone, deglycosylated hCG, does not appear to cause receptor confinement in small membrane compartments in M17 cells.

FUTURE STUDIES AND ANTICIPATED RESULTS

We propose to use hetero-FRET between CFP and YFP on the FRET reporter protein ICUE1 to monitor changes in cAMP levels in M17 cells in response to hormone pulses and increasing concentrations of hCG. ICUE1 (indicator of cAMP using Epac) is a modified chimera of the FRET reporter protein Epac (exchange protein activated by cAMP) that has two fluorophores attached to it, citrine (a modified form of YFP) and ECFP. After transiently transfecting ICUE1 into M17 cells endogenously expressing LH receptors, we will quantitate cAMP production over time in response to hormone pulses and increasing concentrations of constant hCG. Our goal is to select hormone concentrations and to design pulse experiments that accurately represent the constant and pulsatile patterns of LH that are characteristic of pre- and post-menopausal women. However, even with the novel live-cell microscope-based imaging method described

126

here, recreating physiological pulses of LH *in vivo* may prove difficult due to experimental constraints and human error. A more accurate and sensitive method of delivering hormone pulses may be required for this set of experiments, such as using a perfusion chamber to deliver more efficient pulses of hormone to M17 cells.

For hetero-FRET studies of ICUE1, M17 neuroblastoma cells expressing endogenous human LH receptors will be plated overnight in Willco 35 mm^2 #1.5 glass bottom petri dishes (Warner Instruments, Hamden, CT). When cells are at or above 50% confluency, M17 cells will be transiently transfected with 2 μg of ICUE1 DNA in 12 μl of Lipofectamine 2000 according to the Invitrogen Lipofectamine 2000 protocol (Invitrogen Life Technologies, Carlsbad, CA). Transiently transfected cells will be incubated at 37°C in M17 medium for 24 hours and imaged within 48 hours.

To monitor the real-time cAMP changes in M17 cells, FRET between CFP (fluorescence donor) and YFP (fluorescence acceptor) on the FRET reporter protein ICUE1 will be evaluated on individual cells. FRET measurements will be made using a Zeiss Axiovert 200m microscope, 63x water objective and Omega Optical filter sets for imaging CFP and YFP. Metamorph software from Universal Imaging will be used to acquire and analyze images. Imaging analysis of hetero-FRET will be performed using acceptor photobleaching. Cells demonstrating a ring-like fluorescence at the cell's plasma membrane will be selected for imaging, indicating cAMP changes localized at the plasma membrane. We will then measure the intensity of the membrane localized fluorescence donor CFP, in the presence and absence of the fluorescence acceptor YFP. Before photobleaching YFP, CFP and YFP will be imaged separately using a Princeton Instruments 1300YHS ICCD camera using exposure times of 200-1000 ms. After

127

photobleaching YFP for 5 minutes, CFP and YFP will be imaged again. Image backgrounds will be corrected by subtracting the background fluorescence without cells from the emission intensities of fluorescent cells. A decrease in intensity from CFP after photobleaching of YFP is indicative of cAMP binding ICUE1, separating CFP and YFP, resulting in decreases in energy transfer efficiency (%E), as calculated using the following equation and diagrammed in Figure 9.

$$\%E = [(D_{after} - D_{before}) / D_{after}] \times 100$$

Previous experimentation by DiPilato and colleagues using ICUE1 in examining the β-adrenergic receptor has shown that when cAMP is not bound to ICUE1, citrine and ECFP are in close proximity and FRET efficiencies were measured at $29 \pm 3\%$ (163). However once intracellular cAMP levels increased via mechanisms of β-adrenergic receptor signaling, FRET efficiency decreased to $21 \pm 1\%$, and a further decrease in %E was reported with forskolin treatment. In our proposed FRET studies evaluating real-time changes in cAMP in M17 cells due to LH receptor signaling, we expect that values for %E will decrease for cells exposed to saturating concentrations of hCG (100 nM). In addition, we anticipate that M17 cells treated with forskolin, which maximally stimulates adenylate cyclase, will result in a marked reduction of %E as well, at least to the extent of that observed for 100 nM hCG. If no change in %E is detected, we will assume that the levels of LH receptor expressed on M17 cells are not enough to stimulate a change in energy transfer efficiency, thus mirroring the findings reported here using colorimeteric cAMP assay kits. It would also be of great interest to expand this method of detecting changes in real-time cAMP to other events in LH receptor-mediated signal transduction, particularly in desensitization of the LH receptor, where time-dependent changes in

128

cAMP levels have been observed and appear to be critical in reproductive functions such as oocyte meiosis.

Additionally, it would be beneficial to examine a functional consequence of LH-receptor mediated signaling in M17 neuroblastoma cells during this experiment, namely, the processing of amyloid-β from amyloid-β protein precursor, which has been previously described in this cell line (32). We aim to assess the levels of amyloid-β protein with cAMP production using an ELISA kit that is specific for amyloid-β protein and is commercially available from Sigma Aldrich, Inc. (St. Louis, MO).

Our overall hypothesis for this study is that exposing M17 cells to hormone pulses will result in transient mechanisms of signal transduction. Such mechanisms could include transient aggregation of LH receptors on the plasma membrane, as well as transient confinement of receptors in small membrane compartments used for cell signaling that may contribute to increased secretion of amyloid-β. Future studies of imaging signaling events on live cells, such as examining real-time changes in cAMP, will greatly contribute to our understanding of transient signal transduction.

Table 12: cAMP responsiveness of M17 human neuroblastoma cells expressing native LH receptors. Data shown are the mean ± S.E.M.

Cell line	Treatment	Fold increase over basal cAMP levels	cAMP conc (pmol/mL)	n
M17 hLHR	None	1.0^a	4.0 ± 1.2	3
M17 hLHR	100 nM hCG	1.6 ± 0.2^a	6.9 ± 2.9	3
M17 hLHR	20 nM forskolin	2.5 ± 0.9^b	9.1 ± 5.8	3
M17 hLHR	1 nM hCG	1.1 ± 0.3^a	5.1 ± 2.6	3
M17 hLHR	2 x 1 nM hCG	1.1 ± 0.1^a	4.0 ± 0.8	3
M17 hLHR	0.1 nM hCG	1.1 ± 0.1^a	4.6 ± 1.7	3
M17 hLHR	2 x 0.1 nM hCG	1.6 ± 0.6^a	4.2 ± 0.6	2

a,b Values with different superscripts differ significantly ($p < 0.05$).

Table 13: Dose-dependent effects of hCG on individual native LH receptors on M17 human neuroblastoma cells labeled with gold-conjugated hCG or deglycosylated hCG (DG-hCG). Data shown are the mean ± standard deviation; Compartment diameter is mean ± S.E.M.; a,b differ significantly (p<0.05).

Cell line	Au probe	Treatment [hCG]	Number of of particles analyzed	Number of compartments/ 2 min trajectory	D_{0-1} [1] $(10^{-11}\text{cm}^2\text{sec}^{-1})$	$D = L_r^2/4t$ [2] $(10^{-11}\text{cm}^2\text{sec}^{-1})$	Time [3] (t) (sec)	Compartment [4] diameter (L_r) (nm)
M17 hLHR	Au-hCG	None	10	5 ± 1	2.1 ± 0.68	0.86 ± 1.1	25 ± 18	219 ± 22[a]
M17 hLHR	Au-hCG	0.1	10	4 ± 1	2.1 ± 0.48	0.78 ± 1.1	28 ± 20	195 ± 26[a]
M17 hLHR	Au-hCG	1	10	4 ± 2	2.3 ± 0.99	0.35 ± 0.37	27 ± 21	143 ± 17[b]
M17 hLHR	Au-hCG	100	15	5 ± 2	1.9 ± 1.0	0.37 ± 0.39	22 ± 16	131 ± 18[b]
M17 hLHR	Au -hCG	2 x 1	10	6 ± 1	3.5 ± 1.4	0.55 ± 0.79	21 ± 16	151 ± 18[b]
M17 hLHR	Au-DG-hCG	None	10	3 ± 1	2.2 ± 0.73	2.0 ± 3.8	37 ± 33	301 ± 55[a]

[1] D_{0-1}: Diffusion coefficient within compartment calculated from the first two points of MSD vs. time plot as described by Daumas et al. (145).

[2] D represents the diffusion coefficient within a compartment as calculated from compartment size (L_r) and particle residence time (t)

as $D = L_r^2/4t$ as described by Saxton (144).

[3] Average particle residence time for residence within a compartment.

[4] The average diameter of an individual compartment was calculated as described by Daumas et al. (145) and Murase et al. (153).

Table 14: Percent of human LH receptors on M17 cells present in membrane compartments of less than 100 nm and greater than 100 nm. Data shown are the mean ± S.E.M.

Treatment	% hLHR in less than 100 nm compartments	% hLHR in greater than 100 nm compartments	n
Au-hCG probe, 0 nM hCG	2 ± 2^a	98 ± 2	10
Au-hCG probe, 0.1 nM hCG	14 ± 10^a	86 ± 10	10
Au-hCG probe, 1 nM hCG	15 ± 6^a	85 ± 6	10
Au-hCG probe, 100 nM hCG	32 ± 10^b	68 ± 10	15
Au- hCG probe, 2 x 1 nM hCG	19 ± 8^a	81 ± 8	10
Au-DG-hCG probe, 0 nM hCG	7 ± 5^a	93 ± 5	10

a,b Values with different superscripts differ significantly ($p < 0.05$).
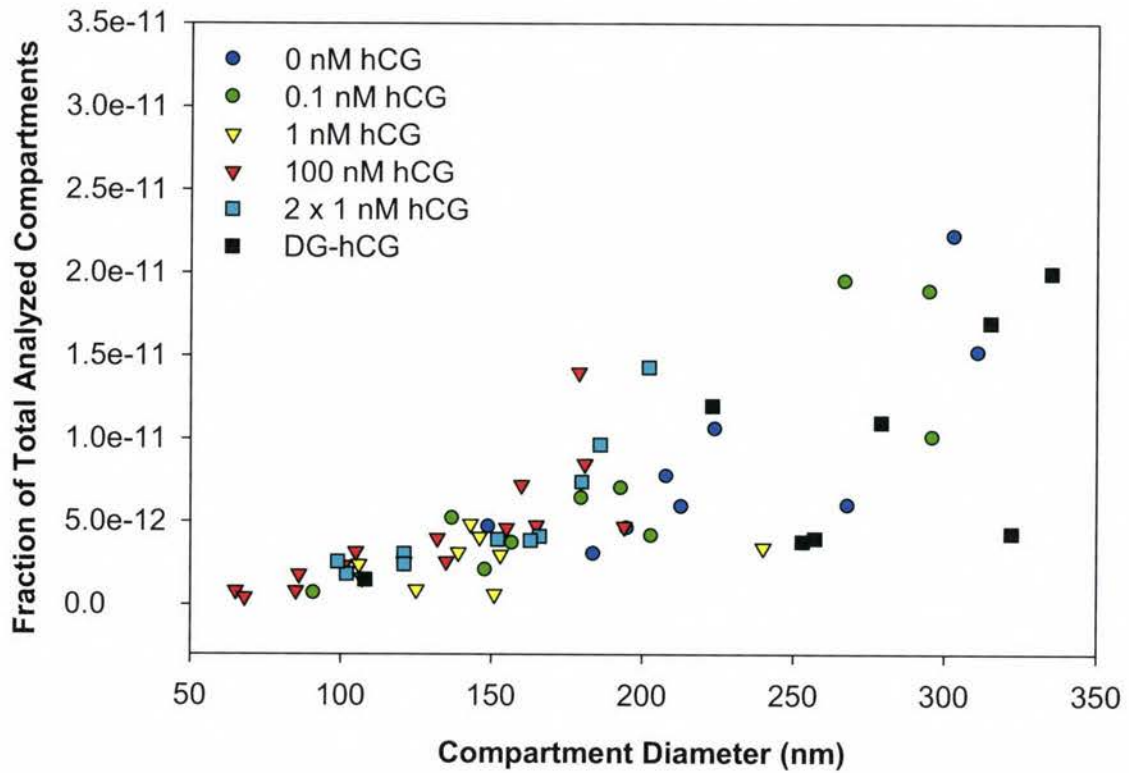
Figure 25: Single particle tracking studies of human LH receptors on M17 neuroblastoma cells. hCG-occupied receptors appeared in significantly smaller compartments and exhibited slower diffusion rates upon additional hCG treatment (0 to 100 nM hCG) when compared to non-functional, untreated receptors (DG-hCG).
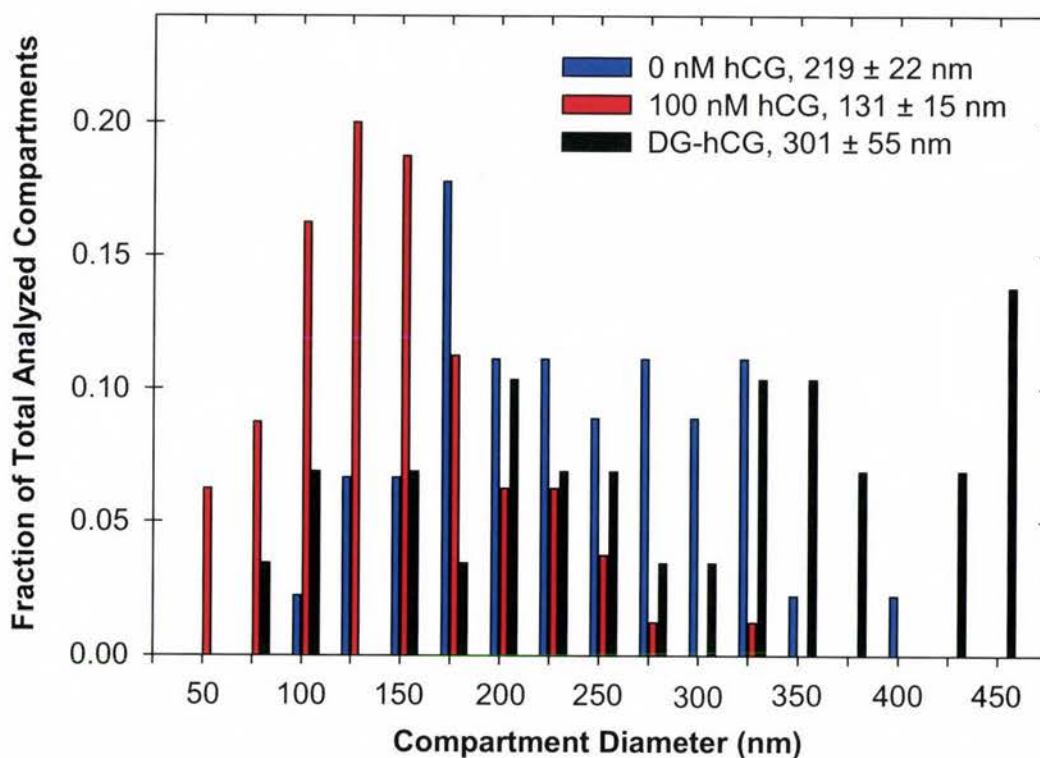
Figure 26: Dose-dependent effects of hCG on the diameter of compartments accessed by individual LH receptors on M17 human neuroblastoma cells. With increasing hormone concentrations, more LH receptors were confined in small membrane compartments with a diameter of less than 100 nm. Receptors labeled with DG-hCG exhibited unconfined lateral diffusion in large compartments.

CHAPTER V

CONCLUSIONS AND FUTURE DIRECTIONS

Fertility is dependent on functional LH receptors, which play an essential role in the normal reproductive function of both male and female mammals by promoting ovulation, follicle maturation, corpus luteum formation and steroidogenesis. A critical regulatory mechanism involved in LH receptor mediated signal transduction is receptor desensitization, which occurs in LH receptors in ovarian follicles leading to ovulation.

We have investigated the organization of LH receptors in the plasma membrane during receptor desensitization and in response to low and high doses of hormone. We observed that desensitized LH receptors not capable of signaling are localized in membrane rafts and in membrane compartments as defined by single particle tracking studies. In addition, biophysical techniques such as fluorescence resonance energy transfer (FRET) and fluorescence correlation spectroscopy (FCS) have revealed that LH receptors demonstrate aggregation with increasing concentrations of hormone and following desensitization. From this information, we have attempted to gain a better understanding of the sequence of events that occurs with hormone binding, signal transduction and receptor desensitization.

LH receptors are localized in membrane rafts following desensitization

After sucrose gradient centrifugation of plasma membrane fractions from CHO cells expressing FLAG-tagged rat or human LH receptors, untreated LH receptors were found in membranes with higher densities. However following desensitization, a significant portion of LH receptors localized in detergent-resistant, low-density fractions characterized as membrane rafts. An important question that arises from these studies is whether LH receptors actually signal in rafts. We have previously demonstrated that LH receptors translocate to membrane rafts following treatment with hormone. Because this event corresponded with increases in intracellular cAMP levels, it appeared that raft translocation may be a requirement for LH receptor-mediated signaling. However here we demonstrated that at least a subpopulation of desensitized LH receptors appear in rafts when the receptors are unable to signal, suggesting that specific molecules involved in either signaling or in desensitization need to be present in rafts for a particular function. The data presented here suggests that membrane rafts may not be essential to cAMP-mediated signaling and that rafts may be involved in other functions such as desensitization.

A useful future experiment would be to probe membrane rafts for β-arrestin-1 and other molecules involved in desensitization. In addition, we could also selectively deplete β-arrestin-1 from CHO cells expressing FLAG-LH-wt receptors using RNAi methods, and then determine if LH receptors were still localized in rafts following desenstization. An alternative method would be to perform immunoprecipitation studies to determine which signaling proteins are associated with LH receptors during signaling and during desensitization.

LH receptors are found in small membrane compartments following desensitization and in response to increasing concentrations of hormone

We have investigated LH receptor organization in the plasma membrane during the 5 hour time course of desensitization using single particle tracking methods. Our data suggests that individual human LH receptors are confined in small membrane compartments following hormone treatment and for several hours during desensitization. Interestingly, desensitized receptors do not signal via cAMP while they are confined. By 5 hours, the majority of LH receptors exhibited unconfined lateral diffusion in large membrane compartments typical of untreated cells. In addition, hormone-treated LH receptors were not confined in small membrane compartments when treated with cytochalasin D, which disrupts the cytoskeleton. This data suggests that the cytoskeleton may serve as a fence that restricts the motion of the LH receptor. It would be of interest to evaluate the effect of β-arrestin-1 depletion on LH receptor desensitization by examining the lateral dynamics of LH receptors expressed in cells lacking β-arrestin-1 using single particle tracking methods.

Additionally, we determined that native LH receptors on KGN human granulosa and M17 human neuroblastoma cells exhibit compartmentalization in response to increasing concentrations of hCG. In both cell lines we observed that, with increasing concentrations of hCG, more hCG-occupied receptors were confined in small membrane compartments, although not to the extent that we observed with FLAG-tagged LH receptors on CHO cells. We also observed confinement of deglycosylated hCG-occupied LH receptors when KGN cells were exposed to saturating concentrations of hCG (100 nM). This suggests that some non-functional hormone-receptors also

redistribute into small membrane compartments in response to hCG. Their movement into small membrane compartments in response to hormone treatment of cells is intriguing, since we expect that they do not participate in signal transduction. Future studies examining the possible interactions between functional and non-functional LH receptors during signal transduction would be helpful in better understanding these findings. For example, FRET experiments using fluorescent functional and non-functional ligands may help to resolve receptor-receptor interactions in small membrane compartments during signal transduction.

Human LH receptors undergo self-association following desensitization and in response to increasing concentrations of hCG

To analyze the self-association or aggregation state of LH receptors in response to hormone treatment and desensitization, we performed homo-FRET and FCS experiments on CHO cells stably expressing human LH-YFP receptors. We found that LH receptors exhibit increased aggregation following desensitization, which also increased in response to increasing concentrations of hCG. The mechanism for receptor aggregation is not known, although receptors may self-associate by transitioning from monomers to dimers/oligomers, or alternatively by forming larger structures containing aggregated receptors.

The aggregation of LH receptors reported here, and the formation of slowly diffusing complexes described by others (90, 96), may be a requirement for receptor desensitization. Perhaps desensitized LH receptors must self-associate and segregate into confined membrane microdomains where LH receptors physically interact with

138

each other as well as proteins needed for uncoupling. These microdomains may allow LH receptors to self-associate in membrane microdomains where β-arrestin-1, ARF6, ARNO and other proteins needed for desensitization are located. These events could facilitate the function of LH receptor desensitization by helping to dampen the cAMP response at the plasma membrane.

Finally, it remains unclear whether membrane rafts and/or membrane compartments detected by SPT represent areas where LH receptors signal. To investigate this question, it may be necessary to gain a better understanding of the sensitive changes in cAMP levels that occur during LH receptor-mediated signal transduction. To better understand these changes, we could perform FRET techniques utilizing a fluorescent probe such as Epac that monitors real-time cAMP levels throughout the time-course of LH receptor desensitization. This experiment will allow us to better quantify the extent of LH receptor desensitization by monitoring dynamic changes in the second messenger molecule cAMP, and could also be used to better define the importance of hormone concentration and hormone pulses on LH receptor-mediated signaling.

In conclusion, this set of experiments has provided a better understanding of the interactions of LH receptors in the plasma membrane during desensitization and in response to increasing concentrations of hormone. We have demonstrated that compartmentalization may be important in signaling by GPCRs. It is thought that the compartmentalization of signals functions in optimizing the signal transduction between a hormone and effector molecules like adenylate cyclase. Together these experiments address the mechanisms of LH receptor desensitization and may lead to a more broad application for addressing fundamental questions about signaling mechanisms used by

membrane receptors. A better understanding of the mechanisms involved in signal transduction of GPCRs may lead to treatments for disease pathologies where receptor-mediated signal transduction is compromised.

REFERENCES

1. **Ascoli M, Fanelli F, Segaloff D** 2002 The lutropin/choriogonadotropin receptor, a 2002 perspective. Endocrine Reviews 23:141-174

2. **Knobil E, Neill J** 1998 Encyclopedia of Reproduction

3. **Conn PM, Huckle WR, Andrews WV, McArdle CA** 1987 The molecular mechanism of action of gonadotroin releasing horrmone (GnRH) in the pituitary. Recent Progress In Hormone Research 43:29-68

4. **Barron A, Verdile G, Martins R** 2006 The role of gonadotropins in Alzheimer's Disease. Endocrine 29:257-269

5. **Jaffe R, Lee P, Midgley AJ** 1969 Serum gonadotropins before, at the inception of, and following human pregnancy. J Clin Endocrinol Metab 29:1281-1283

6. **Catt K, Dufau M** 1991 Gonadotropic hormones: biosynthesis, secretion, receptors and actions. Reproductive Endocrinology:105-155

7. **Chan W-Y** 1998 Molecular, genetic, biochemical, and clinical implications of gonadotropin receptor mutations. Molecular Genetics and Metabolism 63:75 - 84

8. **Fanelli F** 2000 Theorectical study on mutation-induced activation of the luteinizing hormone receptor. Journal of Molecular Biology 296:1333-1351

9. **Shenker A** 2002 Activating mutations of the lutropin choriogonadotropin receptor in precocious puberty. Receptors and Channels 8:3-18

10. **Zheng M, Shi H, Segaloff D, Van Voorhis B** 2001 Expression and localization of luteinizing hormone receptor in the female mouse reproductive tract. Biol Reprod 64:179-187

11. **Lei Z, Mishra S, Zou W, Xu B, Foltz M, Li X, Rao C** 2001 Targeted disruption of luteinizing hormone/human chorionic gonadotropin receptor gene. Mol Endocrinol 15:184-200

12. **Rao C** 1999 A paradigm shift on the targets of luteinizing hormone/human chorionic gonadotropin actions in the body. J Bellevue Obstet Gynecol Soc 15:26-32

13. **Rao C** 1996 The beginning of a new era in reproductive biology and medicine: expression of low levels of functional luteinizing hormone/human chorionic gonadotropin receptors in nongonadal tissues. J Physiol Pharmacol 47:41-53

14. **Lacroix A, Hamet P, Boutin J** 1999 Leuprolide acetate therapy in luteinizing hormone-dependent Cushing's syndrome. N Engl J Med 341:1577-1581

15. **Chakravarti S, Collins W, Forecast J, Newton J, Oram D, Studd J** 1976 Hormonal profiles after the menopause. BMJ 2:784-787

16. **Neaves W, Johnson L, Porter J, Parker CJ, Petty C** 1984 Leydig cell numbers, daily sperm production, and serum gonadotropin levels in aging men. J Clin Endocrinol Metab 59:756-763

17. **Woller M, Everson-Binotto G, Nichols E, et al.** 2002 Aging-related changes in release of growth hormone and luteinizing hormone in female rhesus monkeys. J Clin Endocrinol Metab 87:5160-5167

18. **Reame N, Kelch R, Bietins I, Yu M-Y, Zawacki C, Padmanabhan V** 1996 Age effects of follicle-stimulating hormone and pulsatile luteinizing hormone secretion across the menstrual cycle of pre-menopausal women. J Clin Endocrinol Metab 81:1512-1518

19. **Yen S, Tsai C, Naftolin F, Vandenberg G, Ajabor L** 1972 Pulsatile patterns of gonadotropin release in subjects with and without ovarian function. J Clin Endocrinol Metab 34:671-675

20. **Couzinet B, Lahlou N, Thomas G, Thalabard J, Bouchard P, Roger M, Schaison G** 1991 Effects of gonadotropin releasing hormone antagonist and agonist on the pulsatile release of gonadotropins and alpha subunit in postmenopausal women. Clinical Endocrinology 34:477-483

21. **Manly J, Merchant C, Jacobs D, Small S, Bell K, Ferin M, Mayeux R** 2000 Endogenous estrogen levels and Alzheimer's disease among postmenopausal women. Neurology 54:833-837

22. **Webber K, Casadesus G, Marlatt M, et al.** 2005 Estrogen bows to a new master: the role of gonadotropins in Alzheimer pathogenesis. Annual NY Academy of Sciences 1052:201-209

23. **Craig M, Maki P, Murphy D** 2005 The Women's Health Initiative Memory Study: findings and implications for treatment. Lancet Neurol 4:190-194

24. **Selkoe D** 2004 Cell biology of protein folding: the examples of Alzheimer's and Parkinson's diseases. Nature Cell Biology 6:1054-1061

25. **Emanuele N, Anderson J, Andersen E, Connick E, Baker G, Kirsteins L, Lawrence A** 1983 Extrahypothalamic brain luteinizing hormone: characterization by radioimmunoassay, chromatography, radioligand assay and bioassay. Neuroendocrin 36:254-260

26. **Glass J, McClusky M** 1987 Immunoreactive luteinizing hormone-containing neurons in the brain of the white-footed mouse, Peromyscus leucopus. Experientia 43:188-190

27. **Banks W, Kastin A, Olson G, Olson R** 1993 Neuroendocrin Lett 15:177-182

28. **Lukacs H, Hiatt E, Lei Z, Rao C** 1995 Peripheral and intracerebroventricular administration of human chorionic gonadotropin alters several hippocampus-associated behaviors in cycling female rats. Horm Behav 29:42-58

29. **Lei Z, Rao C** 2001 Neural actions of luteinizing hormone and human chorionic gonadotropin. Semin Reprod Med 19:103-109

30. **Ghinea N, Mai T, Groyer-Picard M, Milgrom E** 1994 How protein hormones reach their target cells. Receptor-mediated transcytosis of hCG through endothelial cells. J Cell Biol 125:87-97

31. **Brett M, Baxendale S** 2001 Motherhood and memory: a review. Psychoneuroendocrinology 26:339-362

143

32. **Bowen R, Verdile G, Liu T, Parlow A, Perry G, Smith M, Martins R, Atwood C** 2004 Luteinizing hormone, a reproductive regulator that modulates the processing of amyloid-β precursor protein and amyloid-β deposition. J Biol Chem 279:20539-20545

33. **Lapthorn AJ, Harris DC, Littlejohn A, Lustbader JW, Canfield RE, Machin KJ, Morgan FJ, Isaacs NW** 1994 Crystal structure of human chorionic gonadotropin. Nature 369:455-461

34. **Dufau ML** 1998 The luteinizing hormone receptor. Annual Review of Physiology 60:461-496

35. **Manjunath P, Sairam M** 1982 Biochemical, biological, and immunological properties of chemically deglycosylated human choriogonadotropin. Journal of Biological Chemistry 257:7109-7115

36. **Sairam M, Bhargavi G** 1985 A role for glycosylation of the α subunit in transduction of biological signal in glycoprotein hormones. Science 229:65-67

37. **Roess DA, Horvat RD, Munnelly H, Barisas BG** 2000 Luteinizing hormone receptors are self-associated in the plasma membrane. Endocrinology 141:4518-4523

38. **Roess DA, Jewell MA, Philpott CJ, Barisas BG** 1997 The rotational diffusion of LH receptors differs when receptors are occupied by hCG versus LH and is increased by Cytochalasin D. Biochimica et Biophysica Acta 1357:98-106

39. **Keutmann H, McIlroy P, Bergert E, Ryan R** 1983 Chemically deglycosylated human chorionic gonadotropin subunits: Characterization and biological properties. Biochemistry 22:3067-3072

40. **Calvo F, Ryan R** 1985 Inhibition of adenylyl cyclase activity in rat corpora luteal tissue by glycopeptides of human chorionic gonadotropin and the α subunit of hCG. Biochemistry 24:1953-1959

41. **Roess DA, Brady CJ, Barisas BG** 2000 Biological function of the LH receptor is associated with slow receptor rotational diffusion. Biochimica et Biophysica Acta 1464:242-250

42. **Rousseau-Merck M, Misrahi M, Atger M, Loosfelt H, Milgrom E, Berger R** 1990 Localization of the human luteinizing hormone/choriogonadotropin receptor gene (LHCGR) to chromosome 2p21. Cytogenet Cell Genet 54:77-79

43. **Jia X-C, Oikawa M, Bo M, Tanaka T, Ny T, Boime I, Hsueh A** 1991 Expression of human luteinizing hormone (LH) receptor: Interaction with LH and chorionic gonadotropin from human but not equine, rat, and ovine species. Molecular Endocrinology 5:759-768

44. **Koo YB, Ji I, Slaughter RG, Ji TH** 1991 Structure of the luteinizing hormone receptor gene and multiple exons of the coding sequence. Endocrinology 128:2297-2308

45. **Tsai-Morris CH, Buczko E, Wang W, Xie S-Z, Dufau ML** 1991 Structural organization of the rat luteinizing hormone (LH) receptor gene. Journal of Biological Chemistry 266:11355-11359

46. **McFarland K, Sprengel R, Phillips H, Kohler M, Rosemblit N, Nikolics K, Segaloff D, Seeburg P** 1989 Lutropin-choriogonadotropin receptor: An unusual member of the G protein-coupled receptor family. Science 245:494-499

47. **Loosfelt H, Misrahi M, Atger M, Saless R, Thi M, Jolivet A, Guiochon-Mantel A, Sar S, Jallal B, Garnier J, Milgrom E** 1989 Cloning and sequencing of porcine LH-hCG receptor cDNA: Variants lacking transmembrane domain. Science 245:525-528

48. **Probst WC, Snyder LA, Schuster DI, Brosius J, Sealfon SC** 1992 Sequence alignment of the G-protein coupled receptor superfamily. DNA and Cell Biology 11:1-20

49. **Minegishi T, Nakamura K, Takakura Y, Miyamoto K, Hasegawa Y, Ibuki Y, Igarashi M** 1990 Cloning and sequencing of human LH/hCG receptor cDNA. Biochemical and Biophysical Research Communications 172:1049-1054

50. **Fredriksson R, Schioth HB** 2005 The repertoire of G-protein-coupled receptors in fully sequenced genomes. Molecular Pharmacology 67

51. **Lefkowitz R** 2007 Seven transmembrane receptors - A brief personal retrospective. Biochimica et Biophysica Acta 1768:748-755

52. **Jacoby E, Bouhelal R, Gerpsacher M, Seuwen K** 2006 The 7 TM G-protein-coupled receptor target family. Chem Med Chem 1:761-782

53. **Tyndall J, Sandilya R** 2005 GPCR agonists and antagonists in the clinic. Medicinal Chemistry 1:405-421

54. **Szidonya L, Cserzo M, Hunyady L** 2008 Dimerization and oligomerization of G-protein-coupled receptors: debated structures with established and emerging functions. Journal of Endocrinology 196:435-453

55. **Segaloff DL, Ascoli M** 1993 The lutropin/choriogonadotropin receptor...4 years later. Endocrine Reviews 14:324-347

56. **Sanchez-Yague J, Rodriquez MC, Segaloff DL, Ascoli M** 1992 Truncation of the cytoplasmic tail of the lutropin/choriogonadotropin receptor prevents agonist-induced uncoupling. Journal of Biological Chemistry 267:7217-7220

57. **Rozell TG, Davis DP, Chai Y, Segaloff DL** 1998 Association of gonadotropin receptor precursors with the protein folding chaperone calnexin. Endocrinology 139(4):1588-1593

58. **Nishi S, Hsu S, Zell K, Hsueh A** 2000 Characterization of two fly LGR (leucine-rich repeat-containing, G protein-coupled receptor) proteins homologus to vertebrate glycoprotein hormone receptors: constitutive activation of wild-type fly LGR1 but not LGR2 in transfected mammalian cells. Endocrinology 141:1-10

59. **Kobe B, Deisenhofer J** 1994 The leucine-rich repeat: a versatile binding motif. Trends Biochem Sci 19:415-421

60. **Kajava A** 1998 Structural diversity of leucine-rich repeat proteins. J Mol Biol 277:519-527

61. **Matzuk MM, Keene JL, Boime I** 1989 Site specificity of the chorionic gonadotropin N-linked oligosaccharides in signal transduction. Journal of Biological Chemistry 264:2409-2414

62. **Sairam MR** 1989 Role of carbohydrates in glycoprotein hormone signal transduction. The FASEB Journal 3:1915-1926

63. **Kawate N, Menon KMJ** 1994 Palmitoylation of luteinizing hormone/human choriogonadotropin receptors in transfected cells. Journal of Biological Chemistry 269:30651-30658

64. **Zhu H, Wang H, Ascoli M** 1995 The lutropin/choriogonadotropin receptor is palmitoylated at intracellular cysteine residues. Molecular Endocrinology 9:141-150

65. **Birnbaumer M** 1995 Mutations and diseases of G protein coupled receptors. J Recept Signal Transd Res 15:133-160

66. **Hipkin RW, Sanchez-Yague J, Ascoli M** 1993 Agonist-induced phosphorylation of the luteinizing hormone/chorionic gonadotropin receptor expressed in a stably transfected cell line. Molecular Endocrinology 7:823-832

67. **Min L, Ascoli M** 2000 Effect of activating and inactivating mutations on the phosphorylation and trafficking of the human lutropin/choriogonadotropin receptor. Molecular Endocrinology 14:1797-1810

68. **Pitcher J, Freedman N, Lefkowitz R** 1998 G protein-coupled receptor kinases. Annu Rev Biochem 67:653-692

69. **Wang Z, Liu X, Ascoli M** 1997 Phosphorylation of the lutropin/choriogonadotropin receptor facilitates uncoupling of the receptor from adenyl cyclase and endocytosis of the bound hormone. Molecular Endocrinology 11:183-192

70. **Lazari MM, Bertrand JE, Makamure K, Liu Z, Benovic JL, Ascoli M** 1998 Mutation of individual serine residues in the C-terminal tail of the lutropin/choriogonadotropin receptor reveal distinct structural requirements for agonist-induced uncoupling and agonist-induced internalization. The Journal of Biological Chemistry 273(29):18316-18324

71. **Gudermann T, Birnbaumer M, Birnbaumer L** 1992 Evidence for dual coupling of the murine luteinizing hormone receptor to adenylyl cyclase and phophoinositide breakdown and Ca^{2+} mobilization. Journal of Biological Chemistry 267:4479-4488

72. **Ji I, Lee C, Song Y, Conn P, Ji T** 2002 *Cis-* and *trans-*activation of hormone receptors: the LH receptor. Molecular Endocrinology 16:1299-1308

73. **Weinberg R** 2007 The Biology of Cancer

74. **Puett D, Li Y, DeMars G, Angelova K, Fanelli F** 2007 A functional transmembrane complex: The luteinizing hormone receptor with bound ligand and G protein. Mol Cell Endocrinol 260-262:126-136

75. **Herrlich A, Kuhn B, Grosse R, Schmid A, Schultz G, Gudermann T** 1996 Involvement of G(s) and G(i) proteins in dual coupling of the luteinizing hormone receptor to adenylyl cyclase and phospholipase C. The Journal of Biological Chemistry 271(28):16764-16772

76. **Zhu X, Gilbert S, Birnbaumer M, Birnbaumer L** 1994 Dual signaling potential is common among G_s-coupled receptors and dependent on receptor density. Molecular Pharmacology 46:460-469

77. **Gudermann T, Nichols C, Levy LO, Birnbaumer M, Birnbaumer L** 1992 Ca^{2+} mobilization by the LH receptor expressed in xenopus oocytes independent of 3',5'-cyclic adenosine monophosphate formation: evidence for parallel activation of two signaling pathways. Molecular Endocrinology 6(2):272-278

78. **Dix CJ, Schumacher M, Cooke BA** 1982 Desensitization of tumor Leydig cells by lutropin: evidence for uncoupling of the lutropin receptor from the guanine nucleotide-binding protein. Biochemistry Journal 202:739-745

79. **Ferguson S** 2001 Evolving concepts in G protein-coupled receptor endocytosis: the role in receptor desensitization and signaling. Pharmacological Reviews 53:1-24

80. **Dohlman HG, Thorner J, Caron MG, Lefkowtz RJ** 1991 Model systems for the study of seven-transmembrane-segment receptors. Annual Review of Biochemistry 60:653-688

81. **Roess DA, Smith SML** 2003 Self-association and raft localization of functional luteinizing hormone receptors. Biol Reprod 69:1765-1770

82. **Krueger K, Daaka Y, Pitcher J, Lefkowitz R** 1997 The role of sequestration in G protein-coupled receptor resensitization. Journal of Biological Chemistry 272:5-8

83. **Lefkowitz R** 1998 G protein-coupled receptors. The Journal of Biological Chemistry 273:18677-18680

84. **Ascoli M** 1996 Functional consequences of the phosphorylation of the gonadotropin receptors. Biochemical Pharmacology 52:1647-1655

85. **Hunzicker-Dunn M, Birnbaumer L** 1975 Adenylyl cyclase activities in ovarian tissues. IV. Gonadotropin-induced desensitization of the luteal adenylyl cyclase throughout pregnancy and pseudopregnancy in the rabbit and the rat. Endocrinology 99:211-222

86. **Downs SM, Hunzicker-Dunn M** 1995 Differential regulation of oocyte maturation and cumulus expansion in the mouse oocyte-cumulus cell complex by site-selective analogs of cyclic adenosine monphosphate. Developmental Biology 172:72-85

87.   **Lindner H, Amsterdam A, Salamon Y, Tsafriri A, Nimrod A, Lamprecht S, Zor U, Koch Y** 1977 Intraovarian factors in ovulation: Determinants of follicular response to gonadotrophins. J Reprod Fertil 51:215-235

88.   **Dekel N, Gliani D, Sherizly I** 1988 Dissociation between the inhibitory and the stimulatory action of cAMP on maturation of rat oocytes. Mol Cell Endocrinol 56:115-121

89.   **Lamm MLG, Hunzicker-Dunn M** 1994 Phosphorylation-independent desensitzation of the luteinizing hormone/chorionic gonadotropin receptor in porcine follicular membranes. Molecular Enocrinology 8(11):1537-1546

90.   **Hunzicker-Dunn M, Barisas G, Song J, Roess DA** 2003 Membrane organization of luteinizing hormone receptors differs between actively signaling and desensitized receptors. J Biol Chem 278:42744-42749

91.   **Mukherjee S, Palczewski K, Gurevich V, Hunzicker-Dunn M** 1999 β-arrestin-dependent desensitization of luteinizing hormone/choriogonadotropin receptor is prevented by a synthetic peptide corresponding to the third intracellular loop of the receptor. Journal of Biological Chemistry 274:12984-12989

92.   **DeWire S, Ahn S, Lefkowitz R, Shenoy S** 2007 Beta-arrestins and cell signaling. Annu Rev Physiol 69:483-510

93.   **Hunzicker-Dunn M, Gurevich V, Casanova J, Mukherjee S** 2002 ARF6: a newly appreciated player in G protein-coupled receptor desensitization. FEBS Letters 521:3-8

94.   **Luborsky J, Slater W, Behrman H** 1984 Luteinizing hormone (LH) receptor aggregation: modification of ferritin-LH binding and aggregation by prostaglandin $F_{2\alpha}$ and ferritin-LH. Endocrinology 115:2217-2225

95.   **Amsterdam A, Berkowitz A, Nimrod A, Kohen F** 1980 Aggregation of luteinizing hormone receptors in granulosa cells: a possible mechanism for desensitization to the hormone. PNAS (USA) 77:3440-3445

96. **Horvat RD, Barisas BG, Roess DA** 2001 Luteinizing hormone receptors are self-associated in slowly diffusing complexes during receptor desensitization. Molecular Endocrinology 15:534-542

97. **Agnati L, Fuxe K, Zoli M, Rondanini C, Ogren SO** 1982 New vistas on synaptic plasticity: the receptor mosaic hypothesis of the engram. Medical Biology 60:183-190

98. **Bouvier M** 2001 Oligomerization of G-protein-coupled transmitter receptors. Nature Reviews Neuroscience 2:274-286

99. **Maggio R, Vogel Z, Wess J** 1993 Coexpression studies with mutant muscarinic/adrenergic receptors provide evidence for intermolecular "cross-talk" between G-protein-linked receptors. PNAS 90:3103-3107

100. **Gouldson P, Higgs C, Smith R, Dean M, Gkoutos G, Reynolds C** 2000 Dimerization and domain swapping in G-protein-coupled receptors: a computational study. Neuropsychopharmacology 23:S60-S77

101. **Schulz A, Grosse R, Schultz G, Gudermann T, Schoneberg T** 2000 Structural implication for receptor oligomerization from functional reconstitution studies of mutant V2 vasopressin receptors. J of Biological Chemistry 275:2381-2389

102. **Lee S, O'Dowd B, Ng G, Varghese G, Akil H, Mansour A, Nguyen T, George S** 2000 Inhibition of cell surface expression by mutant receptors demonstrates that D2 dopamine receptors exist as oligomers in the cell. Molecular Pharmacology 58:120-128

103. **Hebert T, Moffett S, Morello J, Loisel T, Bichet D, Barret C, Bouvier M** 1996 A peptide derived from a beta 2-adrenergic receptor transmembrane domain inhibits both receptor dimerization and activation. J of Biological Chemistry 271:16384-16392

104. **Pfleger K, Eidne K** 2005 Monitoring the formation of dynamic G-protein-coupled receptor-protein complexes in living cells. Biochemical Journal 385:625-637

105. **Singer SJ, Nicolson GL** 1972 The fluid mosaic model of the structure of cell membranes. Cell membranes are viewed as two-dimensional solutions of oriented globular proteins and lipids. Science 175:720-731

106. **Frye LD, Edidin M** 1970 The rapid intermixing of cell surface antigens after formation of mouse-human heterokaryons. Journal of Cell Science 7:319-335

107. **Loor F** 1973 Lectin-induced lymphocyte agglutination. An active cellular process? Experimental Cell Research 82:415-425

108. **Sheets E, Simson R, Jacobsen K** 1995 New insights into membrane dynamics from the analysis of cell surface interactions by physical methods. Current Opinion in Cell Biology 7:707-714

109. **Kusumi A, Koyama-Honda I, Suzuki K** 2004 Molecular dynamics and interactions for creation of stimulation-induced stabilized rafts from small unstable steady-state rafts. Traffic 5:213-230

110. **Day C, Kenworthy A** 2009 Tracking microdomain dynamics in cell membranes. Biochimica et Biophysica Acta 1788:245-253

111. **Patel H, Murray F, Insel P** 2008 G-protein-coupled receptor-signaling components in membrane raft and caveolae microdomains. Handbook of Experimental Pharmacology 186:167-184

112. **Ostrom RS, Post SR, Insel PA** 2000 Stoichiometry and compartmentation in G protein-coupled receptor signaling: implications for therapeutic interventions involving G_s. J Pharmacol Exp Ther 294:407-412

113. **Sheetz MP, Schindler M, Koppel DE** 1980 Lateral mobility of integral membrane proteins is increased in spherocytic erythrocytes. Nature 285:510-511

114. **Edidin M, Stroynowski I** 1991 Differences between the lateral organization of conventional and inositol phospholipid-anchored membrane proteins. A further definition of micrometer scale membrane domains. J Cell Biol 112:1143-1150

115. **Simons K, Ikonen E** 1997 Functional rafts in cell membranes. Nature 387:569-572

116. **Pike L** 2003 Lipid rafts: bringing order to chaos. J Lipid Res 44:655-667

117. **Simons K, Van Meer G** 1988 Lipid sorting in epithelial cells. Biochemistry 27:6197-6202

118. **Simons K, Wandinger-Ness A** 1990 Polarized sorting in epithelia. Cell 62:207-210

119. **Brown D, Rose J** 1992 Sorting of GPI-anchored proteins to glycoplipid-enriched membrane subdomains during transport to the apical cell surface. Cell 68:533-544

120. **Saslowsky D, Lawrence J, Ren X, Brown D, Henderson R, Edwardson J** 2002 Placental alkaline phosphatase is efficiently targeted to rafts in supported lipid bilayers. J Biol Chem 277:26966-26970

121. **White M, Anderson R** 2005 Signaling networks in living cells. Annu Rev Pharmacol Toxicol 45:587-603

122. **Simons K, Toomore D** 2000 Lipid rafts and signal transduction. Nature Reveiws Molecular Cell Biology 1:31-39

123. **Oh P, Schnitzer J** 2001 Segregation of heterotrimeric G proteins in cell surface microdomains. Molecular Biology of the Cell 12:685-698

124. **Insel P, Head B, Patel H, Roth D, Bundey R, Swaney J** 2005 Compartmentation of G-protein-coupled receptors and their signaling components in lipid rafts and caveolae Biochem Soc Trans 33:1131-1134

125. **Sheets ED, Holowka D, Baird B** 1999 Membrane organization in immunoglobulin E receptor signaling. Current Opinion in Chemical Biology 3:95-99

126. **Dietrich C, Volovyk Z, Levi M, Thompson N, Jacobson K** 2001 Partitioning of Thy-1, GM1, and cross-linked phospholipid analogs into lipid rafts reconstitutedin supported model membrane monolayers. PNAS 98(19):10642-10647

127. **Head B, Patel H, Roth D, et al.** 2006 Microtubules and actin microfilaments regulate lipid raft/caveolae localization of adenylyl cyclase signaling components. J Biol Chem 281:26391-26399

128. **Kusumi A, Ike H, Nakada C, Murase K, Fujiwara T** 2005 Single-molecule tracking of membrane molecules: plasma membrane compartmentalization and dynamic assembly of raft-philic signaling molecules. Seminars in Immunology 17:3-21

129. **Pralle A, Keller P, Florin E, Simons K, Hörber J** 2000 Sphingolipid-cholesterol rafts diffuse as small entities in the plasma membrane of mammalian cells. Journal of Cell Biology 148:997-1008

130. **Sako Y, Kusumi A** 1994 Compartmentalized structure of the plasma membrane for receptor movements as revealed by a nanometer-level motion analysis. Journal of Cell Biology 125:1251-1264

131. **Kusumi A, Suzuki K** 2005 Toward understanding the dynamics of membrane-raft-based molecular interactions. Biochimica et Biophysica Acta 1746:234-251

132. **Dietrich C, Yang B, Fujiwara T, Kusumi A, Jacobson K** 2002 Relationship of lipid rafts to transient confinement zones detected by single particle tracking. Biophys J 82:274-284

133. **Fujiwara T, Ritchie K, Murakoshi H, Jacobson K, Kusumi A** 2002 Phospholipids undergo hop diffusion in compartmentalized cell membrane. J Cell Biol 157:1071-1081

134. **Andrews N, Lidke K, Pfeiffer J, Burns A, Wilson B, Oliver J, Lidke D** 2008 Actin restricts FcεRI diffusion and facilitates antigen-induced receptor immobilization. Nature Cell Biology 10:955-963

135. **Garcia-Saez A, Schwille P** 2007 Single molecule techniques for the study of membrane proteins. Appl Microbiol Biotechnol 76:257-266

136. **Bates I, Wiseman P, Hanrahan J** 2006 Investigating membrane protein dynamics in living cells. Biochem Cell Biol 84:825-831

137. **Axelrod D, Koppel DE, Schlessinger J, Elson E, Webb WW** 1976 Mobility measurement by analysis of fluorescence photobleaching recovery kinetics. Biophysical Journal 16:1055-1069

138. **Faulk W, Taylor G** 1971 An immunocolloid method for the electron microscope. Immunochemistry 8:1081-1083

139. **Feldherr C, Marshall J** 1962 The use of colloidal gold for studies of intracellular exchanges in the ameba *Chaos chaos*. J Cell Biol 12:640-645

140. **De Mey J** 1983 Immunocytochemistry: Chapter 6: Colloidal gold probes in immunocytochemistry

141. **Goodman S, Hodges G, Trejdosiewicz L, Livingston D** 1981 Colloidal gold markers and probes for routine application in microscopy. Journal of Microscopy 123:201-213

142. **Goodman S, Hodges G, Livingston D** 1980 Scanning Electron Microscopy: A review of the colloidal gold marker system

143. **Saxton M, Jacobson K** 1997 Single-particle tracking: applications to membrane dynamics. Annual Review of Biophysics and Biomolecular Structure 26:373-399

144. **Saxton M** 1997 Single-particle tracking: the distribution of diffusion coefficients. Biophysical Journal 72(4):1744-1753

145. **Daumas F, Destainville N, Millot C, Lopez A, Dean D, Salomé L** 2003 Confined diffusion without fences of a G protein coupled receptor as revealed by single particle tracking. The Biophysical Journal 84:356-366

146. **Patterson GH, Piston DW, Barisas BG** 2000 Förster distances between green fluorescent protein pairs. Analytical Biochemistry 284:438-440

147. **Zhang J, Campbell R, Ting A, Tsien R** 2002 Creating new fluorescent probes for cell biology. Nature 3:906-918

148. **Lidke D, Nagy P, Barisas B, Heintzmann R, Post J, Kidke K, Clayton A, Arndt-Jovin D, Jovin T** 2003 Imaging molecular interactions in cells by dynamic and static fluorescence anisotropy (rFLIM and emFRET). Biochemical Society Transactions 31:1020-1027

149. **Varma R, Mayor S** 1998 GPI-anchored proteins are organized in submicron domains at the cell surface. Nature 394(20):798-801

150. **Smith S, Lei Y, Liu J, Cahill M, Hagen G, Barisas B, Roess D** 2006 Luteinizing hormone receptors translocate to plasma membrane microdomains after binding of human chorionic gonadotropin. Endocrinology 147:1789-1795

151. **Lei Y HG, Smith SM, Liu J, Barisas G, Roess DA** 2007 Constitutively-active human LH receptors are self-associated and located in rafts. Mol Cell Endocrinol 260-262:65-72

152. **Kusumi A, Sako Y, Yamamoto M** 1993 Confined lateral diffusion of membrane receptors as studied by single particle tracking (nanovid microscopy). Effects of calcium-induced differentiation in cultured epithelial cells. Biophysical Journal 65:2021-2040

153. **Murase K, et al.** 2004 Ultrafine membrane compartments for molecular diffusion as revealed by single molecule techniques. Biophysical Journal 86:4075-4093

154. **Guan R, Feng X, Wu X, Zhang M, Zhang X, Hebert T, Segaloff D** 2009 Bioluminescence resonance energy transfer studies reveal constitutive dimerization of the human lutropin receptor and a lack of correlation between receptor activation and the propensity for dimerization. J Biol Chem 284:7483-7494

155. **Ritchie K, Iino R, Fujiwara T, Murase K, Kusumi A** 2003 The fence and picket structure of the plasma membrane of live cells as revealed by single molecule techniques. Molecular Membrane Biology 20:13-18

156. **Roess DA, Niswender GD, Barisas BG** 1988 Cytochalasins and colchicine increase the lateral mobility of human chorionic gonadotropin-occupied luteinizing hormone receptors on ovine luteal cells. Endocrinology 122:261-269

157. **Lei Y, Hagen G, Smith S, Barisas B, Roess D** 2005 Chimeric GnRH-LH receptors and LH receptors lacking C-terminus palmitoylation sites do not localize to plasma membrane rafts. Biochem Biophys Res Commun 337:430-434

158. **Nishi Y, Yanase T, Mu Y, Oba K, Nawata H, et al.** 2001 Establishment and characterization of a steroidogenic human granulosa-like tumor cell line, KGN, that expresses functional follicle-stimulating hormone receptor. Endocrinology 142:437-445

159. **Kawate N, Peegel H, Menon K** 1997 Role of palmitoylation of conserved cystine residues of lutenizing hormone/human choriogonadotropin receptors in receptor down-regulation. Molecular and Cellular Endocrinology 127:211-219

160. **Jin H, Zastawny R, George S, O'Dowd B** 1997 Elimination of palmitoylation sites in the human dopamine D1 receptor does not affect receptor-G protein interaction. Eur J Pharmacol 324:109-116

161. **Ponimaskin E, Heine M, Joubert L, Sebben M, Bickmeyer U, Richter D, Dumuis A** 2002 The 5-hydroxytryptamine (4a) receptor is palmitoylated at two different sites, and acylation is critically involved in regulation of receptor constitutive activity. J Biol Chem 277:2534-2546

162. **Qanbar R, Bouvier M** 2003 Role of palmitoylation/depalmitoylation reactions in G-protein-coupled receptor function. Pharmacological Therapeutics 97:1-33

163. **DiPilato L, Cheng X, Zhang J** 2004 Fluorescent indicators of cAMP and Epac activation reveal differential dynamics of cAMP signaling within discrete subcellular compartments. PNAS (USA) 101:16513-16518

LIST OF ABBREVIATIONS

Aβ:	beta amyloid
AβPP:	amyloid beta protein precursor
AC:	adenylate cyclase
ACTH:	adrenocorticotropic hormone
AD:	Alzheimer's Disease
ARF6:	ADP-ribosylation factor, isotype 6
ARNO:	ADP-ribosylation factor nucleotide-binding site opener
Asn:	asparagine
ATP:	adenosine triphosphate
Au:	gold
β_2-AR:	beta 2 adrenergic receptor
BRET:	bioluminescence resonance energy transfer
BSA:	bovine serum albumin
BSS:	hank's balanced salt solution
Ca^{2+}:	calcium
cAMP:	cyclic adenosine monophosphate
cDNA:	complementary deoxyribonucleic acid
CFP:	cyan fluorescent protein
CHO:	chinese hamster ovary

CL:	corpus luteum
CO_2:	carbon dioxide
Cys:	cysteine
D:	diffusion coefficient
D +:	desensitization treatment
D_{after}:	donor fluorescence after acceptor photobleaching
D_{before}:	donor fluorescence before acceptor photobleaching
DAG:	1,2-diacylglycerol
DG-hCG:	deglycosylated-human chorionic gonadotropin
DIG:	detergent-insoluble, glycolipid-enriched complex
DMEM:	dulbecco's modified minimum essential medium
DRM:	detergent-resistant membrane
%E:	energy transfer efficiency
ECD:	extracellular domain
ECFP:	enhanced cyan fluorescent protein
eCG:	equine chorionic gonadotropin
EDTA:	ethylenediaminetetraacetic acid
emFRET:	energy migration fluorescence resonance energy transfer
Epac:	exchange protein activated by cAMP
Fab:	fraction antigen binding
FBS:	fetal bovine serum
FCS:	fluorescence correlation spectroscopy
FET:	fluorescence energy transfer

159

FITC:	fluorescein isothiocyanate
FLAG:	a short hydrophilic 8-amino acid peptide
	(Asp-Tyr-Lys-Asp-Asp-Asp-Asp-Lys)
FMPP:	familial male-limited precocious puberty
FPR:	fluorescence photobleaching recovery
FRAP:	fluorescence recovery after photobleaching
FRET:	fluorescence resonance energy transfer
FSH:	follicle-stimulating hormone or follitropin
G418:	geneticin
G_i:	inhibitory g protein
G_s:	stimulatory g protein
GDP:	guanosine diphosphate
GEF:	guanine exchange factor
GFP:	green fluorescent protein
GM1:	membrane ganglioside
GnRH:	gonadotropin releasing hormone
GnRHR:	gonadotropin releasing hormone receptor
GPCR:	g protein-coupled receptor
GPI:	glycosylphosphatidylinositol
GRK:	g protein-coupled receptor kinase
GTP:	guanosine triphosphate
hCG:	human chorionic gonadotropin
hetero-FRET:	heterotransfer fluorescence resonance energy transfer

hLHR:	human luteinizing hormone receptor
homo-FRET:	homotransfer fluorescence resonance energy transfer
HPG:	hypothalamic-pituitary-gonadal
ICUE1:	indicator of cAMP using Epac
IP3:	inositol 1,4,5-triphosphate
LGR:	leucine-rich repeat-containing g protein-coupled receptor
LH:	luteinizing hormone
LHR:	luteinizing hormone receptor
LRR:	leucine-rich repeat
M3:	muscarinic
M_f:	mobile fraction
mAb:	monoclonal antibody
MβCD:	methyl-beta cyclodextrin
MEM:	minimum essential medium
MES:	2-(N-morpholino)ethanesulfonic acid
mRNA:	messenger ribonucleic acid
MSD:	mean square displacement
MSK:	membrane skeleton
N.A.:	numerical aperture
NaCl:	sodium chloride
NGF:	nerve growth factor
PBS:	phosphate buffered saline
PDGF-β:	platelet-derived growth factor beta

PIP2:	phosphatidylinositol 4,5-biphosphate
PKA:	protein kinase A
PKC:	protein kinase C
PLC:	phospholipase C
PMT:	photomultiplier tube
r:	anisotropy
r_o:	Förster distance
RET:	resonance energy transfer
rLHR:	rat luteinizing hormone receptor
SDS-PAGE:	sodium dodecylsulfate polyacrylamide gel electrophoresis
Ser:	serine
SFVI:	single fluorescent molecule video imaging
SPT:	single particle tracking
TGF-β:	transforming growth factor beta
Thr:	threonine
TM:	transmembrane
TPA:	time-resolved phosphoresence anisotropy
TrITC:	tetramethyl rhodamine isothiocyanate
TSH:	thyroid-stimulating hormone or thyrotropin
VFP:	visible fluorescent protein
Wt:	wild type
YFP:	yellow fluorescent protein
3i:	third intracellular loop